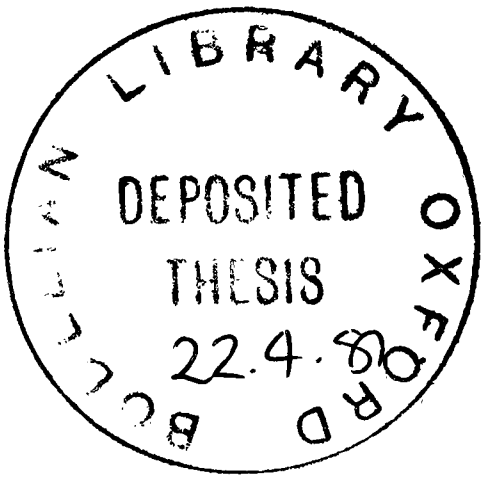
A MICROSCOPIC THEORY OF THE ALPHA-NUCLEUS OPTICAL POTENTIAL

ANGELA BONACCORSO

SOMERVILLE COLLEGE



A Thesis submitted for the Degree of Doctor of Philosophy at the University of Oxford

December 1980

A MICROSCOPIC THEORY OF THE ALPHA-NUCLEUS OPTICAL POTENTIAL

Angela Bonaccorso, Somerville College, Oxford

Abstract of thesis submitted for the degree of Doctor of Philosophy.
Michaelmas Term 1980

ABSTRACT

A semiclassical theory of the optical potential based on Feynman's path integral formalism is proposed.

The new approach gives an expression for the time integral of the optical potential in terms of the ground state to ground state transition amplitude. The transition amplitude is first calculated by perturbation theory. Then the formalism is applied to the study of the imaginary part of the optical potential for α-elastic scattering on ^{16}O and ^{40}Ca. The projectile is treated as a point-like particle and the target is described by the shell model. The relative motion is calculated in a semiclassical approximation. The intermediate states of the target are 1p-1h states and the centre-of-mass spurious excitations are explicitly calculated. The absorption of flux from the elastic channel due only to collective excitations is evaluated by taking as intermediate states only the giant quadrupole and monopole states. The relation to phenomenological potentials is clarified by comparing time integrals along classical trajectories.

In order to test the validity of perturbation theory the ground state to ground state transition amplitude is also calculated by solving a set of coupled channel equations. Time integrals of the imaginary part of the optical potential are compared with the results obtained by perturbation theory. Information about the real part of the potential is also extracted. Finally a comparison is made with other theories of the optical potential which use perturbation theory. Some final remarks and suggestions for future developments conclude this work.

TABLE OF CONTENTS

	Page
ABSTRACT	(ii)
TABLE OF CONTENTS	(iii)
ACKNOWLEDGEMENTS	(vi)
TABLE OF UNITS AND CONSTANTS	(viii)
INTRODUCTION	1
Chapter I - THEORETICAL APPROACHES TO THE OPTICAL POTENTIAL	4
I-1 Feshbach's Potential	4
I-2 Folding Potentials	8
Chapter II - THE PATH INTEGRAL APPROACH	12
II-1 Motivation	12
II-2 Feynman's Propagator	13
II-3 The Reduced Propagator	19
Chapter III - IMAGINARY PART OF OPTICAL POTENTIAL CALCULATED BY PERTURBATION THEORY	25
III-1 Transition Amplitude in Perturbation Theory	25
III-2 The Model for α-Scattering	27
Appendix III	35
Chapter IV - THE EFFECTIVE INTERACTION	41
Appendix IV	48
Chapter V - A SIMPLE APPLICATION	51
V-1 - Correlation Function	51
V-2 - Choice of the Path $\underline{r}(t)$	55
V-3 - Straight Line Trajectory	58
Tables V	

		Page
Chapter VI	- THE SPURIOUS CENTRE-OF-MASS EXCITATIONS	61
VI-1	Introduction	61
VI-2	Correction to the $1\hbar\omega$ Excitations	62
VI-3	Correction to the $2\hbar\omega$ Excitations	66
	Appendix VI	70
	Tables VI	
Chapter VII	- THE ROLE OF COLLECTIVE EXCITATIONS	74
VII-1	Review of the Theoretical and Experimental Situation	74
VII-2	Collective Excitations and the Imaginary Part of the Optical Potential	76
	Appendix VII	84
	Tables VII	
Chapter VIII	- SEMICLASSICAL TREATMENT OF THE RELATIVE MOTION	86
	Appendix VIII	90
	Figures VIII	
Chapter IX	- NUMERICAL RESULTS	91
IX-1	Calculations with Straight Line Trajectories	91
IX-2	Comparison with Phenomenological Potentials	93
IX-3	Calculations with Classical Trajectories	96
	Figures IX	
Chapter X	- NON PERTURBATIVE CALCULATION OF THE OPTICAL POTENTIAL	101
X-1	Coupled Equations	101
X-2	Real Part of the Optical Potential	103
X-3	Results	106
	Tables X	

Page

Chapter XI - COMPARISON TO OTHER APPROACHES 108

XI-1 Introduction 108

XI-2 N. Vinh Mau's Calculations and the Path Integral Approach 109

XI-3 The Path Integral Approach and the Microscopic Model of De Vries and Peng. 114

CONCLUSIONS 120

REFERENCES 125

ACKNOWLEDGEMENTS

My years in Oxford constitute an unforgettable experience and I would like to express my gratitude to all those who have been near to me in this period.

To my supervisor, Dr. D.M. Brink, I owe thanks more than to everyone else. I would like to thank him first of all for offering me the possibility of coming to Oxford and working with him. Nothing I can say here would be enough to describe how our weekly discussions have clarified to me the fascinating world of Nuclear Physics. Also, I would like to mention the infinite patience with which Dr. Brink has continued to direct my work, in particular during the last period of preparation of this thesis, and to read and comment on my manuscript.

Prof. M. Di Toro suggested first, and in the end almost forced me to leave my beloved Sicily and come to Oxford. Now I thank him for that and for continuing to help and encourage me through these years. I benefitted from several discussions with him, in particular during his visit to Oxford last Spring.

I would like to thank Prof. R.J. Elliott for the warm atmosphere I have enjoyed at the Department of Theoretical Physics and for the help I received from him on several occasions.

Many members and visitors of the Department of Theoretical Physics and of the Nuclear Physics Laboratory have shown interest in my work. Several discussions with Dr. J.R. Rook have clarified to me many problems. I received also interesting comments and suggestions from Dr. N. Rowley, Drs. B. Crowley, P. E. Hodgson, R. Lipperheide, A. Marchant, E. Mavrommatis and Ica Stancu have contributed with their comments to my work.

During the last year I have enjoyed in Room 6.3 the company of J. Lopes-Neto, R. Lindsay, G. Maddison and S. Marsh. From all of them I have received help in solving different problems. I would like to thank in particular R. Linsday for revealing to me many secrets of the IBM/195 machine and for discussions on optical potential and related matters.

Although they are quite far away, my friends and colleagues from the Theory Group of the Physics Department in Catania, in particular Drs. M. Baldo, F. Catara, A. Insolia, U. Lombardo, G. Giansiracusa and R. Pucci, have been able to participate in my progress and I am grateful to them for what they have been doing for me.

I thank Mrs. Verena Brink for reading and correcting my English throughout several parts of this thesis and for the many delightful hours I have spent in her house.

Mrs. Judy Cullen has been the most friendly, fast and expert typist I have ever met in my life.

Finally I would like to thank my husband, Ken Konishi, for all the reasons which we know but it would be too long to enumerate here. Without his constant help I would have never been able to finish this work.

I have used for my numerical calculations the IBM/195 machine of Rutherford Laboratory and I would like to thank the staff there and at the Oxford terminal for their help.

Financial support from the British Council and the Catania Branch of the I.N.F.N. and of the C.S.F.N.S.M. is gratefully acknowledged.

TABLE OF UNITS AND CONSTANTS

$1g = (5.610 \pm 0.00011) \times 10^{26}$ MeV

1 eV $= 1.6021 \times 10^{-12}$ erg

1 MeV $= 1.6021 \times 10^{-6}$ erg

$\hbar = 1.0545 \times 10^{-27}$ erg·sec $= 6.58218 \cdot 10^{-22}$ MeV·sec

$c = 2997930 \pm 03$ km sec^{-1}

$\sim 3.10^{23}$ fm sec$^{-1} = 30 \cdot 10^{22}$ fm·sec^{-1}

$e^2 = (1.60210 \cdot 10^{-19})^2$ Coulb$^2 = 1.44189$ MeV·fm

$m_n = 939.550 \pm 004$ MeV $= 1.67474 \pm 0.00010 \cdot 10^{-24}$ gm

$m_p = 938.256 \pm 004$ MeV $= 1.67243 \pm 0.00010 \cdot 10^{-24}$ gm

$m_\alpha = 3727.377$ MeV $= 6.6442 \pm 0.0012 \cdot 10^{-24}$ gm

$\frac{m_p + m_n}{2} = 938.903$ MeV $= 1.04322$ MeV$(10^{-22}$ sec$)^2 \cdot$ fm^{-2}

In our calculations the following units were used

SPACE = FERMI

TIME = 10^{-22} SEC

ENERGY = MeV

MASS = MEV·SEC^2/FERMI^2

CHARGE^2 = MeV· FERMI

Throughout this thesis the following parameters are used

a , range of the effective potential Eq.(IV-6)

V_o , strength of the effective potential

β , harmonic oscillator parameter Eq.(A-III-11)

ω ; harmonic oscillator frequency

$\gamma = a^2\beta^2$; $\alpha = 1 + \gamma$

$\underline{r}_o \equiv \underline{r}(t)$, path of the α-particle

μ , reduced mass

ABBREVIATIONS

O.P.	Optical potential
H.O.	Harmonic oscillator
S.M.	Shell model
G.D.R.	Giant dipole resonance
G.Q.R.	Giant quadrupole resonance

INTRODUCTION

Since its first introduction in 1958[1] the optical-model potential has been widely used to describe scattering of nucleons and composite particles of nuclei.

As it is shown in ref.(2), the optical-model potential is the single particle operator which, introduced in the one-body Schrödinger equation, yields the elastic part of the full many-channel wave function. But as Feshbach already pointed out in his paper[2] the "generalised optical-model potential" is complex, non-local, and energy-dependent, therefore it is very difficult to calculate without the introduction of several approximations.

However, it has been successfully applied in the framework of a phenomenological approach in which its form factor has been chosen on the grounds of nuclear structure considerations and its parameters have been adjusted in order to fit the experimental data.

In spite of its complexity, several attempts have been made to calculate the optical potential[3,4,5], but they have been mainly concerned with the calculation of the real part of the O.P. (optical potential), while the imaginary part has been treated phenomenologically due to its further complexity, as it depends on all the possible inelastic channels. Only recently N. Vinh Mau[6] has obtained the imaginary as well as the real part of the optical potential for alpha-elastic scattering on ^{40}Ca using a 2nd order-perturbation-theory approximation to the Feshbach potential.

In this work we have tried to derive both the real and imaginary parts of the O.P. for alpha elastic scattering using a semiclassical approach[7], although much of the attention has

been devoted to the imaginary part, as it is the one that still is not fully understood in terms of a nuclear excitation mechanism.

The reason for studying alpha-scattering and in a semiclassical framework will be clarified later. Here we would just like to remark that the alpha-particle is the simplest composite projectile to be used when starting to construct a nucleus-nucleus potential and that semiclassical theories have been shown to be fairly good approximations to the study of heavy-ion reactions; so we hope that from our results it would be possible to shed some light on the problem of an ion-ion potential.

After a brief review of Feshbach's and the folding theory of the optical potential, we present in Chapter II a new approach based on Feynman's path integral formalism. The form of the optical potential that we derive is model-independent and gives the time integral of the optical potential along the path of relative motion $\underline{r}(t)$ in terms of the amplitude for a ground state to ground state transition. In Chapter III this amplitude is evaluated by perturbation theory and then the shell model description of the target is introduced. Our formalism requires the use of an effective α-nucleon interaction and this point is discussed in Chapter IV.

Chapters V-VI-VII-IX are devoted to the imaginary part of the optical potential only. In Chapter V we present a simple application of the new formalism proposed in the case of a target of ^{16}O. A characteristic of the path integral approach is its explicit dependence on the path of the relative motion $\underline{r}(t)$. The choice of the path is also discussed in Chapter V. Chapter VI is devoted to the calculation of the centre-of-mass spurious excitations which affect our shell

model results. In Chapter VII we show how in path integral approach the excitations due only to the giant quadrupole and monopole resonances can be calculated.

Chapter VIII contains the description of the calculation of the projectile trajectory $\underline{r}(t)$. In Chapter IX we discuss some of the results already presented in Chapters V and VI and make a comparison with phenomenological potentials. In Chapter X we go back to the original problem of the evaluation of the ground state to ground state transition amplitude and calculate it by solving a set of coupled channel equations. The results for the time integral of the imaginary part of the potential are compared with the results obtained by perturbation theory. The time integral of the real part of the potential is also calculated and the second order correction is separated from the first order term.

Finally in Chapter XI we compare our formulae for the optical potential obtained by perturbation theory with other approaches to the optical potential which also use the perturbation approximation.

This thesis finishes with some conclusions on the validity of the new approach proposed and with some suggestions for future developments.

Several chapters contain appendices, tables and figures. They are numbered according to the chapter to which they belong.

Chapter I

THEORETICAL APPROACHES TO THE OPTICAL POTENTIAL

In the first part of this chapter we review the original formulation of the optical potential due to Feshbach[1,2] and its application to α-nucleus scattering by N. Vinh Mau[6]. The second part describes the so-called folding potential and a related work by De Vries and Peng[9]. The detailed comparison between these approaches and our own will be made later in chapter XI.

I-1 Feshbach's potential

The problem of studying the scattering of two nuclei corresponds to finding the solution of the Schrödinger equation

$$H\,\Phi = E\,\Phi \qquad \text{(I-1)}$$

where H is the total hamiltonian of the system

$$H = H_1 + H_2 + T_o + V_{12} \qquad \text{(I-2)}$$

given by the sum of the internal hamiltonians of the two nuclei H_1 and H_2, plus the kinetic energy of relative motion T_o, plus the two-body interaction potential of the two nuclei V_{12}.

The wave function Φ can be written as an expansion in terms of the wave functions $\phi_i(1)$, $\phi_j(2)$ which are eigenstates of H_1 and H_2 with eigenvalues $\varepsilon_i(1)$ and $\varepsilon_j(2)$

$$\Phi = \sum_{ij} \psi_{ij}\, \varphi_i(1)\, \varphi_j(2) \qquad \text{(I-3)}$$

where $\psi_{ij} = -\psi_{ji}$

Using the orthonormality of the ϕ's the solution of Eq.(I-1) can be reduced to the solution of the set of coupled equations

$$\left(\varepsilon_\kappa(1) + \varepsilon_{\kappa'}(2) + T_0 + V_{\kappa\kappa;\kappa'\kappa'} - E\right)\psi_{\kappa\kappa'} = -\sum_{\substack{i\neq\kappa \\ j\neq\kappa'}} V_{\kappa i\,;\,\kappa' j}\ \psi_{ij} \tag{I-4}$$

where

$$V_{\kappa i;\,\kappa' j} \equiv \langle \varphi_\kappa(1)\varphi_{\kappa'}(2)|V_{12}|\varphi_i(1)\varphi_j(2)\rangle$$

From Eq.(I-4) Feshbach obtained an uncoupled equation for the amplitude ψ_{oo} of the elastic channel:

$$\left(T_0 + V_{opt} - E\right)\psi_{oo} = 0 \tag{I-5}$$

where the optical potential takes into accountthe coupling to all inelastic channels and it is defined by

$$V_{opt} = \langle\varphi_0(1)\varphi_0(2)|V_{12}|\varphi_0(1)\varphi_0(2)\rangle + \langle\varphi_0(1)\varphi_0(2)|V_{12}\,Q\,\frac{1}{E - H_{QQ} + i\varepsilon}\,Q\,V_{12}|\varphi_0(1)\varphi_0(2)\rangle \tag{I-6}$$

where $\phi_o(1)$ and $\phi_o(2)$ are the ground state wave functions of the two nuclei and Q is the operator which projects off the ground state.

The first term in Eq.(I-6) is real and can be written, by introducing the density functions of the two nuclei, as

$$\langle \varphi_0(1)\varphi_0(2)|V_{12}|\varphi_0(1)\varphi_0(2)\rangle = \int d^3r_1 \int d^3r_2 \; \rho(r_1) V_{12} \rho(r_2) \qquad \text{(I-7)}$$

The second term contains both real and imaginary parts.
The imaginary part takes into account the loss of flux from the elastic channel.

Ref.(6) makes a perturbation approximation of the optical potential Eq.(I-6) by neglecting $Q\, V_{12}\, Q$ in H_{QQ} and calculates the optical potential for α-elastic scattering on ^{40}Ca. The calculations are carried out under the assumption that the α-particle is without internal structure and that its wave functions inside the target are plane waves with momentum $k_\alpha^2 = (2m\alpha/\hbar^2)(\varepsilon_\alpha - V_{\alpha N}^{(o)})$ and that the α-incident energy E_α is higher than the important target excitation energies E_M. The α-nucleus optical potential is then

$$\begin{aligned} V_{\alpha N} &= V_{\alpha N}^{(o)} + \sum_{\Pi \neq 0} f(m_\alpha, s_\alpha)\langle \varphi_0 | V_{\alpha n} | \varphi_\Pi \rangle \langle \varphi_M | V_{\alpha n} | \varphi_0 \rangle \\ &= V_{\alpha N}^{(o)} + \Delta V_{\alpha N} \end{aligned} \qquad \text{(I-8)}$$

where $V_{\alpha N}^{(o)}$ is the folding potential of Eq.(I-7) and it is purely real; $V_{\alpha n}$ is the α-nucleon effective interaction $V_{\alpha n} = \Sigma_i V_{\alpha n}(i)$, ϕ_o and ϕ_M are the wave functions of the ground state and of the excited states of the target, respectively.

$f(m_\alpha, s_\alpha)$ is the Green's function, which according to ref.(6) is given by

$$f(m_\alpha, s_\alpha) = -\frac{m_\alpha}{2\pi\hbar^2} \; \frac{e^{i K_{M\alpha}(r) s_\alpha}}{s_\alpha} \; \frac{K_M}{K_{M\alpha}(r)} \qquad \text{(I-9)}$$

where

$$\underline{S}_\alpha = \underline{r}_\alpha - \underline{r}_\alpha' \quad ; \quad \underline{R}_\alpha = \frac{\underline{r}_\alpha + \underline{r}_\alpha'}{2} \quad . \qquad \text{(a)}$$

$$K^2_{n\alpha} = \frac{2m_\alpha}{\hbar^2}\left(E_\alpha - V^{(o)}_{\alpha N} - E_n\right) \quad . \qquad \text{(b)} \qquad \text{(I-10)}$$

$$K^2_n = \frac{2m_\alpha}{\hbar^2}\left(E_\alpha - E_n\right) \qquad \text{(c)}$$

It is assumed that all strongly excited states are concentrated around an average energy $\bar{E}_M$ with $E_\alpha >> \bar{E}_M$, such that the momentum K_M can be replaced by

$$\bar{K}_n \simeq K_o = \sqrt{\frac{2m_\alpha}{\hbar^2} E_\alpha} \quad . \qquad \text{(I-11)}$$

Furthermore in the expression of $K_{M\alpha}$ the folding potential is very large compared to E_M. This implies that $K_{M\alpha}$ can be approximated by

$$K_{n_\alpha} \simeq \bar{K}_\alpha = \sqrt{\frac{2m_\alpha}{\hbar^2}\left(E_\alpha - V^{(o)}_{\alpha N}\right)} \quad . \qquad \text{(I-12)}$$

With the above assumption the Green's function $f(m_\alpha, s_\alpha)$ becomes independent of the excited states M and the summation in Eq.(I-8) is only on the matrix elements of $V_{\alpha n}$. The term $\Delta V_{\alpha N}$ in Eq.(I-8) is non-local. A local equivalent potential can be obtained by using the Perey-Saxon approximation[8]

$$\Delta V_{\alpha N}(\underline{r}) = 4\pi \int_0^\infty j_0(K_{o\alpha} s_\alpha)\, V\left(\underline{r} + \frac{1}{2}\underline{s}_\alpha, \underline{r} - \frac{1}{2}\underline{s}_\alpha\right) s_\alpha^2\, d s_\alpha \qquad \text{(I-13)}$$

where

$$j_0(K_{o\alpha} s_\alpha) = \frac{\sin(K_{o\alpha} s_\alpha)}{K_{o\alpha} s_\alpha}$$

and $K_{o\alpha}$ is given by Eq.(I-10,b) for M = 0.

$$\Delta V_{\alpha N}(\underline{r}) = -\frac{i}{\hbar}\sum_{M\neq 0}\left(\frac{K_M}{K_{M\alpha}(r)\,K_{o\alpha}(r)}\,\frac{m_\alpha}{\hbar}\right)\int_0^\infty d s_\alpha \Big[e^{i s_\alpha (K_{M\alpha}(r)-K_{o\alpha}(r))} - e^{i(K_{M\alpha}(r)+K_{o\alpha}(r))s_\alpha}\Big]\langle\varphi_0|V(r+\tfrac{1}{2}s)|\varphi_M\rangle\langle\varphi_M|V(r-\tfrac{1}{2}s)|\varphi_0\rangle \tag{I-14}$$

$$= -\frac{i}{\hbar}\sum_{M\neq 0}\left(\frac{K_M}{K_{M\alpha}(r)\,K_{o\alpha}(r)}\,\frac{m_\alpha}{\hbar}\right)\int_0^\infty d s_\alpha\, e^{i s_\alpha (K_{M\alpha}(r)-K_{o\alpha}(r))} \times \langle\varphi_0|V(r+\tfrac{1}{2}s)|\varphi_M\rangle\langle\varphi_M|V(r-\tfrac{1}{2}s)|\varphi_0\rangle$$

where the integral containing the rapidly oscillating factor $e^{i(K_{M\alpha}+K_{o\alpha})s_\alpha}$ has been neglected.

Eq.(I-14) will be discussed in chapter XI where we will show the analogy with a formula coming from the formalism we will present in chapters II and III.

II-2 Folding Potentials

The folding procedure described in the previous section (cf. Eq.(I-7)) has been generalized by several authors[3,4,5] to obtain both the real and the imaginary part of the optical potential.

In this case the optical potential is given by

$$V_{opt}(\underline{r}) = \int d^3\underline{r}_1 \int d^3\underline{r}_2\, \rho(\underline{r}_1)\rho(\underline{r}_2)\, g(\underline{r}_{12}) \tag{I-15}$$

where $g(\underline{r}_{12})$ is an effective G-matrix which describes the nucleon-nucleon interaction.

In the high energy limit g can be simplified[4] to

$$g(\underline{r}+\underline{r}_1-\underline{r}_2) = -\frac{2\pi}{m}\hbar^2 f(0)\,\delta(\underline{r}+\underline{r}_1-\underline{r}_2) \qquad \text{(I-16)}$$

where m is the nucleon mass and f(o) is the complex forward amplitude for nucleon-nucleon scattering.

In this case the O.P. reads

$$V_{opt}(\underline{r}) = -\frac{2\pi\hbar^2}{m} f(0)\int d^3\underline{r}'\,\rho_1(\underline{r}'-\underline{r})\,\rho_2(\underline{r}') \qquad \text{(I-17)}$$

and its imaginary part is

$$\begin{aligned} \mathrm{Im}\,V_{opt}(\underline{r}) &= -\frac{2\pi\hbar^2}{m}\,\mathrm{Im}\,f(0)\int d^3\underline{r}'\,\rho_1(\underline{r}'-\underline{r})\rho_2(\underline{r}') \\ &= -\frac{1}{2}\hbar v\,\sigma_T^{nn}\int d^3\underline{r}'\,\rho_1(\underline{r}'-\underline{r})\,\rho_2(\underline{r}') \end{aligned} \qquad \text{(I-18)}$$

where σ_T^{nn} is the nucleon-nucleon total reaction cross section given by the optical theorem

$$\sigma_T^{nn} = \frac{4\pi}{K}\,\mathrm{Im}\,f(0) \qquad \text{and} \qquad K = \frac{mv}{\hbar}$$

If we consider a point-like projectile, we find

$$V_{opt}(\underline{r}) = \int d^3\underline{r}\,\rho(\underline{r})\,g(\underline{r}_{12}) \qquad \text{(I-19)}$$

where $\rho(\underline{r})$ is the target density function, and $g(\underline{r}_{12})$ at high energies is

$$g(\underline{r}-\underline{r}') = -\frac{2\pi\hbar^2}{m} f(0)\,\delta(\underline{r}-\underline{r}') \qquad \text{(I-20)}$$

The optical potential becomes then

$$V_{opt}(\underline{r}) = -\frac{2\pi\hbar^2}{m} f(0)\rho(\underline{r}) \qquad \text{(I-21)}$$

and its imaginary part is

$$\mathrm{Im}\, V_{opt}(\underline{r}) = -\frac{1}{2}\hbar v\, \sigma_T^{nn}\rho(\underline{r}) \qquad \text{(I-22)}$$

De Vries and Peng[9] have recently used a semiclassical microscopic model to obtain the nucleus-nucleus reaction cross section $\sigma_R(E)$. They show that at medium energies $\sigma_R(E)$ is neither a constant nor equal to the geometric limit, as it is commonly assumed. Rather they give indication that in the region of incident energy per nucleon $50 < E_i/n < 600$ MeV, σ_R shows a deep fall off reminiscent of the nucleon-nucleon cross section σ_T^{nn}. Therefore they propose that in the above region of energies the nucleus-nucleus collision is dominated by the nucleon-nucleon interactions, rather than by collective (hydrodynamic) effects.

Within the Glauber's approximation[26] they found the following expression for the cross section

$$\sigma_R = 2\pi\int d^2b \left\{1 - \exp\left(-\int \sigma_T^{nn}\rho(r)\, dz\right)\right\} \qquad \text{(I-23)}$$

If we now use the folding expression of the imaginary part of the optical potential, Eq.(I-22), obtained within the same approximation as De Vries and Peng model, (i.e. in the high energy limit), we find that the reaction cross section can be written as

$$\sigma_R = 2\pi \int d^2b \left\{ 1 - \exp\left(\frac{2}{\hbar} \int dt \ \mathrm{Im}\, V_{opt}(\underline{r}(t)) \right) \right\} \qquad \text{(I-24)}$$

where we used $\underline{r}(t) = \underline{v}t + \underline{b} = \underline{z} + \underline{b}$.

In the next chapter we shall see how to obtain an expression for σ_R similar to (I-2-4), starting from a different approach to the optical potential.

Chapter II

THE PATH INTEGRAL APPROACH

II-1 Motivation

This chapter is devoted to the derivation of a formula for the O.P. within the framework of Feynman's path integral formalism.

Feynman's formulation of Quantum Mechanics allows for a simple understanding of all those processes in which semiclassical approximations are applicable. In fact, as we shall show in the following section, Feynman's expression for the propagator for motion between two space-time points, is a functional integral over all continuous paths between the two points. The evaluation of the path integral becomes rather easy to perform when stationary phase approximation is applicable: in this case one would expand the integrand about "points" of stationary phase, which are in fact nothing but the classical trajectories between the two end points.

We can then see that the possibility of defining classical trajectories is a crucial step in the application of such semi-classical approximations.

At this stage we would like to make a few remarks about the physics of heavy-ion collisions as it seems to us the best example of a nuclear process in which a semiclassical description is applicable.

By the term heavy-ions we usually mean the nuclei with A > 10. When two such nuclei collide at an energy well above the Coulomb barrier, say $(E - V_B) \sim 100$ MeV, the wave length in the relative motion

$$\lambda\!\!\!^{-} \equiv \frac{\lambda}{\pi} = \left(\sqrt{\frac{A_1 A_2}{A_1 + A_2} \frac{\hbar^2}{2m(E - V_B)}} \right)^{-1} \text{ fm}$$

is of the order of 0.1 fm if $A_1 \sim A_2 \sim 10$, and it is smaller than a characteristic length a of the interaction potential (typically $a \sim 0.7$ fm)[10].

Therefore, these collisions can frequently be treated in the classical limit and the concept of classical trajectory can be restored. For this reason the formalism that we shall soon describe appears to be appropriate to the study of relative motion in heavy-ion scattering.

But one of the main requirements for the description of such collisions is to know the ion-ion potential. This is a problem that has already been attacked from several points of view[11,12], although each of them is more a model to describe a particular kind of reaction, rather than a general theory for the interaction.

The general problem of an ion-ion interaction constructed starting from first principles has, in our opinion, still to be solved.

We have then taken the simplest point of view, which is to try to construct a potential which can reproduce the simplest kind of scattering, the elastic one, with the simplest projectile that can still be considered an "ion", although not really "heavy", the α-particle.

The existence of much experimental data that we can attempt to understand with the help of our microscopic potential constitutes one more reason to start with the simple alpha-particle.

II-2 Feynman's propagator[13,14]

If we prepare a one-dimensional quantum mechanical system in a state $|q,t>$, which is an eigenstate of the coordinate Q_H at time t, with eigenvalue q, namely:

$$Q_H \, |q,t\rangle_H = q \, |q,t\rangle_H \tag{II-1}$$

where

$$Q_H(t) = e^{iHt} \, Q_S \, e^{-iHt}$$

$$|q\rangle = e^{-iHt} \, |q,t\rangle_H \tag{II-2}$$

and H is the hamiltonian of the system, Q_S is the operator in the Schrödinger picture and Q_H is the same in the Heisenberg picture, then the probability of finding it in a state $\langle q'|$ at time t' is:

$$F(q',t';q,t) = {}_H\langle q',t'|q,t\rangle_H = \langle q'| e^{-iH(t'-t)} |q\rangle \tag{II-3}$$

Let us now divide the time interval $[t,t']$ in $\underline{n}$ equal segments of length:

$$\varepsilon = \frac{t'-t}{n} \tag{II-4}$$

and define

$$t_\ell = \ell\varepsilon + t$$
$$t' = n\varepsilon + t \tag{II-4'}$$

Introducing (n - 1) resolutions of the identity in Eq.(II-3), we have

$$F(q',t';q,t) = \int dq_1(t_1) \int dq_2(t_2) \int \cdots \int dq_{n-1}(t_{n-1}) \langle q',t'|q_{n-1},t_{n-1}\rangle \cdot \tag{II-5}$$
$$\times \langle q_{n-1},t_{n-1}|q_{n-2},t_{n-2}\rangle \cdots \langle q_1,t_1|q,t\rangle$$

where we dropped the subscript H but we are still considering the state $|q,t>$ in the Heisenberg picture.

For sufficiently large $\underline{n}$ the time interval $t_\ell - t_{\ell-1}$ can be made as small as we like, and we can write:

$$\begin{aligned} \langle q', \varepsilon | q, 0 \rangle &= \langle q' | e^{-i\varepsilon H} | q \rangle \\ &= \delta(q-q') - i\varepsilon \langle q' | H | q \rangle + O(\varepsilon^2) \end{aligned} \tag{II-6}$$

where we expanded the exponential, as ε is very small:

$$e^{-i\varepsilon H} = 1 - i\varepsilon H + O(\varepsilon^2)$$

If we assume that we are dealing with scattering by a potential, our hamiltonian should be of the form:

$$H = \frac{1}{2} P^2 + V(Q) \tag{II-6'}$$

with P and Q operators.

Then the second term of the R.H.S. of Eq.(II-6) can be written (by Fourier transform):

$$\begin{aligned} \langle q' | H(P,Q) | q \rangle &= \frac{1}{2} \langle q' | -\nabla^2 | q \rangle + \langle q' | V(Q) | q \rangle \\ &= \frac{1}{2} \int \frac{dp}{2\pi} e^{ipq'} (-\nabla^2) e^{-ipq} + \langle q' | q \rangle V(q) \\ &= \int \frac{dp}{2\pi} e^{ip(q'-q)} \left\{ \frac{1}{2} p^2 + V(q) \right\} \\ &= \int \frac{dp}{2\pi} e^{ip(q'-q)} H\left(p, \frac{q+q'}{2}\right) \end{aligned} \tag{II-7}$$

where we used the fact that the operator V(Q) is diagonal in the coordinate representation and therefore

$$\langle q' | V(Q) | q \rangle = \delta(q'-q)\, V(q)$$
$$= \delta(q'-q)\, V\left(\frac{q+q'}{2}\right) \quad ;$$

$H(p, \frac{q + p'}{2})$ is now the classical hamiltonian.

Substituting Eq.(II-7) in (II-6) we find:

$$\langle q_\ell, t_\ell | q_{\ell-1}, t_{\ell-1} \rangle = \int \frac{dp}{2\pi}\, e^{ip(q_\ell - q_{\ell-1})} - i\varepsilon \int \frac{dp}{2\pi}\, e^{ip(q_\ell - q_{\ell-1})} \times H\left(p, \tfrac{1}{2}(q+q')\right) \qquad \text{(II-8)}$$
$$= \int \frac{dp}{2\pi}\, e^{ip(q_\ell - q_{\ell-1})} \left\{ 1 - i\varepsilon H \right\}$$

Up to the first order in ε we can make the following approximation in Eq.(II-8):

$$e^{-i\varepsilon H} = 1 - i\varepsilon H$$

Inserting the result of Eq.(II-8) into Eq.(II-5) we find:

$$F(q', t'; q, t) = \lim_{n\to\infty} \int \prod_1^{n-1} dq_i \prod_1^{n} \frac{dp_i}{2\pi} \times \qquad \text{(II-9)}$$
$$\times \exp\left\{ i \sum_1^n \left[p_j (q_j - q_{j-1}) - H\left(p_j, \tfrac{1}{2}(q_j + q_{j-1})\right)(t_j - t_{j-1}) \right] \right\} .$$

Note in Eq.(II-9) that there are n integrations over p and only n-1 integrations over q. This is because there are no end point restrictions on the p integration.

Introducing the notation

$$\int \left[\frac{dq\,dp}{2\pi\hbar}\right] = \int \prod_{1}^{n-1}{}_i \prod_{1}^{n}{}_j \frac{dq_i\,dp_j}{(2\pi\hbar)^n}$$

we can write Eq.(II-9) as follows:

$$F(q',t';q,t) = \int\left[\frac{dq\,dp}{2\pi\hbar}\right] \exp\left\{\frac{i}{\hbar}\int_t^{t'}\left[p\dot{q} - H(p,q)\right] d\tau\right\} \qquad \text{(II-10)}$$

Where we have restored $\hbar = 1$ to indicate that the functional integration is over all phase space volume $\int \frac{\Delta q\,\Delta p}{\hbar}$ for all times between t and t'.

If the hamiltonian is of the form (II-6'), the p-integration on the R.H.S. of Eq.(II-9) can be performed using[15]:

$$\int_{-\infty}^{\infty}\frac{dp}{2\pi} e^{i\varepsilon\left(p\dot{q} - \frac{1}{2}p^2\right)} = (2\pi i\varepsilon)^{-\frac{1}{2}} \exp\left(\frac{i}{2}\varepsilon\dot{q}^2\right)$$

and we obtain:

$$F(q',t';q,t) = \int \mathfrak{D}q \exp\left\{i\int_t^{t'} \mathcal{L}(q,\dot{q})\,d\tau\right\} \qquad \text{(II-11)}$$

where

$$\mathfrak{D}q = \prod_{1}^{n-1}{}_i \frac{dq_i}{(2\pi i\varepsilon)^{1/2}}$$

and $\mathfrak{D}q$ in Feynman's formalism indicates the sum over all paths between q(t) and q'(t')

We wish to remark at this point that the derivation of the Feynman's propagator presented in this chapter has the nice feature of giving the explicit expression for the normalization factor $\frac{1}{(2\pi i\varepsilon)^{1/2}}$; this allows us to perform the limit in Eq.(II-9) and therefore define the measure in the space of paths.

In Eq.(I-11) $\mathcal{L}$ is the lagrangian

$$\mathcal{L} = \frac{1}{2}\dot{q}^2 - V(q) \tag{II-12}$$

and the time development of the system described by $\mathcal{L}$, between t and t' is generated by the action:

$$S = \int_t^{t'} \mathcal{L}(q, \dot{q})\, d\tau \tag{II-12'}$$

and $q_o = q(t)$

$q_n = q'(t')$

Introducing explicitly the mass $\underline{m}$ of the particle scattered by a potential $V(\underline{r}(t))$ we can generalise the above result to scattering in three dimensions

$$F(\vec{r}', t'; \vec{r}, t) = \int_{\vec{r}(t)}^{\vec{r}(t')} \mathcal{D}\vec{r}(\tau)\, e^{\frac{i}{\hbar} S[\vec{r}(\tau)]} \tag{II-13}$$

$$= \int_{\vec{r}(t)}^{\vec{r}(t')} \mathcal{D}\vec{r}(\tau)\, e^{\frac{i}{\hbar} S_0}\, e^{-\frac{i}{\hbar} V}$$

where

$$\mathcal{S}[\underline{r}(\tau)] = \int_t^{t'} d\tau \left\{ \frac{1}{2} m (\dot{\underline{r}}(\tau))^2 - V(\underline{r}(\tau)) \right\} \qquad \text{(II-13')}$$

$$= \int_t^{t'} d\tau \left[\frac{1}{2} m (\dot{\underline{r}}(\tau))^2 \right] - \int_t^{t'} d\tau \, V(\underline{r}(\tau))$$

$$= \quad S_0 \quad - \quad V$$

$$S_0 = \int_t^{t'} d\tau \left[\frac{1}{2} m (\dot{\underline{r}}(\tau))^2 \right]$$

$$V = \int_t^{t'} d\tau \; V(\underline{r}(\tau))$$

and $\mathcal{D}\underline{r}(\tau)$ indicates the sum over all paths between $\underline{r}(t)$ and $\underline{r}'(t')$.

II-3 The Reduced Propagator[16]

In this section we shall consider in more detail the collision between two nuclei in the reference frame in which the centre-of-mass of the target and projectile is at rest at the origin.

The total hamiltonian is:

$$H_{Tot} = T(\underline{r}(t)) + h_1(x_1) + h_2(x_2) + V_{12}(\underline{r}(t), x) \qquad \text{(II-14)}$$

where $T = \frac{1}{2}\mu\dot{r}^2$ is the kinetic energy of relative motion, $\underline{r}(t)$ is the path of relative motion and in this case corresponds to the projectile trajectory, μ is the reduced mass, h_1 and h_2 and x_1 and x_2 are respectively the internal hamiltonians and set of space, spin and isospin coordinates for the two nuclei, x stands for both x_1 and x_2 setting:

$$H(\underline{r}(t), x) = h_1(x_1) + h_2(x_2) + V_{12}(\underline{r}(t), x) \qquad \text{(II-15)}$$

we can define the internal hamiltonian as:

$$h(x) = \lim_{r \to \infty} H(\underline{r}(t), x) \tag{II-16}$$

Let us now restrict ourselves to collisions such that the initial and final state of the system of the two nuclei are eigenstates of h(x), i.e.

$$\begin{aligned} h(x)\,\varphi_\alpha(x) &= \varepsilon_\alpha\,\varphi_\alpha(x) \\ h(x)\,\varphi_\beta(x) &= \varepsilon_\beta\,\varphi_\beta(x) \end{aligned} \tag{II-17}$$

The probability of transition from the state $|\underline{r}', \alpha\rangle$ to the state $\langle \underline{r}'', \beta|$, eigenstates of $H_{TOT}(\underline{r}(t), x)$, is:

$$\begin{aligned} F_{\beta\alpha}(\underline{r}'', t''; \underline{r}', t') &= \langle \underline{r}'', \beta | e^{-i H_{TOT}(t''-t')} | \underline{r}', \alpha \rangle \\ &= \iint dx''\,dx'\,\varphi_\beta^*(x'')\,F(\underline{r}'', x'', t''; \underline{r}', x', t')\,\varphi_\alpha(x') \end{aligned} \tag{II-18}$$

and

$$F(\underline{r}'', x'', t''; \underline{r}', x', t') = \langle \underline{r}'', x'' | e^{-i H_{TOT}(t''-t')} | \underline{r}', x' \rangle \tag{II-19}$$

Feynman's expression for the propagator eq. (II-18) can be obtained applying the method already described in section (II-1). In the present case the equivalent of eq. (II-11) is:

$$F_{\beta\alpha}(\underline{r}'', t''; \underline{r}', t') = \lim_{n\to\infty} \iint dx' dx'' \, \varphi_\beta^*(x'') \left\{ \int \prod_1^{n-1} \frac{d^3\underline{r}_i}{(2\pi i\varepsilon)^{3/2}} \right.$$

$$\left. \times \exp\left[i \sum_1^n \varepsilon \left[\frac{1}{2} \left(\frac{r_{j-1} - r_j}{\varepsilon} \right)^2 - H\left(\frac{r_{j+1} + r_j}{2}, x \right) \right] \right] \right\} \varphi_\alpha(x') \qquad \text{(II-19')}$$

$$= \lim_{n\to\infty} \int \prod_1^{n-1} \frac{d^3\underline{r}_i}{(2\pi i\varepsilon)^{3/2}} \exp\left[i \sum_1^n \varepsilon \left[\frac{1}{2} \left(\frac{r_{j-1} - r_j}{\varepsilon} \right)^2 \right] \right. \times$$

$$\times \lim_{\varepsilon\to 0} \langle \beta | \exp\left[-i \sum_1^n H_{t_j} \varepsilon \right] | \alpha \rangle$$

where

$$H_{t_j} \equiv H\left[\underline{r}(t'' - j\varepsilon), x \right] \qquad \text{(II-20)}$$

but the second term of eq. (II-19') is nothing but the transition amplitude for the target to go from state α to β, when the projectile passes on the path $\underline{r}(t)$, as

$$U(\underline{r}(t), t'', t') = \lim_{\varepsilon\to 0} \exp\left[-i \sum_1^n H_{t_j} \varepsilon \right] \qquad \text{(II-21)}$$

is the time evolution operator of the system. So we finally have

$$F_{\beta\alpha}(r'', t''; r', t') = \int_{\underline{r}'(t')}^{\underline{r}''(t'')} \mathcal{D}(\underline{r}(t)) \, e^{i S_0[\underline{r}(t)]/\hbar} \quad T_{\beta\alpha}[\underline{r}(t)] \quad , \qquad \text{(II-22)}$$

$$T_{\beta\alpha}[\underline{r}(t)] = \langle \beta | U | \alpha \rangle \, . \qquad \text{(II-23)}$$

U satisfy the Schrödinger equation

$$i\hbar \frac{\partial U}{\partial t} = H(\underline{r}(t), x) U \qquad \text{(II-24)}$$

In the case in which α and β are both the ground state of the system, comparing Eqs. (II-13) and (II-22), suggests for the optical potential an equation

$$\int_{t'}^{t''} V_{opt}(\underline{r}(t))\,dt = i\hbar \ln \langle 0|U(\underline{r}(t), t'', t')|0\rangle \qquad \text{(II-25)}$$

where

$$V_{opt}(\underline{r}(t)) = Re\, V_{opt}(\underline{r}(t)) + i\, Im\, V_{opt}(\underline{r}(t)) \qquad \text{(II-25')}$$

Eq. (II-25) has in principle to be satisfied for all path $\underline{r}(t)$ between t' and t" in order to give the same path integrals and therefore the same elastic scattering propagators in Eqs. (II-13) and (II-22).

But the functional dependence on the path $\underline{r}(t)$ of the R.H.S. of Eq. (II-25) is rather more complicated than the functional dependence of the optical potential which appears in the L.H.S. of Eq. (II-25). Therefore we do not expect to be able to satisfy Eq. (II-25) for all paths, also because we are using here an optical potential which is local, while the optical potential of Feshbach's theory is non-local and energy-dependent (cf. Chapter I, section 1).

However, not all paths in the path integrals Eqs. (II-13), (II-22) are equally important. We will try, therefore, to select the class of important paths which give the main contribution to the path integrals, and then to satisfy Eq. (II-25) for this class of paths.

The way to obtain such a class of important paths will be discussed later in this work (Chapters II, VIII and IX).

The probability that no transition occurs during the scattering can be obtained from equation (II-25) in the following way:

$$-\frac{i}{\hbar}\int_{t'}^{t''} V_{opt}(\underline{r}(t))\,dt = \ln \langle o|U(\underline{r}(t), t'', t')|o\rangle$$

$$\exp\left\{-\frac{i}{\hbar}\int_{t'}^{t''} \mathrm{Re}\, V_{opt}(\underline{r}(t))\,dt + \frac{1}{\hbar}\int_{t'}^{t''} \mathrm{Im}\, V_{opt}(\underline{r}(t))\,dt\right\} = \langle o|U|o\rangle \qquad \text{(II-25")}$$

$$\exp\left\{\frac{2}{\hbar}\int_{t'}^{t''} \mathrm{Im}\, V_{opt}(\underline{r}(t))\,dt\right\} = |\langle o|U|o\rangle|^2 .$$

Note that we expect Im V_{opt} to be negative. This is consistent with Eq. (II-25) because $|\langle o|U|o\rangle|^2 \leq 1$.

Equation (II-25") is not unexpected in view of a result obtained by Koeling and Malfliet[17], who calculated the S-matrix for elastic scattering in a semiclassical approximation. In the case in which the lagrangian contains a complex potential whose imaginary part is a smooth functional of the path, they obtain

$$S = \exp\left\{\frac{i}{\hbar}\int_{t'}^{t''}\left[\frac{1}{2}m\left(\dot{\underline{r}}(t)\right)^2 - V(\underline{r}(t))\right]dt + \frac{1}{\hbar}\int_{t'}^{t''} W(\underline{r}(t))\,dt\right\}, \qquad \text{(II-26)}$$

where $W(r) = \mathrm{Im}\, V_{opt}(r)$ and $\underline{r}(t)$ is the path that satisfies the minimum condition:

$$\delta\int_{t'}^{t''} \mathrm{Re}\left[\mathcal{L}\left(\underline{r}(t), \dot{\underline{r}}(t)\right)\right]dt = 0. \qquad \text{(II-27)}$$

In this case the reaction cross section is:

$$\sigma_R = \frac{\pi}{k^2}\left(1 - |S|^2\right) = \frac{\pi}{k^2}\left[1 - \exp\left(\frac{2}{\hbar}\int_{t'}^{t''} W(\underline{r}(t))\,dt\right)\right] \qquad \text{(II-28)}$$

for each partial wave

The term $\exp\left(\frac{2}{\hbar}\int_{t'}^{t''} W(\underline{r}(t))\,dt\right)$ represents the probability of a ground state to ground state transition; therefore we conclude:

$$P_{0\to 0} = |\langle 0|\, U(\underline{r}(t), t'', t')\, |0\rangle|^2 \qquad \text{(II-29)}$$

$$= \exp\left(\frac{2}{\hbar}\int_{t'}^{t''} W^{-}(\underline{r}(t))\, dt\right) .$$

This equation is identical to (II-25").

Chapter III

IMAGINARY PART OF THE OPTICAL POTENTIAL CALCULATED BY PERTURBATION THEORY

III-1 Transition Amplitude in Perturbation Theory

In the case of scattering of strongly absorbed particles, the elastic scattering and then the optical potential, give information only on the surface region of the target or alternately, on the tail of the potential. In this region the nuclear potential should be weak enough to allow for calculation of Eq. (II-25) by perturbation theory.

The perturbation theory expansion of the evolution operator U between t' and t" is in general given by[18]

$$U(t'',t') = U^{(0)}(t'',t') + \sum_{1}^{\infty} {}_{n} U^{(n)}(t'',t') \qquad \text{(III-1)}$$

where $U^{(0)}$ is the evolution operator for the unperturbed hamiltonian

$$U^{(0)}(t'',t') = \exp\left[-i H^{(0)}(t''-t')/\hbar\right] \qquad \text{(III-1')}$$

and the n.th term is given by

$$U^{(n)}(t'',t') = \frac{1}{(i\hbar)^n} \int_{t''>t_n>t_{n-1}>\dots>t_1>t'} dt_n\, dt_{n-1} \dots dt_1\, U^{(0)}(t'',t_n)\, V(t_n) \times \qquad \text{(III-1")}$$

$$\times U^{(0)}(t_n,t_{n-1})\, V(t_{n-1}) \dots U^{(0)}(t_2,t_1)\, V(t_1)\, U^{(0)}(t_1,t')$$

Therefore the transition amplitude from the ground state to the ground state, to second order, is

$$\langle 0|U|0\rangle = \langle 0|U^{(0)}|0\rangle + \sum_1^\infty{}_n \langle 0|U^{(n)}|0\rangle$$

$$= 1 + \frac{1}{i\hbar}\int_{-\infty}^{\infty} dt\, \langle 0|V|0\rangle + \tag{III-2}$$

$$+ \frac{1}{(i\hbar)^2}\sum_n \int_{-\infty}^{\infty} dt \int_{-\infty}^{t} dt' \langle 0|V(t)|n\rangle\langle n|V(t')|0\rangle e^{\frac{i}{\hbar}(\varepsilon_0-\varepsilon_n)(t-t')} .$$

Taking the logarithm of both sides of Eq. (III-2) multiplying by $i\hbar$ and substituting into Eq. (II-25) we obtain:

$$\int_{-\infty}^{\infty} V_{opt}(\underline{r}(t))\,dt = \int_{-\infty}^{\infty} \langle 0|V[\underline{r}(t),x]|0\rangle\, dt - \tag{III-3}$$

$$- \frac{i}{\hbar}\sum_{n\neq 0} \int_{-\infty}^{\infty} dt \int_{-\infty}^{t} dt' \langle 0|V[\underline{r}(t),x]|n\rangle\langle n|V[\underline{r}(t'),x]|0\rangle \times$$

$$\times\, e^{\frac{i}{\hbar}(\varepsilon_0-\varepsilon_n)(t-t')} .$$

The imaginary part of this equation is shown to be equivalent to (see Appendix III-1)

$$\int_{-\infty}^{\infty} \mathrm{Im}\, V_{opt}(\underline{r}(t))\,dt = -\frac{1}{2\hbar}\sum_{n\neq 0}\left|\int_{-\infty}^{\infty} dt\, \langle n|V(\underline{r}(t),x)|0\rangle\, e^{\frac{i}{\hbar}(\varepsilon_n-\varepsilon_0)t}\right|^2 . \tag{III-4}$$

From what was shown at the end of Chapter II, the L.H.S. of Eq. (III-4) can be interpreted as the total absorption for the projectile trajectory $\underline{r}(t)$.

On the other hand, the factor under the summation symbol in Eq.(III-4) is the quantum mechanical first order probability for the transition from the ground state $|0\rangle$ to an excited state $|n\rangle$. Eq. (III-4) therefore states that the total absorption is given by the sum of the probabilities of transition from the ground state to all possible excited states.

III-2 The Model for α-scattering

From now on we shall concentrate on the scattering of α-particles on closed-shell nuclei. The possibility of an extension to non-closed-shell targets will be briefly outlined in the final discussion.

The semiclassical formalism developed in the previous chapter can be applied to α-particles.

The condition $aK \gtrsim 1$ [10] is satisfied in this case, where $K = \frac{1}{\lambda\!\!\!^{-}}$ is the inverse of the wave length for relative motion and a is the potential diffuseness, i.e.

$$K = \lambda\!\!\!^{-1} = \sqrt{\frac{A_1 A_2}{A_1+A_2}\,\frac{\hbar^2}{2m(E-V_B)}} \quad \text{fm}^{-1}$$

$$\simeq \sqrt{\frac{A_1 A_2}{A_1+A_2}\,\frac{20}{(E-V_B)}} \quad \text{fm}^{-1} \quad ,$$

and

$$a \simeq 0.65 \text{ fm}.$$

For $(E - V_B) \simeq 50$ MeV, we find indeed:

$$\alpha + {}^{16}O \quad : \quad K = 2.86 \text{ fm}^{-1} \quad , \quad aK \simeq 1.8 \quad ,$$

$$\alpha + {}^{40}Ca \quad : \quad K = 3.03 \text{ fm}^{-1} \quad , \quad aK \simeq 1.9 \quad .$$

Eq.(II-3) and Eq.(III-4) have been obtained without any specification of the states $|0>$ and $|n>$, and of the potential $(V(\underline{r}(t), x)$. In our calculations we choose to describe the α as a point-particle.

At high energy this should be a reasonable approximation; furthermore, inside the nuclear potential of the target, the α is accelerated and so the probability of break-up should be small. These assumptions imply that we can neglect antisymmetrization effects in the internal wave function of the α and in the α-nucleus wave-function.

The target is described as a system of independent particles inside a three-dimensional isotropic harmonic oscillator potential. The characteristic parameter of the oscillator is chosen so as to reproduce the radius of the nucleus under consideration[19]. A description of the H.O. (harmonic oscillator) shell model is contained in Appendix III, part 3.

$|0\rangle$ and $|n\rangle$ are then Slater determinants and so the internal antisymmetrization of the target is automatically taken into account.

Furthermore we assume that the α-nucleus interaction can be approximated by the sum of α-nucleon interactions. This point is discussed in detail in Chapter IV.

The hamiltonian $H(\underline{r}_\alpha(t),\underline{r})$ of Eq.(II-14) is then given by:

$$\begin{aligned} H(\underline{r}_\alpha(t),\underline{r}) &= \sum_1^A i \left(\frac{p_i^2}{2m} + \frac{1}{2} m\omega^2 \underline{r}_i^2 \right) + \sum_1^A i\, V(\underline{r}_i - \underline{r}_\alpha(t)) \\ &= \sum_1^A i \left\{ h_{oi}(\underline{r}_i) + V(\underline{r}_i - \underline{r}_\alpha(t)) \right\} \\ &= \sum_1^A i \; h_i(\underline{r}_\alpha(t), \underline{r}_i) \end{aligned} \qquad \text{(III-5)}$$

where A is the target mass number,

$\underline{r}_\alpha(t)$ is the α-particle position relative to the centre of the H.O. potential, m is the nucleon mass, $\underline{r}_i$ is the internal coordinate of the i^{th} nucleon in the target, while $\underline{r}$ stands for the set of all the $\underline{r}_i$, $h_{oi}(\underline{r}_i)$ and $h_i(\underline{r}_\alpha(t),\underline{r})$ are single-particle hamiltonians. They satisfy the Schrödinger equations

$$h_{oi}(\underline{r}_i)\,\chi_i(\underline{r}_i) = \varepsilon_i\,\chi_i(\underline{r}_i) \tag{III-6}$$

$$h_i(\underline{r}_\alpha(t),\underline{r})\,\varphi_i(\underline{r}_\alpha(t),\underline{r}) = E_i\,\varphi_i(\underline{r}_\alpha(t),\underline{r}) \tag{III-6'}$$

The functions $\phi_i(\underline{r}_\alpha(t),\underline{r})$ can be expressed as a linear combination of $\chi_i(\underline{r}_i)$'s which form a complete orthonormal set,

$$\varphi_i(\underline{r}_\alpha(t),\underline{r}) = \sum_1^N{}_j\, a_{ij}(t)\,\chi_j(\underline{r}_j)\,e^{-\frac{i}{\hbar}\varepsilon_j t} \tag{III-7}$$

$N \geqslant A$.

We now insert Eq.(III-7) in (III-6'), multiply both sides by $\chi^*_K(\underline{r}_K)$, and integrate in $d^3\underline{r}$ to obtain:

$$\dot{a}_{iK}(t) = -\frac{i}{\hbar}\sum_1^N{}_j\, a_{ij}(t)\,V_{Kj}(\underline{r}_\alpha(t))\,e^{i\omega_{Kj}t} \tag{III-8}$$

where

$$\omega_{Kj} = \frac{\varepsilon_K - \varepsilon_j}{\hbar} \tag{III-9}$$

and

$$V_{Kj}(\underline{r}_\alpha(t)) = \langle \chi_K | V(\underline{r} - \underline{r}_\alpha(t)) | \chi_j \rangle = \int d^3\underline{r}\,\chi^*_K(\underline{r})\,V(\underline{r} - \underline{r}_\alpha(t))\,\chi_j(\underline{r}) \tag{III-10}$$

Eq.(III-8) can be solved by perturbation theory. We take the boundary conditions

$$\varphi_i \underset{t\to-\infty}{\longrightarrow} \chi_i \qquad i = 1, 2, \ldots, A. \tag{III-11}$$

as we want our system to be in a state with definite energy before any perturbation is applied.

This implies that to the second order of perturbation the coefficients a_{iK}, which are solutions of Eq.(III-8), are given by:

$$a_{i\kappa}(t) = \delta_{i\kappa} + a^{(1)}_{i\kappa}(t) + a^{(2)}_{i\kappa}(t) \quad , \tag{III-12}$$

where

$$a^{(1)}_{i\kappa}(t) = (i\hbar)^{-1} \int_{-\infty}^{t} V_{\kappa i}(t') e^{i\omega_{\kappa i} t'} \, dt' \tag{III-13}$$

$$a^{(2)}_{i\kappa}(t) = (i\hbar)^{-2} \sum_{n} \int_{-\infty}^{t} dt' \int_{-\infty}^{t'} dt'' \, e^{i\omega_{\kappa n} t'} V_{\kappa n}(t') e^{i\omega_{ni} t''} V_{ni}(t'') \tag{III-13'}$$

From the orthonormalization condition for the ϕ_i,

$$\langle \varphi_\kappa | \varphi_{\kappa'} \rangle = \delta_{\kappa\kappa'} \tag{III-14}$$

it follows:

$$\langle \sum_i^N a^*_{i\kappa}(t) \chi^*_i \, e^{i\varepsilon_i t/\hbar} | \sum_j^N a_{j\kappa'}(t'') \chi_j \, e^{-i\varepsilon_j t/\hbar} \rangle = \tag{III-14'}$$

$$= \sum_i^N a^*_{i\kappa}(t) a_{i\kappa'}(t')$$

$$= \delta_{\kappa\kappa'} \quad .$$

This gives some restrictions on $a^{(1)}_{iK}$ and $a^{(2)}_{iK}$.

From the first order terms in Eq.(III-14') we obtain:

$$a^{(1)}_{KK'} + a^{(1)*}_{K'K} = 0 \quad , \qquad \text{(III-15)}$$

$$A^{(1)} = -A^{(1)\dagger}$$

where $(A^{(1)})_{KK'} \equiv a^{(1)}_{K\,K'}$.

The second order terms in Eq.(III-14') give :

$$\sum_i^N a^{(1)}_{Ki}\, a^{(1)}_{iK'} = a^{(2)}_{KK'} + a^{(2)*}_{K'K} \qquad \text{(III-15')}$$

$$\left[A^{(1)}\right]^2 = A^{(2)} + A^{(2)\dagger}$$

and $(A^{(2)})_{KK'} \equiv a^{(2)}_{KK'}$

Eq.(III-12) can be written as,

$$A = 1 + \bar{A} = 1 + A^{(1)} + A^{(2)} \quad .$$

We now come back to the evaluation of the factor <O|U|O> in Eq.(II-25), which in the model we have just been describing, becomes:

$$\begin{aligned} \langle O|U|O\rangle &= \langle \bar{\Phi}\,|\,\bar{\Phi}'\rangle \\ &= \det \langle \chi_i \,|\, \varphi_K \rangle \\ &= \det \{a_{iK}\} \\ &= \det (1+\bar{A}) \end{aligned} \qquad \text{(III-16)}$$

where $\bar{\Phi}, \bar{\Phi}'$ are Slater determinants.

Eq.(III-16) is obtained applying Thouless theorem[20]. Taking the logarithm of both sides in Eq.(III-16) we find:

$$
\begin{aligned}
\ln \langle 0|U|0\rangle &= \ln \det (1+\bar{A}) \\
&= \mathrm{Tr} \ln (1+\bar{A}) \\
&= \mathrm{Tr}\left(A^{(1)} + A^{(2)} - \frac{1}{2}\left(A^{(1)}\right)^2 + \dots \right) \\
&= \mathrm{Tr}\, A^{(1)} + \mathrm{Tr}\left(A^{(2)} - \frac{1}{2}\left(A^{(1)}\right)^2 \right) \\
&= \sum_{\kappa}^{A} a^{(1)}_{\kappa\kappa} + \sum_{\kappa}^{A}\left(a^{(2)}_{\kappa\kappa} - \frac{1}{2}\sum_{n}^{A} a^{(1)}_{\kappa n} a^{(1)}_{n\kappa} \right) \\
&= (i\hbar)^{-1} \sum_{n<} \int_{-\infty}^{t} \langle n|V|n\rangle\, dt' + \\
&\quad + (i\hbar)^{-2} \sum_{\substack{n< \\ \kappa>}} \int_{-\infty}^{t} dt' \int_{-\infty}^{t'} dt'' \langle n|V|\kappa\rangle\langle \kappa|V|n\rangle\, e^{i\omega_{\kappa n}(t'-t'')} ,
\end{aligned}
\qquad \text{(III-17)}
$$

where $n<$ labels the A occupied states of the set $\{\chi(r)\}$, and $K>$ labels all the unoccupied ones. The term $\mathrm{Tr}\left[A^{(2)} - \frac{1}{2}(A^{(1)})^2\right]$ is calculated in Appendix II, part 2. Eqs. (III-3) and (III-4), within the shell model description of the target become then:

$$
\begin{aligned}
\int_{-\infty}^{\infty} V_{opt}(\underline{r}_\alpha | t))\, dt &= \sum_{n<} \int_{-\infty}^{\infty} \langle n|V[\underline{r}-\underline{r}_\alpha(t)]|n\rangle\, dt \; - \\
&\quad - \frac{i}{\hbar} \sum_{\substack{n< \\ \kappa>}} \int_{-\infty}^{\infty} dt \int_{-\infty}^{t} dt' \langle n|V[\underline{r}-\underline{r}_\alpha(t)]|\kappa\rangle \cdot \\
&\quad \times \langle \kappa|V[\underline{r}-\underline{r}_\alpha(t')]|n\rangle\, e^{\frac{i}{\hbar}(\varepsilon_n-\varepsilon_\kappa)(t-t')} .
\end{aligned}
\qquad \text{(III-18)}
$$

$$
\int_{-\infty}^{\infty} \mathrm{Im}\, V_{opt}(\underline{r}(t))\, dt = -\frac{1}{2\hbar} \sum_{\substack{n< \\ \kappa>}} \left| \int_{-\infty}^{\infty} dt\, \langle n|V[\underline{r}-\underline{r}_\alpha(t)]|\kappa\rangle \cdot e^{\frac{i}{\hbar}(\varepsilon_\kappa-\varepsilon_n)t} \right|^2 . \qquad \text{(III-19)}
$$

Equations (III-18) and (III-19) are essentially the same as (III-3) and (III-4) but the approximations made are different.

Equations (III-3,4) are obtained by a perturbation expansion of $\langle 0|U|0\rangle$ up to second order. Equations (III-18,19) are obtained from a perturbation expansion of the single particle amplitudes a_{ij} up to second order but the expression for $\langle 0|U|0\rangle$ includes some higher order effects such as multiparticle excitations.

For the method of section III-1 to be valid it is necessary that change in $\langle 0|U|0\rangle$ should be small. While the method of the present section requires only that the changes in the single-particle amplitudes a_{ij} should be small.

From Eq.(III-1?) it follows that the transition amplitude is given by

$$\langle 0|U|0\rangle = \det e^{\left[A^{(1)} + A^{(2)} - \frac{1}{2}(A^{(1)})^2\right]} \qquad \text{(III-20)}$$

But from Eqs.(III-13,13') it can be seen that

$$A^{(1)} = \{a_{ik}^{(1)}\} \propto V_0$$

$$A^{(2)} = \{a_{ik}^{(2)}\} \propto V_0^2$$

where V_0 is the strength of the effective interaction.

Now, substituting the exponential in Eq.(III-20) with its series expansion in powers of V_0, we get

$$\langle 0|U|0\rangle = \det\left\{1 + V_0\,\tilde{A}^{(1)} + V_0^2\,\tilde{A}^{(2)} - \frac{1}{2}V_0^2\,\tilde{A}^{(1)2} + \right.$$
$$\left. + \frac{1}{2}\left[V_0^2\,\tilde{A}^{(1)2} + V_0^4\,\tilde{A}^{(2)} + \frac{1}{4}V_0^4\,\tilde{A}^{(1)4} + \ldots\right] + \ldots\right\} \qquad \text{(III-20')}$$

where

$$\tilde{A}^{(1)} \equiv A^{(1)} / V_o$$

$$\tilde{A}^{(2)} \equiv A^{(2)} / V_o^2$$

The above equation for $\langle 0|U|0\rangle$ shows that the transition amplitude thus calculated contains contributions from any power of V_o. The transition amplitude Eq.(III-2) to second order contains instead only contributions from terms proportional to V_o and V_o^2.

Within an independent particle model of the target we have then obtained a much more accurate expression for $\langle 0|U|0\rangle$.

The difference between Eq.(III-2) and (III-20) comes from a different application of perturbation theory. In the first case it was applied to the motion of the nucleus as a whole (by means of U), while in the second case it was applied to the single particle motion (by means of the coefficients a_{ij}).

Appendix III

Part 1

In Chapter III, section 1, we obtained the following expression

$$\int_{-\infty}^{\infty} V_{opt}(\underline{r}(t))\,dt = \int_{-\infty}^{\infty} \langle 0|V[\underline{r}(t),x]|0\rangle\,dt - \frac{i}{\hbar}\sum_{n\neq 0}\int_{-\infty}^{\infty} dt \int_{-\infty}^{t} dt' \langle 0|V[\underline{r}(t),x]|n\rangle\langle n|V[\underline{r}(t'),x]|0\rangle \cdot e^{\frac{i}{\hbar}(\varepsilon_0-\varepsilon_n)(t-t')} \tag{A-III-1}$$

The first order term is purely real; the second order term is complex, its imaginary part is given by

$$\int_{-\infty}^{\infty} I_m V_{opt}(\underline{r}(t))\,dt = -\frac{1}{\hbar} Re\left\{\sum_{n\neq 0}\int_{-\infty}^{\infty} dt \int_{-\infty}^{t} dt' \langle 0|V(\underline{r}(t),x)|n\rangle \langle n|V[\underline{r}(t'),x]|0\rangle e^{\frac{i}{\hbar}(\varepsilon_0-\varepsilon_n)(t-t')}\right\} \tag{A-III-2}$$

$$= -\frac{1}{\hbar}\int_{-\infty}^{\infty} dt \int_{-\infty}^{t} dt'\, Re\, f(t,t')$$

where

$$f(t,t') \equiv \sum_{n\neq 0} \langle 0|V[\underline{r}(t),x]|n\rangle\langle n|V[\underline{r}(t'),x]|0\rangle e^{\frac{i}{\hbar}(\varepsilon_0-\varepsilon_n)(t-t')} \tag{A-III-3}$$

The properties of f(t,t') are:

$$f^*(t,t') = f(t',t),$$

$$f(t,t') = u(t,t') + i v(t,t') \tag{A-III-4}$$

$$f^*(t,t') = u(t,t') - i v(t,t')$$

$$= u(t',t) + i v(t',t)$$

with

$$u(t,t') = u(t',t)$$

$$v(t,t') = -v(t',t)$$

The real part of f(t,t') is symmetric. It follows then

$$\int_{-\infty}^{\infty} dt \int_{-\infty}^{t} dt' \, Re\, f(t,t') = \frac{1}{2} \int_{-\infty}^{\infty} dt \int_{-\infty}^{\infty} dt' \, Re\, f(t,t') \qquad \text{(A-III-5)}$$

Inserting this in the R.H.S. of Eq.(A-III-2) we obtain

$$\int_{-\infty}^{\infty} Im\, V_{opt}(\underline{r}(t))\, dt = -\frac{1}{2\hbar} \sum_{n\neq 0} \int_{-\infty}^{\infty} dt \int_{-\infty}^{\infty} dt' \langle 0|V[\underline{r}(t,x)]|n\rangle \cdot$$

$$\times \langle n|V[\underline{r}(t'),x]|0\rangle e^{\frac{i}{\hbar}(\varepsilon_0-\varepsilon_n)(t-t')} \qquad \text{(A-III-6)}$$

$$= -\frac{1}{2\hbar} \sum_{n\neq 0} \left| \int_{-\infty}^{\infty} dt \, \langle n|V[\underline{r}(t),x]|0\rangle e^{\frac{i}{\hbar}(\varepsilon_n-\varepsilon_0)t} \right|^2$$

Part 2

Proof of Eq.(III-17)

$$Tr\left[A^{(2)} - \frac{1}{2}(A^{(1)})^2\right] = \sum_{\kappa}^{A} \left(a^{(2)}_{\kappa\kappa} - \frac{1}{2}\sum_{n}^{A} a^{(1)}_{\kappa n}\, a^{(1)}_{n\kappa}\right)$$

$$= (i\hbar)^{-2} \sum_{\kappa}^{A} \Bigg\{ \sum_{n}^{A} \int_{-\infty}^{t} dt' \int_{-\infty}^{t'} dt''\, V_{\kappa n}(t')\, V_{n\kappa}(t'')\, e^{i\omega_{\kappa n}(t'-t'')}$$

$$+ \sum_{A+1}^{N}{}_{n} \int_{-\infty}^{t} dt' \int_{-\infty}^{t'} dt''\, V_{\kappa n}(t')\, V_{n\kappa}(t'')\, e^{i\omega_{\kappa n}(t'-t'')} \qquad \text{(A-III-7)}$$

$$- \frac{1}{2} \sum_{n}^{A} \int_{-\infty}^{t} dt'\, V_{\kappa n} \int_{-\infty}^{t} dt''\, V_{n\kappa}(t'')\, e^{i\omega_{\kappa n}(t'-t'')}$$

$$= (i\hbar)^{-2} \sum_{1}^{A}{}_{\kappa} \sum_{A+1}^{N}{}_{n} \int_{-\infty}^{t} dt' \int_{-\infty}^{t'} dt''\, V_{\kappa n}(t')\, V_{n\kappa}(t'')\, e^{i\omega_{\kappa n}(t'-t'')}$$

where we used Eqs.(III-13) and (III-13') and

$$V_{rn}(t) = V_{nr}(t)^* = V_{nr}(t) \tag{A-III-8}$$

$$\frac{1}{\ell}\sum_{\substack{n\\ \kappa}}^{H}\left|\int_{-\infty}^{t} dt'\, V_{rn}(t')\, e^{i\omega_{rn}t'}\right|^2 = \frac{1}{\ell}\sum_{\substack{n\\ \kappa}}^{A}\left\{\int_{-\infty}^{t}dt'\int_{-\infty}^{t}dt''\, V_{rn}(t')V_{nr}(t'')\cdot\right.$$

$$\left.\times e^{i\omega_{rn}(t'-t'')}\right|_{t'<t''} +$$

$$\left.+\int_{-\infty}^{t}dt'\int_{-\infty}^{t}dt''\, V_{rn}(t')V_{nr}(t'')\; e^{i\omega_{rn}(t'-t'')}\right|_{t'>t''} \tag{A-III-9}$$

$$= \sum_{\substack{n\\ \kappa}}^{A}\int_{-\infty}^{t}dt'\int_{-\infty}^{t'}dt''\, V_{rn}(t')V_{nr}(t'')\, e^{i\omega_{rn}(t'-t'')}.$$

Part 3

The one-dimension harmonic oscillator wave functions are:

$$\varphi_n(\beta x) = \left(\frac{\beta}{\pi^{\frac{1}{2}}\, 2^n\, n!}\right) e^{-\frac{1}{2}\beta^2x^2}\, H_n(\beta x) \tag{A-III-10}$$

where $H_n(\beta x)$ are the Hermite polynomials given by

$$H_0(\beta x) = 1,$$

$$H_1(\beta x) = 2\beta x,$$

$$\vdots$$

$$H_{n+1}(\beta x) = 2\beta x\, H_n(\beta x) - 2n\, H_{n-1}(\beta x).$$

β is a parameter whose dimension is the inverse of a length; its definition is:

$$\beta = \sqrt{\frac{m\,\omega}{\hbar}} \qquad \text{(A-III-11)}$$

where m is the nucleon mass given by the average of the proton and neutron mass, and ω is the characteristic frequency of the oscillator. In shell model calculations one usually derives ω from[20]

$$\hbar\omega = 40\ A^{-1/3} \quad [\text{MeV}] = \begin{matrix} 15.87\ \text{MeV} & ^{16}O \\ 11.70\ \text{MeV} & ^{40}Ca \end{matrix}$$

in order to fit the nuclear mean square radius. A is the nuclear mass number. β is therefore given by:

$$\beta = \frac{\sqrt{m\hbar\omega}}{\hbar} = 0.155228\sqrt{\hbar\omega} \quad [\text{fm}^{-1}] = \begin{matrix} 0.61\ \text{fm}^{-1} & ^{16}O \\ 0.53\ \text{fm}^{-1} & ^{40}Ca \end{matrix} \qquad \text{(A-III-11')}$$

For our future purposes it is useful to give here some values of the normalization constant of the w.f. (A-III-10)

$$N_0^2 = \frac{\beta}{\sqrt{\pi}} \;;\; N_1^2 = \frac{\beta^2}{2\sqrt{\pi}} \;;\; N_2^2 = \frac{\beta}{2^3\sqrt{\pi}} \;;$$

$$N_3^2 = \frac{\beta}{3\cdot 2^4\cdot\sqrt{\pi}} \;;\; N_4^2 = \frac{\beta}{3\cdot 2^2\sqrt{\pi}} \qquad \text{(A-III-12)}$$

Our calculations have been performed in cartesian coordinates, the total three-dimensional wave functions are then

$$\varphi_n(\beta r) = \varphi_{n_x}(\beta x)\,\varphi_{n_y}(\beta y)\,\varphi_{n_z}(\beta z) \qquad \text{(A-III-12)}$$

Throughout this work the following notation for the state corresponding to the wave function (Eq.(A-III-12) has been used

$$|n\rangle = |n_x\, n_y\, n_z\rangle \qquad \text{(A-III-12')}$$

The spectrum of the harmonic oscillator is given in Fig.(III-1)

$N=n_x+n_y+n_z$ (principal quantum number)	Degeneracy	Total Number of Particles(*)	Wave Functions
5	42	112	
4	30	70	
3	20	40	$\{\,\|3\,0\,0\rangle, \|0\,3\,0\rangle, \|0\,0\,3\rangle, \|2\,1\,0\rangle, \|2\,0\,1\rangle, \|1\,1\,2\rangle, \|1\,2\,0\rangle, \|0\,1\,2\rangle, \|0\,2\,1\rangle, \|1\,1\,1\rangle$
2	12	20	$\{\,\|2\,0\,0\rangle, \|0\,2\,0\rangle, \|0\,0\,2\rangle, \|1\,1\,0\rangle, \|0\,1\,1\rangle, \|1\,0\,1\rangle$
1	6	8	$\|1\,0\,0\rangle, \|0\,1\,0\rangle, \|0\,0\,1\rangle$
0	2	2	$\|0\,0\,0\rangle$

(*) Isospin is not taken into account

Harmonic oscillator operators of creation and annihilation (in one-dimension)

Definition

$$a_x = -\frac{\beta}{\sqrt{2}}\left(x + \frac{i}{m\omega}\, p_x\right)$$

$$a_x^+ = -\frac{\beta}{\sqrt{2}}\left(x - \frac{i}{m\omega}\, p_x\right) \qquad \text{(A-III-13)}$$

$$x = \frac{a_x + a_x^+}{\sqrt{2}\,\beta}$$

$$\frac{p_x}{\hbar} = \beta\,\frac{a_x - a_x^+}{\sqrt{2}}$$

Properties

$$a_i^\dagger |n_i\rangle = \sqrt{n_i+1}\ |n_i+1\rangle$$
$$a_i |n_i\rangle = \sqrt{n_i}\ |n_i-1\rangle \qquad n_i \neq 0$$
$$a_i |n_i\rangle = 0 \qquad n_i = 0 \qquad \text{(A-III-14)}$$

Commutation relations

$$[a_i, a_j^\dagger] = \delta_{ij}$$
$$[a_i, a_j] = 0 = [a_i^\dagger, a_j^\dagger] \qquad \text{(A-III-15)}$$

$i, j \equiv x, y, z.$

Chapter IV

THE EFFECTIVE INTERACTION

In Eq.(II-14) for the total hamiltonian describing the scattering process, we introduced a term $V_{12}(\underline{r}(t),x)$. It represents the projectile-target effective interaction and it is a function of the relative coordinate $\underline{r}(t)$ of the projectile with respect to the target, and of the set x of internal coordinates of both nuclei.

In Chapter III we restricted our study to the scattering of α-particles, within the framework of an independent-particle model for the target. The last assumption implies that the α-particle interacts separately with each nucleon in the target and that the total interaction V_{12} is given by the sum of the α-nucleon interactions.

We noticed also that the α-particle is a strongly absorbed projectile and therefore its elastic scattering with the target nucleus is sensitive only to the nuclear surface. In this region of low nuclear density one expects very little probability for multiple scattering and a less crucial role of the Pauli principle as compared to more internal regions.

It should therefore be appropriate to assume that the interaction of the α with a bound nucleon is the same as the one with a free nucleon.

These assumptions allowed us to introduce in Eq.(III-5) an α-nucleus interaction of the form

$$V(\underline{r}_\alpha(t), \underline{r}) = \sum_1^A V_i(\underline{r}_i - \underline{r}_\alpha(t)) \,. \qquad \text{(IV-1)}$$

in which the α-i^{th} nucleon interaction is a function only of the α-i^{th} nucleon relative distance $(\underline{r}_i - \underline{r}_\alpha(t))$.

The problem that arises at this stage is the choice of the α-nucleon effective interaction $V_i(\underline{r}_i - \underline{r}_\alpha(t))$.

In principle if we were to obtain a completely self-consistent theoretical construction of the nucleus-nucleus potential, we should have gone back and calculated the nucleon-α optical potential from the first principles. This might look at first sight straightforward in the case of α-nucleon interaction, for the following reason.

The first excited state of the α-particle lies at about 20 MeV, which is quite a high energy. As a consequence, the Feshbach optical potential of Chapter I could be calculated taking only the first order term which does not contain contributions from any excited state. That term actually corresponds to our first order term in the perturbation expansion: its form is

$$V^{(1)}_{\alpha n}(\underline{r}) = \langle 0 | V_{nn}(\underline{r} - \underline{r}') | 0 \rangle = \int_{-\infty}^{\infty} \rho_\alpha(\underline{r}') V_{nn}(\underline{r} - \underline{r}')\, d^3\underline{r}' \qquad \text{(IV-2)}$$

It is purely real and it could be calculated just folding a nucleon-nucleon effective interaction into the α-particle ground state density ρ_α.

Such calculations can be improved further by introducing an exchange term in Eq.(IV-2), which takes into account the antisymmetrization effects, leading to a non-local effective interaction of the kind

$$V^{(1)}_{\alpha n}(\underline{r}, \underline{r}') = \delta(\underline{r} - \underline{r}') \int_{-\infty}^{\infty} \rho(\underline{r}_1) V_{nn}(\underline{r} - \underline{r}_1)\, d^3\underline{r}_1 - \rho(\underline{r}, \underline{r}') V_{nn}(\underline{r} - \underline{r}') \qquad \text{(IV-3)}$$

This approach has been followed by several authors who either use a density dependent[21-a] or independent[21-b] nucleon-nucleon interaction.

However, the attempts in this direction have encountered certain difficulties related to the non-locality of the form of Eq.(IV-3) and to the density-dependence of the nucleon-nucleon interaction.

The solutions of the first problem already proposed are essentially two. One due to N. Vinh Mau[21-a] and collaborators consists of approximating the α-nucleon non-local potential with a local one before folding into the target density; on the other hand, Love and Satchler[22] propose to use a zero-range pseudo-potential which simulates single nucleon exchange.

Besides, the use of a density-dependent interaction, although essential for a correct treatment of the nuclear properties in a Hartree-Fock type of approach like Eq.(IV-3), involves a further difficulty related to the definition of the local-density and the treatment of the rearrangement terms. The last two points are widely discussed in ref.(21-a_4) in which some new results are also presented for the α-^{40}Ca real potential.

As we already explained in Chapter II, our principle aim is however, the construction of a microscopic theory for the imaginary part of the α-nucleus optical potential. For this purpose it seemed to us more appropriate to start with a phenomenological α-nucleon effective interaction, rather than to try to calculate it in a truly microscopic approach.

Phenomenological effective interactions are usually local potentials fitted first to the low-energy nucleon-α scattering data and the parameters are adjusted so as to reproduce many-body effects like the

exchange effects[23]. In applying them to nuclei, modifications to the parameters are made in order to reproduce the experimental α-nucleus cross sections and angular distributions.

Phenomenological effective interactions for α-scattering have been studied in great detail by D.F. Jackson and various collaborators[23]. The fits to experimental data are very good and these potentials seem to be sufficiently reliable to to be used in microscopic calculations.

We used the potential (H') of ref.(23-b). It is a gaussian given by

$$V(r) = V_0 \; e^{-r^2/a^2} \qquad \text{(IV-4)}$$

where

$$V_0 = -53.8 \text{ MeV} \quad ; \quad a = 1.9 \text{ fm.} \qquad \text{(IV-5)}$$

The potential of Eq.(IV-4) was obtained renormalizing a potential due to Bernstein[24]. It gave excellent agreement with the s-wave phase shifts for n + α scattering up to 22 MeV and good agreement with the angular distributions for p + α scattering at 10 MeV, 17.5 MeV and 31 MeV.

The α-nucleus effective interaction was then constructed, folding the interaction of Eq.(IV-4) into the target density.

Targets ^{40}Ca and ^{58}Ni have been studied in detail. The ground state densities have been calculated in the potential of ref.(25). Details about the fits can be found in the original ref.(23-b).

In the last part of this chapter we observe the way in which changes

in the α-nucleon potential affect the α-nucleus potential.

A particularly interesting fact in the fits of ref.(23b) is that any set of the parameters V_o and a satisfying the relation

$$V_o\, a^6 = \text{const.} \qquad \text{(IV-6)}$$

give equally good α-nucleus-scattering cross sections. The actual value of the constant depends on the target but the relation

$$V_o\, a^6 = (2.6 \pm 0.2) \cdot 10^3 \ \text{MeV} \cdot \text{fm}^6, \qquad \text{(IV-7)}$$

holds for a range of nuclei including in particular ^{40}Ca and ^{58}Ni.

Relation (IV-7) is interesting because one usually requires that different effective interactions are equivalent if they give the same folding potential

$$V_{folding} = \int \rho(\underline{r})\, V(\underline{r}-\underline{r}')\, d^3\underline{r} \qquad \text{(IV-8)}$$

where $\rho(\underline{r})$ is the nuclear distribution function which can be parametrized as

$$\rho(\underline{r}) = \rho_0 \left(1 + e^{(r-R)/a}\right)^{-1} . \qquad \text{(IV-9)}$$

If the α-particle is inside the target then $\rho(r)$ is approximately constant $\rho(\underline{r}) \simeq \rho_o$, and therefore from Eq.(IV-8) it follows that:

$$V_{folding} = \rho_0 \int V(\underline{r}-\underline{r}')\, d^3\underline{r} \qquad \text{(IV-10)}$$

where the integral is the so-called volume integral of the effective interaction.

For a gaussian effective interaction of the type given in Eq.(IV-4) the volume integral is

$$V.I. \equiv \int V(r-r')\, d^3r = \pi^{3/2}\, a^3\, V_0 \,. \qquad \text{(IV-11)}$$

If the scattering probes the internal region of the target, the value of the relation Eq.(IV-11) has to be constant when changing the parameters in Eq.(IV-4).

A somewhat different situation occurs when the scattering is sensitive only to the surface of the nuclear distribution. This is in fact the case for α-scattering at forward angles.

In this case, due to the small dimension of the α-particle compared to the target one, one can approximate $\rho(\underline{r})$ with the nuclear matter distribution. $\rho(\underline{r})$ has then an exponential form in one coordinate and it is constant in the other two. In this case the folding potential also has an exponential shape with effective strength. Potentials for which Eq.(IV-12) has the same value will be very similar in the surface region. We find then

$$V_{folding} = \rho_0 \int e^{-\beta r}\, V(\underline{r}-\underline{r}')\, d^3\underline{r} \qquad \text{(IV-12)}$$

$$= \rho_0\, \pi^{3/2}\, a^3\, V_0\, e^{\beta^2 a^2/4}$$

In this case one can argue that the quantity to be conserved when changing the parameters in the effective interaction, is not the volume integral

$$V.I. \propto a^3 V_0$$

but rather a combination of the type:

$$V.I.\ e^{\beta^2 a^2/4} \sim a^6 V_0 \ .$$

Appendix IV

Matrix Elements of the Effective Interaction

In order to calculate Eq.(III-19) we need the matrix elements of the effective interaction Eq.(IV-6) between the wave functions Eq.(A-III-12).

They can be obtained using the proprieties of the Hermite polynomials, in particular their definition in terms of the generating function:

$$e^{2tx - t^2} = \sum_0^\infty n \quad \frac{H_n(x)\, t^n}{n!} \,, \tag{A-IV-1}$$

$$H_n(x) = \frac{d^n}{dt^n} \; e^{2tx - t^2} \Big|_{t=0} \,. \tag{A-IV-1'}$$

We want matrix elements of the type $\langle n|V|m\rangle$, where $|n\rangle$ and $|m\rangle$ are defined in Eq.(A-III-12') and V in Eq.(IV-6).

In this case the following propriety holds

$$\langle n | V | m \rangle = \langle n_x | V_x | m_x \rangle \langle n_y | V_y | m_y \rangle \langle n_z | V_z | m_z \rangle \tag{A-IV-2}$$

The one-dimension matrix elements are given by:

$$\langle n_x | V_x | m_x \rangle = C \int H_n(\beta x)\, e^{-\beta^2 x}\, e^{-(x-x')^2/a^2}\, H_m(\beta x)\, dx \tag{A-IV-3}$$

$$= C \frac{d^n}{ds^n} \frac{d^m}{dt^m} \int e^{2s\beta x - s^2}\, e^{-\beta^2 x^2}\, e^{-(x-x')^2/a^2}\, e^{2t\beta x - x^2}\, dx \Big|_{\substack{s=0 \\ t=0}}$$

where

$$= C \frac{d^n}{ds^n} \frac{d^m}{dt^m} F(s,t) \Big|_{\substack{s=0 \\ t=0}}$$

$$C = V_0 \frac{\beta}{\sqrt{\pi}\; 2^{(n+m)/2} \sqrt{n!\, m!}} \tag{A-IV-4}$$

and

$$F(s,t) = \int_{-\infty}^{\infty} dx \exp\left\{2\beta t x - t^2 - \frac{(x-x')^2}{a^2} - \beta^2 x^2 + 2s\beta x - s^2\right\} \qquad \text{(A-IV-5)}$$

$$= a\sqrt{\frac{\pi}{\alpha}} \exp\left\{(-s^2 - \beta^2 x'^2 + 2\beta x' s - t^2 + 2\beta x' t + 2\gamma s t)/a\right\}$$

where

$$\gamma \equiv a^2\beta^2$$
$$\alpha \equiv 1 + \gamma \qquad \text{(A-IV-6)}$$

The n^{th} and m^{th} derivatives with respect to s and t in Eq.(A-IV-3) are easily obtained if we note that they are nothing but the coefficients of the s^n and t^m terms respectively, in the series expansion of the exponential in Eq.(A-IV-5).

Putting $V_{nm} \equiv \langle n_x | V_x | m_x \rangle$, the analytical form of the matrix elements V_{mo} is given by:

$$V_{mo} = \left(\frac{\gamma}{\alpha}\right)^{1/2} \frac{e^{-\bar{x}^2}}{(m!)^{1/2}(2\alpha)^{m/2}} H_m(\bar{x}) \qquad \text{(A-IV-7)}$$

where

$$\bar{x} \equiv \frac{\beta x'}{\sqrt{\alpha}} \qquad \text{(A-IV-8)}$$

The following recurrence formula gives all the other matrix elements:

$$V_{m,n} = \frac{\gamma-1}{\gamma}\sqrt{\frac{m}{n}}\, V_{m-1,n-1} - \frac{1}{\gamma}\sqrt{\frac{m+1}{n}}\, V_{m+1,n-1} + \qquad \text{(A-IV-9)}$$
$$+ \frac{\sqrt{2}\beta x'}{\gamma\sqrt{n}}\, V_{m,n-1}.$$

Eq.(A-IV-9) has been obtained in the following way. First we calculate the commutator $\left[a_x^+, V_x\right]$, where a_x^+ is the creation operator defined in Eq.(A-III-13) and $V_x = V_o\, e^{-(x - x_o)^2/a^2}$

$$\left[a^+_x, V\right] = \left(a_x + a_x^+ - \sqrt{2}\,\beta\, x'\right) \frac{V_x}{\gamma}$$

and then

$$V_x\, a^+_x = \left(1 - \frac{1}{\gamma}\right) a^+_x V_x - \frac{a_x V_x}{\gamma} + \frac{\sqrt{2}\beta}{\gamma}\, x'\, V_x$$

Using this result in the calculation of the matrix elements of V, we obtain in one dimension:

$$\langle m|V|1\rangle = \langle m|Va^+|0\rangle$$
$$= \left(1 - \frac{1}{\gamma}\right)\langle m|a^+V|0\rangle - \frac{1}{\gamma}\langle m|aV|0\rangle + \frac{\sqrt{2}\beta x'}{\gamma}\langle m|V|0\rangle$$

from which it follows by successive application of a^+:

$$\sqrt{m}\; V_{m,n} = \left(1 - \frac{1}{\gamma}\right)\sqrt{m}\; V_{m-1,\,n-1} - \frac{1}{\gamma}\sqrt{m+1}\; V_{m+1,\,n-1}$$
$$+ \sqrt{\frac{2}{\gamma}}\,\beta x'\; V_{m,\,n-1}.$$

The following gaussian integral has often been used:

$$\int_{-\infty}^{\infty} x^m\, e^{-(\alpha x^2 + \beta x + \gamma)}\, dx = \frac{e^{(\beta^2 - 4\alpha\gamma)/4\alpha}}{\alpha^{(m+1)/2}} \int_{-\infty}^{\infty} \left(y - \frac{\beta}{2\sqrt{\alpha}}\right)^m e^{-y^2}\, dy.$$

Chapter V

A SIMPLE APPLICATION

Introduction

In this chapter a simple application of the formalism discussed in chapters II and III, will be presented.

The time integral of the imaginary part of the optical potential will be calculated for α-scattering on a target of ^{16}O.

In section 1 we show how the R.H.S. of Eq.(III-19) can be calculated using the so-called correlation function.

In section 2 the choice of the path is discussed and in section 3 it is shown how the calculation can be performed analytically in the case of a straight line trajectory.

V-1 Correlation function

In this section we present in detail the calculation of Eq.(III-19) for a target of ^{16}O including only simple modes of excitation, namely the $1\hbar\omega$ and $2\hbar\omega$ particle-hole excitations.

Instead of calculating the corresponding matrix elements of the effective interaction, according to the formulae given in Appendix III, we wish to use another method.

Let us define the correlation function as:

$$C_V(\underline{r}_0, \underline{r}_0') = \int_{-\infty}^{\infty} d^3\underline{r}\, d^3\underline{r}'\, C_0(\underline{r}, \underline{r}')\, V(|\underline{r}-\underline{r}_0|)\, V(|\underline{r}'-\underline{r}_0'|) \qquad (V\text{-}1)$$

where $\underline{r}_0$, $\underline{r}_0'$, represent the position of the centre of the α-particle and $C_0(\underline{r}, \underline{r}')$ is the correlation function for the case in which the interaction is replaced by a δ-function

$$V(|\underline{r}-\underline{r}_d|) \Rightarrow \delta(\underline{r}-\underline{r}_0). \qquad \text{(V-2)}$$

$Co(\underline{r},\underline{r}')$ is then defined by

$$C_0(\underline{r},\underline{r}') = 4 \sum_{n<} \varphi_n^*(\underline{r})\varphi_n(\underline{r}') \sum_{k>} \varphi_k^*(\underline{r}')\varphi_k(\underline{r}) \qquad \text{(V-3)}$$

$\phi_n(\underline{r})$ are the single particle orbital wave functions, in our case given by Eq.(A-III-12); the label n < is for occupied states in the H.O.S.M., while k > stands for unoccupied states. The single-particle wave functions in Eq.(III-19) contain spin and isospin parts. In this thesis we deal with states which are spin and isospin saturated and the interaction $V(\underline{r} - \underline{r}_0)$ is independent of spin and isospin. Hence the summation over spin and isospin quantum numbers can be calculated to give the factor 4 which is included in Eq.(V-3)

Substituting Eq.(V-1) in Eq.(III-19) we obtain

$$\int_{-\infty}^{\infty} I_m V(\underline{r}(t))\,dt = -\frac{1}{2\hbar}\int_{-\infty}^{\infty}dt\int_{-\infty}^{\infty}dt'\, e^{i\omega_{kn}(t-t')} C_V(\underline{r}(t),\underline{r}(t')) \qquad \text{(V-4)}$$

1-a Calculation of C_0 for the $1\hbar\omega$ transition (k = n + 1 in Eq.(V-3)).

According to the spectrum of the H.O.S.M. given in Fig.(III-1), page 39, ^{16}O is obtained by filling the first two shells, corresponding to N = 0 and N = 1. The $1\hbar\omega$ excitations come from transitions satisfying the condition $\Delta N = 1$; in ^{16}O this corresponds only to the transition from the level N = 1 to the one with N = 2. Therefore in Eq.(V-3) $\sum_{n<}$ means the sum over the orbital wave functions with principal quantum number N = 1 and $\sum_{k>}$ means the sum over those with

N = 2. Using the wave functions defined in Eqs.(A-III-12) and (A-III-10) we get

$$C_0(\underline{r},\underline{r}') = 4\pi^{-3}\beta^6 e^{-\beta^2(\underline{r}^2+\underline{r}'^2)}\beta^2(\underline{r}\cdot\underline{r}')\left[4\beta^2(\underline{r}\cdot\underline{r}')^2 - 2\beta^2(\underline{r}^2+\underline{r}'^2)+3\right]. \qquad (V\text{-}5)$$

Substituting Eq.(V-5) in Eq.(V-1) for C_v, and using the interaction Eq.(IV-6), we obtain

$$C_v(\underline{r}_0,\underline{r}_0') = \int V(|\underline{s}-\underline{r}(t)|)\, V(|\underline{s}'-\underline{r}(t')|)\, C_0(\underline{s},\underline{s}')\, d^3\underline{s}\, d^3\underline{s}'$$

$$= 4V_0^2\pi^{-3}\beta^6 e^{-(\underline{r}^2+\underline{r}'^2)/a^2} \times$$

$$\times \int e^{2[(\underline{r}_0\cdot\underline{s})+(\underline{r}_0'\cdot\underline{s}')]/a^2} e^{-(\underline{s}^2+\underline{s}'^2)\alpha/a^2} \times \qquad (V\text{-}6)$$

$$\times \left\{\beta^2(\underline{s}\cdot\underline{s}')\left[4\beta^4(\underline{s}\cdot\underline{s}')^2 - 2\beta^2(\underline{s}^2+\underline{s}'^2)+3\right]\right\} d^3\underline{s}\, d^3\underline{s}' ,$$

where $\gamma \equiv a^2\beta^2$; $\alpha = 1 + \gamma$.

In order to calculate the R.H.S. of Eq.(V-6), let us define the following integral:

$$\overline{I}(\underline{r}_0,\underline{r}_0') = \int d^3\underline{s}\, d^3\underline{s}'\, e^{-(\underline{s}^2+\underline{s}'^2)\alpha/a^2} e^{2[(\underline{r}_0\cdot\underline{s})+(\underline{r}_0'\cdot\underline{s}')]/a^2} \qquad (V\text{-}7)$$

$$= \left(\frac{\pi a^2}{\alpha}\right)^3 e^{(r_0^2+r_0'^2)/a^2\alpha}$$

then we have

$$C_V(\underline{r}_0,\underline{r}_0') = 4V_0^2\pi^3\beta^6 e^{-(\underline{r}_0^2+\underline{r}_0'^2)/a^2}\left\{\sum_i \frac{a^4\beta^2}{4}\left(\frac{\partial}{\partial r_{0i}}\frac{\partial}{\partial r_{0i}'}\right)\cdot\right.$$

$$\left.\left[\frac{a^8\beta^4}{4}\left(\sum_i \frac{\partial}{\partial r_{0i}}\frac{\partial}{\partial r_{0i}'}\right)^2 - \frac{a^4\beta^2}{2}\left(\nabla_{r_0}^2+\nabla_{r_0'}^2\right)+3\right\}\cdot\right. \qquad \text{(V-8)}$$

$$\times \underline{I}(\underline{r}_0,\underline{r}_0')$$

$$= 4V_0^2\frac{\gamma^3}{\alpha^7}e^{-\beta^2(\underline{r}_0^2+\underline{r}_0'^2)/\alpha}\beta^2(\underline{r}_0\cdot\underline{r}_0')\left[\frac{4\beta^4}{\alpha^2}(\underline{r}_0\cdot\underline{r}_0')^2+\right.$$

$$\left.+\frac{2}{\alpha}(2\gamma-1)\beta^2(\underline{r}_0^2+\underline{r}_0'^2)+(8\gamma^2-4\gamma+3)\right],$$

where we used Eq.(A-IV-6).

V-1-b Calculation of C_o for the $2\hbar\omega$ transition ($k = n+2$ in Eq.(V-3)).

The $2\hbar\omega$ transitions, in first order, are given by the transitions for which $\Delta N = 2$, i.e. the one from the level with $N = 0$ to the level $N = 2$, plus the transition from level $N = 1$ to level $N = 2$.

Using the same notation as in (1-a) we find now

$$C_o(\underline{r},\underline{r}') = 4\pi^{-3}\beta^6 e^{-\beta^2(\underline{r}^2+\underline{r}'^2)}\left\{\frac{8}{3}\beta^8(\underline{r}\cdot\underline{r}')^4 - 4\beta^6(\underline{r}\cdot\underline{r}')^2(\underline{r}^2+\underline{r}'^2)\right.$$

$$\left.+2\beta^4(\underline{r}\cdot\underline{r}')^2+\beta^2(\underline{r}^2+\underline{r}'^2)+\frac{23}{2}\right\}. \qquad \text{(V-9)}$$

$$C_V(\underline{r}_0,\underline{r}_0') = 4V_0^2\frac{\gamma^3}{\alpha^7}e^{-\beta^2(\underline{r}_0^2+\underline{r}_0'^2)}\left[h_1+h_2\frac{\beta^2}{\alpha}(\underline{r}_0^2+\underline{r}_0'^2)+\right.$$

$$\left.+h_3\frac{\beta^4}{\alpha^2}(\underline{r}_0\cdot\underline{r}_0')^2+h_4\frac{\beta^8}{\alpha^4}(\underline{r}_0+\underline{r}_0')^4+\right.$$

$$+ h_5 \frac{\beta^4}{\alpha^2} \left(\underline{r}_0^2 + \underline{r}_0'^2\right)^2 + h_6 \frac{\beta^6}{\alpha^3} \left(\underline{r}_0 \cdot \underline{r}_0'\right)^2 \left(\underline{r}_0^2 + \underline{r}_0'^2\right) \qquad \text{(V-10)}$$

where

$$h_1 = \frac{3}{2}\left(6\gamma^2 + 2\gamma + 1\right),$$

$$h_2 = -\left(6\gamma^2 - 3\gamma + 1\right),$$

$$h_3 = 4\left(3\gamma^2 - \gamma + 3\right),$$

$$h_4 = \frac{8}{3}, \qquad \text{(V-11)}$$

$$h_5 = -2\gamma,$$

$$h_6 = 4\gamma - 4.$$

The time dependence of the integrands of Eq.(V-4) comes through the path $\underline{r}(t)$. In order to perform the integral we have therefore to give the explicit form of $\underline{r}(t)$. The simplest case is when $\underline{r}(t)$ is a linear function of t, in which case the time integral can be done analytically.

Let us therefore discuss the choice of the path.

V-2 Choice of the path r(t)

In chapter II we have shown that our approach is equivalent to the one of Koeling and Malfliet. In their formula the path is chosen in order to satisfy the condition of minimal action, Eq.(II-27,) where only the real part of the lagrangian enters. The path obtained in this way is real.

Following Koeling and Malfliet, we can apply the minimum condition on the real part of the action Eq.(II-13') which generates the scattering we are dealing with.

Then our path is given by

$$\delta\left(\mathrm{Re}\ S(\underline{r}(t))\right) = 0 \tag{V-12}$$

where

$$S(\underline{r}(t)) = \int_{-\infty}^{\infty} dt \left\{ \frac{1}{2}\mu \left(\dot{\underline{r}}(t)\right)^2 - V_{opt}(\underline{r}(t)) \right\} \tag{V-13}$$

and

$$V_{opt}(\underline{r}(t)) = \mathrm{Re}\, V_{opt}(\underline{r}(t)) + i\, \mathrm{Im}\, V_{opt}(\underline{r}(t)).$$

From Eq.(V-12) the classical equation of motion follows:

$$\mu\, \ddot{\underline{r}}(t) = -\frac{\partial}{\partial \underline{r}} \left\{ \mathrm{Re}\, V_{opt}(\underline{r}(t)) \right\} \tag{V-14}$$

and μ is the reduced mass.

Thus we get the prescription that the path appearing in our formalism is the classical trajectory that the projectile follows when moving in the real part of the optical potential.

From Feshbach's theory and N. Vinh Mau calculations we already know that Re V_{opt} is mainly given by the first order term in Eq.(I-6) and hence it can be calculated by the folding procedure discussed in chapter IV.

In cases in which the imaginary part of the potential is not negligible, however, the path should be taken so as to give a minimum

of the action corresponding to the full lagrangian: this will lead to an imaginary path. Indeed, we shall see in chapter VIII that the approximation of a classical real path breaks down for trajectories with an impact parameter such as to give an orbiting. In such a case the projectile is expected to have a strong interaction with the target and as a consequence the imaginary potential should not be neglected compared to the real potential.

This critical value of the impact parameter corresponds to the grazing angular momentum, i.e., the one for which the incident energy is equal to the top of the barrier of the effective potential

$$V(r) = V_N(r) + V_C(r) + \frac{\hbar^2}{2\mu} \frac{\ell(\ell+1)}{r^2}$$

given by the sum of the nuclear plus Coulomb plus centrifugal potentials.

In order to test the validity of the approach so far proposed, we made a first set of calculations supposing that the potential in Eq.(V-14) is zero. In this case the trajectory is a straight line with constant velocity and all the calculations can be done analytically. This is related to the Glauber[26] approximation and it is expected to work under the following conditions:

$$\text{i)} \quad ka > 1 \quad .$$
$$\text{i)} \quad V/E \ll 1 \quad . \qquad \text{(V-15)}$$

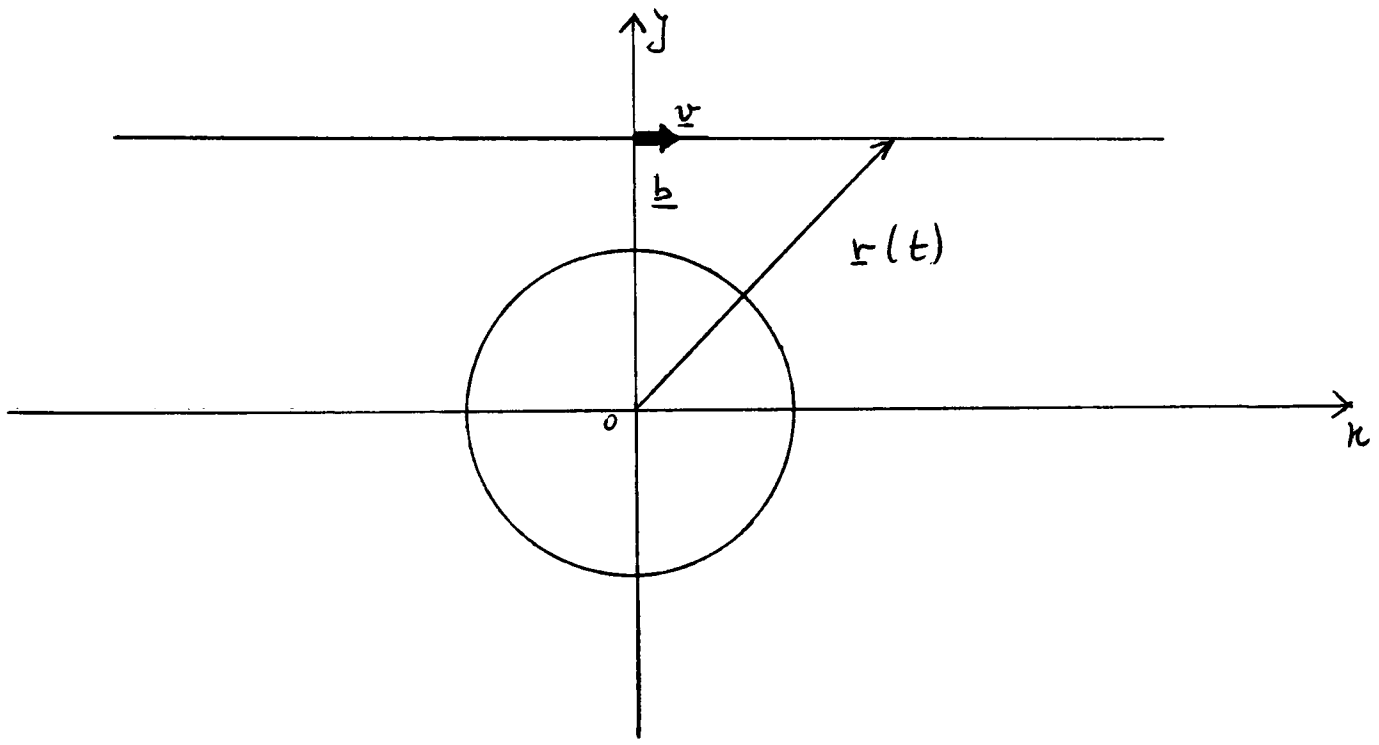
Condition (i) gives the limit of applicability of semiclassical approximations and has already been shown to be satisfied (Chapter III, Section 2) in the case of α-scattering.

Condition (ii) is also a reasonable approximation if the absorption (i.e. Im V_{opt}) is strong because then only grazing collisions are important. In fact, for a peripheral path the α-particle interacts only with the tail of the potential; while for trajectories that penetrate well inside the potential there is complete absorption and the details of Im V_{opt} are not important.

V-3 Straight line trajectory

In order to calculate Eq.(V-4) we introduce a cartesian frame of reference with the origin in the centre of mass of the target nucleus, the x-axis parallel to the trajectory and the y-axis along the direction of the impact parameter. Then the trajectory is given by

$$\underline{r}(t) = \underline{v}t + \underline{b} \qquad \text{with} \qquad \underline{v} \perp \underline{b} \tag{V-16}$$



We now substitute Eqs.(V-16) in the R.H.S. of Eq.(V-4) and change variables twice in the following way

$$\tau = \frac{t-t'}{2} \quad ; \quad \tau' = \frac{t+t'}{2} \quad ; \quad dt\, dt' = 2\, d\tau\, d\tau' \tag{V-17}$$

$$s = \beta v \tau \quad ; \quad s' = \beta v \tau' \quad ; \quad ds = \beta v\, d\tau \quad ; \quad ds' = \beta v\, d\tau' \tag{V-17'}$$

and s is now a dimensionless variable leading to

$$\text{R.H.S. (of Eq. (V-5))} = -e^{-\beta^2 b^2/\alpha} \frac{V_0^2}{\hbar \beta^2 v^2} \int_{-\infty}^{\infty} ds\, ds'\, e^{-2(s^2+s'^2)/\alpha}\, e^{2i\frac{k}{\beta}s} \times P(s,s') , \tag{V-18}$$

where P(s,s') is a polynomial in s,s' depending on the actual form of $C_v(\underline{r}(t), \underline{r}'(t'))$.

Performing the s' integration and changing again variable to

$$y = s - i\frac{k\alpha}{2\beta} \quad ; \quad d = \frac{k\alpha}{2\beta} \quad ; \quad k = \frac{\bar{\omega}}{v} \quad ; \quad \bar{\omega} = \omega_{rn} \tag{V-17''}$$

we get

$$\text{R.H.S.} = -\frac{e^{-\beta^2 b^2/\alpha} V_0^2}{\hbar \beta^2 v^2} \int_{-\infty}^{\infty} ds\, e^{-2s^2/\alpha}\, e^{2i\frac{k}{\beta}s}\, f(s)$$

$$= -\frac{e^{-\beta^2 b^2/\alpha} V_0^2}{\hbar \beta^2 v^2}\, e^{-2d^2/\alpha} \int_{-\infty}^{\infty} dy\, e^{-\frac{2}{\alpha}y^2}\, f(y) \tag{V-18'}$$

$$= -e^{-\beta^2 b^2/\alpha} e^{-2d^2/\alpha} \frac{V_0^2}{\hbar \beta^2 v^2}\, I(d)$$

where

$$f(s) = g_1 s^2 + g_2 s^4 + \ldots + g_n s^{2n} + g_{n+1} , \tag{V-19}$$

$$\bar{I}(d) = c_1 d^2 + c_2 d^4 + \dots + c_n d^{2n} + c_{n+1}. \qquad \text{(V-19')}$$

In Eqs.(V-19,19') the coefficients g and c depend on the impact parameter b as well as on the coefficients of the polinomial P(s,s'). The degree of the polinomials f(s) and I(d) is always even and depends on the order of excitation being considered. It is $2n = 6$ for $1\hbar\omega$ excitations, $2n = 8$ for $2\hbar\omega$ ones and so on.

The numerical values of Eq.(V-18') are given in Table (V-1) for ^{16}O.

In Table (V-2) we give the results for ^{40}Ca, obtained using the computing code OPTPOT.

The results of Tables (V-1,2) are not as yet physically meaningful, since they include the spurious centre-of-mass excitations and the procedure to eliminate them constitutes the subject of the next chapter.

TABLE (V-1)
^{16}O

E_α (MeV)	$1\hbar\omega$ b = 0 fm		$1\hbar\omega$ b = 1.6 fm		b = 3.024 fm		$2\hbar\omega$ b = 0 fm	
	Analytical	Numerical	Analytical	Numerical	Analytical	Numerical	Analytical	Numerical
10	24.24	24.12	21.88	21.84	9.84	9.84	0.02	0.02
20	66.64	66.52	48.08	48.00	20.16	20.16	1.92	1.84
30	67.68	67.60	50.00	49.96	21.40	21.40	7.59	7.60
40	57.48	57.44	45.24	45.20	20.16	20.16	13.90	13.80
50	47.04	47.04	39.16	39.76	18.40	18.44	17.71	17.68
60	38.48	38.48	34.92	34.92	16.80	16.80	19.38	19.32
70	30.00	31.80	28.76	30.88	14.72	15.32	19.71	19.68
80	26.56	26.56	27.52	27.52	14.04	14.04	19.32	19.28
90	22.48	22.48	24.76	24.76	12.96	12.96	18.60	18.56
100	19.20	19.20	22.48	22.48	11.96	11.96	17.73	17.72
110	16.60	16.60	20.24	20.52	11.16	11.16	16.89	16.84
120	14.48	14.48	18.60	18.88	10.44	10.44	16.07	16.04

Values of $-\int \mathrm{Im}\, V(\underline{r}(t))\, dt$ $\left[\mathrm{MeV}\cdot 10^{-22}\ \mathrm{sec}\right]$, from Eq.(III-19) with straight line trajectory

TABLE (V-2)

^{40}Ca

b = 0 fm

E_α (MeV)	1ħω	2ħω	3ħω	4ħω	5ħω	6ħω	7ħω	8ħω
10	59.40	7.23	2.00	0.46	0.25	0.07	0.04	0.01
20	98.99	12.30	0.62	0.007	0.0005	0.0001	0.00007	0.00003
30	89.09	26.51	3.29	0.15	0.002	0.00002	5.0×10^{-8}	0.0×10^{-8}
40	71.32	35.99	7.24	0.66	0.035	0.0009	0.00001	9.0×10^{-8}
50	56.34	38.94	11.47	1.56	0.14	0.008	0.002	0.000005
60	44.99	38.31	14.75	2.79	0.36	0.034	0.002	0.00007
70	36.51	36.25	16.73	4.12	0.70	0.08	0.008	0.0005
80	30.11	33.84	17.63	5.31	1.13	0.17	0.02	0.002
90	25.21	31.51	17.80	6.22	1.62	0.31	0.04	0.005
100	21.38	29.40	17.51	6.82	2.08	0.48	0.08	0.01
110	18.35	27.55	16.96	7.17	2.48	0.67	0.14	0.02
120	15.91	25.94	16.27	7.31	2.79	0.86	0.21	0.03

Numerical values of $-\int_{-\infty}^{\infty}$ Im V ($\underline{r}$(t))dt (MeV.10^{-22} sec), from Eq.(III-19) with straight line trajectory.

TABLE (V-3)

^{40}Ca

b = 2.05 fm

E_α(Me)	1ħω	2ħω	3ħω	4ħω	5ħω	6ħω	7ħω	8ħω	C.M.1	C.M.2
10	61.12	1.49	0.00	0.00	0.00	0.00	0.00	0.02	19.65	0.005
20	75.09	12.63	0.48	0.00	0.00	0.00	0.00	0.00	52.31	0.005
30	66.33	23.51	2.65	0.11	0.00	0.00	0.00	0.00	51.44	0.058
40	56.12	29.43	5.78	0.53	0.03	0.00	0.00	0.00	44.67	0.15
50	47.74	31.18	8.72	1.27	0.12	0.01	0.00	0.00	38.20	0.21
60	41.19	30.62	10.85	2.19	0.29	0.03	0.00	0.00	32.91	0.23
70	36.06	29.03	12.07	3.11	0.56	0.07	0.01	0.00	28.70	0.24
80	31.98	27.08	12.60	3.90	0.88	0.14	0.02	0.00	25.33	0.23
90	28.69	25.08	12.65	4.48	1.21	0.25	0.04	0.00	22.60	0.22
100	25.98	23.18	12.41	4.86	1.52	0.37	0.07	0.01	20.37	0.20
110	23.72	21.44	12.00	5.08	1.78	0.50	0.11	0.02	18.51	0.19
120	21.81	19.86	11.51	5.17	1.98	0.62	0.16	0.03	16.48	0.18

The same as Table (V-2) with b = 2.05 fm. C.M.1 and C.M.2 are centre-of-mass corrections discussed in Chapter VI

TABLE (V-4)

^{40}Ca

b = 4.10 fm

E_α(MeV)	1ħω	2ħω	3ħω	4ħω	5ħω	6ħω	7ħω	8ħω	C.M.1	C.M.2
10	29.12	0.43	0.0009	0.0	0.0	0.0	$0.13\ 10^{-5}$	0.006	6.79	0.0003
20	33.09	4.69	0.13	0.0008	$0.87\ 10^{-6}$	0.0	0.0	0.0	16.17	0.004
30	29.07	8.33	0.83	0.032	0.0004	$02\ 10^{-5}$	0.0	0.0	17.03	0.03
40	25.03	9.94	0.17	0.007	0.0001	$0.17\ 10^{-5}$	$0.1\ 10^{-7}$	0.0	16.29	0.05
50	21.75	10.35	2.66	0.40	0.03	0.001	0.00005	$0.8\ 10^{-5}$	14.89	0.06
60	19.15	10.18	3.24	0.68	0.09	0.008	0.0004	0.00001	13.55	0.07
70	17.07	9.75	3.58	0.94	0.17	0.023	0.002	0.0001	12.35	0.07
80	15.38	9.24	3.74	1.16	0.27	0.04	0.005	0.0005	11.32	0.07
90	13.99	8.71	3.77	1.32	0.36	0.07	0.01	0.001	10.42	0.07
100	12.82	8.19	3.73	1.42	0.44	0.11	0.02	0.003	9.65	0.07
110	11.83	7.70	3.64	1.49	0.51	0.14	0.03	0.006	8.98	0.07
120	10.98	7.26	3.52	1.52	0.57	0.17	0.04	0.009	8.41	0.07

The same as Table (V-3) with b = 4.10 fm.

TABLE (V-5)

^{40}Ca

b = 0 fm

E_α (MeV)	$1\hbar\omega$	$2\hbar\omega$	$3\hbar\omega$	$4\hbar\omega$	$5\hbar\omega$	$6\hbar\omega$	$7\hbar\omega$	C.M.1	C.M.2
10	50.05	39.88	17.87	28.51	6.91	15.53	8.01	32.46	0.44
20	10.05	13.29	7.38	3.89	2.36	1.01	0.73	6.54	0.15
30	8.26	12.72	7.02	3.96	2.03	1.12	0.56	5.42	0.14
40	7.03	12.23	6.79	3.88	1.98	1.12	0.50	4.65	0.13
50	6.11	11.86	6.55	3.78	1.99	1.03	0.58	4.07	0.12
60	5.41	11.54	6.31	3.68	1.94	1.04	0.55	3.62	0.12
70	4.84	11.27	6.08	3.58	1.90	1.03	0.53	3.25	0.11
80	4.38	11.03	5.87	3.48	1.85	1.01	0.53	2.95	0.11
90	3.99	10.82	5.66	3.38	1.81	0.99	0.53	2.69	0.11
100	3.66	10.62	5.47	3.29	1.76	0.97	0.52	2.47	0.10
110	3.37	10.44	5.28	3.20	1.72	0.95	0.51	2.29	0.10
120	3.12	10.27	5.11	3.12	1.67	0.93	0.50	2.12	0.10

The same as Tables (V-2,3,4) but with classical trajectories

TABLE (V-6)

^{40}Ca

b = 2.05 fm

E_α (MeV)	$1\hbar\omega$	$2\hbar\omega$	$3\hbar\omega$	$4\hbar\omega$	$5\hbar\omega$	$6\hbar\omega$	$7\hbar\omega$	C.M.1	C.M.2
10	46.61	8.46	29.73	16.34	7.17	7.07	1.51	29.27	0.065
20	10.74	13.04	7.15	4.48	1.73	1.54	0.43	6.96	0.15
30	9.10	12.40	7.33	3.86	2.16	0.98	0.68	5.96	0.14
40	8.02	11.73	7.17	3.84	2.04	1.05	0.56	5.27	0.13
50	7.24	11.17	7.01	3.74	1.99	1.07	0.52	4.77	0.12
60	6.64	10.70	6.84	3.63	1.97	1.04	0.54	4.37	0.12
70	6.17	10.29	6.66	3.52	1.93	1.02	0.54	4.06	0.11
80	5.80	9.92	6.50	3.41	1.88	1.01	0.53	3.81	0.11
90	5.48	9.58	6.33	3.29	1.84	0.99	0.52	3.60	0.10
100	5.22	9.28	6.18	3.18	1.79	0.97	0.52	3.42	0.10
110	5.00	9.00	6.02	3.08	1.74	0.95	0.51	3.27	0.10
120	4.81	8.74	5.88	2.98	1.70	0.92	0.50	3.14	0.09

The same as Table (V-5) with b = 2.05 fm

TABLE (V-6)

^{40}Ca

b = 2.05 fm

E_α (MeV)	$1\hbar\omega$	$2\hbar\omega$	$3\hbar\omega$	$4\hbar\omega$	$5\hbar\omega$	$6\hbar\omega$	$7\hbar\omega$	C.M.1	C.M.2
10	46.61	8.46	29.73	16.34	7.17	7.07	1.51	29.27	0.065
20	10.74	13.04	7.15	4.48	1.73	1.54	0.43	6.96	0.15
30	9.10	12.40	7.33	3.86	2.16	0.98	0.68	5.96	0.14
40	8.02	11.73	7.17	3.84	2.04	1.05	0.56	5.27	0.13
50	7.24	11.17	7.01	3.74	1.99	1.07	0.52	4.77	0.12
60	6.64	10.70	6.84	3.63	1.97	1.04	0.54	4.37	0.12
70	6.17	10.29	6.66	3.52	1.93	1.02	0.54	4.06	0.11
80	5.80	9.92	6.50	3.41	1.88	1.01	0.53	3.81	0.11
90	5.48	9.58	6.33	3.29	1.84	0.99	0.52	3.60	0.10
100	5.22	9.28	6.18	3.18	1.79	0.97	0.52	3.42	0.10
110	5.00	9.00	6.02	3.08	1.74	0.95	0.51	3.27	0.10
120	4.81	8.74	5.88	2.98	1.70	0.92	0.50	3.14	0.09

The same as Table (V-5) with b = 2.05 fm

TABLE (V-7)

^{40}Ca

b = 4.10 fm

E_α (MeV)	$1\hbar\omega$	$2\hbar\omega$	$3\hbar\omega$	$4\hbar\omega$	$5\hbar\omega$	$6\hbar\omega$	$7\hbar\omega$	C.M.1	C.M.2
10	23.98	14.77	11.16	24.25	5.81	3.50	2.98	11.29	0.15
20	12.89	12.48	7.70	4.27	1.93	1.37	0.51	8.39	0.15
30	11.96	11.56	7.97	3.92	2.12	1.04	0.61	7.89	0.14
40	11.39	10.58	7.98	3.93	2.04	1.06	0.54	7.57	0.14
50	11.00	9.73	7.90	3.92	2.02	1.05	0.53	7.37	0.13
60	10.72	8.98	7.73	3.90	1.99	1.04	0.53	7.24	0.12
70	10.50	8.33	7.50	3.86	1.95	1.03	0.52	7.16	0.11
80	10.33	7.77	7.24	3.81	1.91	1.01	0.52	7.10	0.10
90	10.18	7.29	6.95	3.74	1.86	1.00	0.51	7.07	0.10
100	10.04	6.88	6.65	3.66	1.81	0.97	0.51	7.04	0.09
110	9.90	6.52	6.35	3.57	1.75	0.95	0.50	7.02	0.08
120	9.77	6.22	6.04	3.47	1.69	0.92	0.49	6.99	0.08

The same as Table (V-5) with b = 4.10 fm

Chapter VI

THE SPURIOUS CENTRE-OF-MASS EXCITATIONS

VI-1 Introduction

It is well known that whenever calculations are made with shell-model functions, an appropriate subtraction of the centre-of-mass motion contribution is necessary[27].

The reason for the appearance of the spurious states is that when one introduces the harmonic oscillator potential, three extra degrees of freedom are brought into the system, namely the coordinates of the centre of the potential, which do not have any physical meaning. As a consequence the wave functions calculated in such a potential do not depend only on the intrinsic coordinates of the nucelus, as they should, but also on $\underline{R} \equiv (R_x, R_y, R_z)$, the centre-of-mass coordinate of the nucleus.

The above mentioned spurious states correspond to motions of the nucleus as a whole.

There are several methods to identify and eliminate these spurious excitations, depending on the problem one is interested in. For the purposes of this work this can be done as follows.

In the equation (III-3) for the time integral of the imaginary part of the optical potential, the sum over all possible excited states $\sum_{n\neq 0}$ contains states $|n\rangle$ which can be obtained operating with the centre of mass coordinate operator $\underline{R}$ on the ground state $|0\rangle$.

As we shall see shortly in detail the application of any component of $\underline{R}$ on the ground state produces an excitation with energy $1\hbar\omega$, the application of $\underline{R}^2$ an excitation with energy $2\hbar\omega$, and so on.

All states obtained in this way, by applying R_x, R_y, R_x, and R_x^2, R_y^2 $R_z^2, R_xR_y, R_xR_z, R_yR_z$ have to be subtracted from the sum $\sum_{n\neq 0}$.

Let us define

$$\mathcal{R}_x = -\frac{1}{2\hbar}\int_{-\infty}^{\infty}dt\int_{-\infty}^{\infty}dt'\ \langle 0|V(\underline{r}-\underline{r}_0)R_x^\dagger|0\rangle N_x^2\langle 0|R_x V(\underline{r}'-\underline{r}_0')|0\rangle e^{\frac{i}{\hbar}\omega_{10}(t-t')}$$

$$\mathcal{R}_{xx} = -\frac{1}{2\hbar}\int_{-\infty}^{\infty}dt\int_{-\infty}^{\infty}dt'\ \langle 0|V(\underline{r}-\underline{r}_0)(R_x^\dagger)^2|0\rangle N_{xx}^2\langle 0|R_x^2 V(\underline{r}'-\underline{r}_0')|0\rangle e^{\frac{i}{\hbar}\omega_{20}(t-t')}$$

$$\mathcal{R}_{xy} = -\frac{1}{2\hbar}\int_{-\infty}^{\infty}dt\int_{-\infty}^{\infty}dt'\ \langle 0|V(\underline{r}-\underline{r}_0)R_u^\dagger R_y^\dagger|0\rangle N_{xy}^2\langle 0|R_u R_y V(\underline{r}'-\underline{r}_0')|0\rangle e^{\frac{i}{\hbar}\omega_{20}(t-t')}$$

$$\int_{-\infty}^{\infty}\mathrm{Im}\,V_{opt}(\underline{r}(t))\,dt = -\frac{1}{2\hbar}\sum_{n\neq 0}\int_{-\infty}^{\infty}dt\int_{-\infty}^{\infty}dt'\ \langle 0|V(\underline{r}-\underline{r}_0')|n\rangle\langle n|V(\underline{r}'-\underline{r}_0')|0\rangle e^{\frac{i}{\hbar}\omega_{n0}(t-t')}$$

$$-\mathcal{R}_{xx}-\mathcal{R}_{yy}-\mathcal{R}_{zz}-\mathcal{R}_{xx}-\mathcal{R}_{xy}-\mathcal{R}_{xz}-\mathcal{R}_{yy}$$
$$-\mathcal{R}_{yz}-\mathcal{R}_{zz}.$$

Then Eq.(III-3) should read:

Section 2 and 3 below are devoted to the detailed calculation of these corrections to the $1\hbar\omega$ and $2\hbar\omega$ excitations, respectively.

VI-2 Corrections to the $1\hbar\omega$ excitations

In this section we compute the effects of the vector operator $R \equiv (R_x, R_y, R_z)$ on the ground state $|0\rangle$ of the target nucleus.

Due to the spherical symmetry of $|0\rangle$ (we are dealing with closed shell nuclei), we shall simply show the calculations with R_x.

First we calculate the normalization constant N_x of the operator R_x. It is defined by

$$N_x^2 \langle 0 | R_x^2 | 0 \rangle = 1. \tag{VI-2}$$

Introducing the creation and annihilation operators defined in Eq.(A-III-13), the operator R_x can be written as

$$\begin{aligned} R_x &= \Sigma_i x_i \\ &= \frac{1}{\sqrt{2}\beta} \Sigma_i (a_{xi} + a^+_{xi}) \\ &= A_x + A^+_x \end{aligned} \tag{VI-3}$$

where

$$A_x \equiv \frac{1}{\sqrt{2}\beta} \Sigma_i a_{xi} \tag{VI-4}$$

and then

$$\begin{aligned} \langle 0 | R_x^2 | 0 \rangle &= \langle 0 | A_x^2 + A_x^{+2} + A_x^+ A_x + A_x A_x^+ | 0 \rangle \\ &= \langle 0 | A_x A_x^+ | 0 \rangle \\ &= \langle 0 | A^+_x A_x + [A_x, A^+_x] | 0 \rangle \\ &= \frac{1}{2\beta^2} \sum_1^A i \langle 0 | [a_{xi}, a^+_{xi}] | 0 \rangle \\ &= \frac{A}{2\beta^2} \end{aligned} \tag{VI-5}$$

where we used the fact that:

$$\langle 0 | A_x^{+2} | 0 \rangle = 0 \; ; \quad \langle 0 | A_x^2 | 0 \rangle = 0 ; \; \langle 0 | A^+_x A_x | 0 \rangle = 0$$

Using the result of Eq.(VI-5), from Eq.(VI-2) we finally obtain

$$N_x = N_y = N_z = \beta \sqrt{\frac{2}{A}} \tag{VI-6}$$

where A is the mass number

We wish now to calculate matrix elements of the type

$$N_x \langle 0 | R_x \; V(\underline{r} - \underline{r}_0) | 0 \rangle \tag{VI-7}$$

where we can replace the operator R_x by A_x defined in Eq.(VI-4) since it operates on the ground state from the right.

Then we have

$$\langle 0|R_x V|0\rangle = \langle 0|A_x V|0\rangle = \langle 0|VA_x + [A_x, V]|0\rangle = \langle 0|[A_x, V]|0\rangle \qquad \text{(VI-8)}$$

because $A_x|0\rangle = 0$.

Next we calculate the commutator $[A_x, V]$, using Eq.(VI-4) and the definition of a_{xi} given in Appendix III, and the representation of p_x as

$$p_x = -i\hbar \frac{\partial}{\partial x}$$

$$[A_x, V] = \frac{1}{\sqrt{2}\beta}\left[\sum_i a_{xi}, \sum_j V(r_j - r_0)\right]$$

$$= \frac{1}{\sqrt{2}\beta} \sum_i [a_{xi}, V_i]$$

$$= \frac{1}{\sqrt{2}\beta} \sqrt{\frac{m\omega}{2\hbar}} \left[\left(x_i + \frac{i}{m\omega} p_{xi}\right), V_i\right] \qquad \text{(VI-9)}$$

$$= \frac{1}{\sqrt{2}\beta} \frac{\beta}{\sqrt{2}} \frac{i}{m\omega} [p_{xi}, V_i]$$

$$= \frac{1}{2\beta^2} \frac{\partial V_i}{\partial x_i}$$

Inserting the result of Eq.(VI-9) in Eq.(VI-7) we find:

$$N_x \langle 0|R_x V|0\rangle = \beta \frac{\sqrt{2}}{\sqrt{A}} \frac{4}{2\beta^2} \sum_i \langle i| \frac{\partial V}{\partial x} |i\rangle \qquad \text{(VI-10)}$$

$$= \frac{4}{\sqrt{2}\beta\sqrt{A}} \sum_i \int_{-\infty}^{\infty} \varphi_i(\underline{r}) \frac{\partial V(\underline{r} - \underline{r}_0)}{\partial x} \varphi_i(\underline{r})\, d^3\underline{r}$$

where $|i\rangle$ are now single particle orbital states and the factor 4 comes from the summation over the spin and isospin part of the wave functions. Note that the single particle orbital wave functions $\phi_i(\underline{r})$ are real.

Using the definition of the density function

$$\rho(\underline{r}) = \sum_i |\varphi_i(\underline{r})|^2$$

it follows:

$$\text{R.H.S. of Eq.(VI-10)} = \frac{4}{\beta\sqrt{2A}} \int_{-\infty}^{\infty} \rho(\underline{r}) \frac{\partial V(\underline{r}-\underline{r}_0)}{\partial x} \, d^3\underline{r} \qquad \text{(VI-10')}$$

$$= -\frac{4}{\beta\sqrt{2A}} \int_{-\infty}^{\infty} V(\underline{r}-\underline{r}_0) \frac{\partial \rho(\underline{r})}{\partial x} \, d^3\underline{r}$$

where we have integrated by parts and used the fact that

$$[\rho(\underline{r})\ V\ (\underline{r} - \underline{r}_0)]_{-\infty}^{+\infty} = 0.$$

The analytical expression of the density function and the result of Eq.(VI-10') for ^{16}O and ^{40}Ca are:

^{16}O :

$$\rho(\underline{r}) = \frac{\beta^3}{\pi^{3/2}} e^{-\beta^2\underline{r}^2} (1 + 2\beta^2\underline{r}^2) \qquad \text{(VI-11)}$$

$$N_x \langle 0|R_x V|0\rangle = \sqrt{2}\ \frac{a^3\beta^3}{\alpha^3} V_0 e^{-\beta^2 r_0^2/\alpha} \frac{\beta\mu_0}{\sqrt{\alpha}} \left\{ \frac{2\beta^2 r_0^2}{\alpha} + (4\gamma - 1) \right\} \qquad \text{(VI-12)}$$

^{40}Ca:

$$\rho(\underline{r}) = \frac{\beta^3}{\pi^{3/2}} e^{-\beta^2\underline{r}^2} \left(2\beta^4\underline{r}^4 + \frac{5}{2}\right) \qquad \text{(VI-11')}$$

$$N_x \langle 0|R_x V|0\rangle = \frac{2}{\sqrt{5}} \frac{a^3\beta^3}{\alpha^4} V_0\ e^{-\beta^2 r_0^2/\alpha} \frac{\beta\mu_0}{\sqrt{\alpha}} \times \qquad \text{(VI-12')}$$

$$\times \left\{ \frac{2\beta^4 r_0^4}{\alpha^2} + (10\gamma - 4)\frac{\beta^2 r_0^2}{\alpha} + \left(10\gamma^2 - 5\gamma + \frac{5}{2}\right) \right\}$$

The numerical results for Q_x, Q_y, Q_z are given in Table (VI-1) and (VI-2), together with the results for the full Eq.(VI-1).

As in chapter V we used a path $\underline{r}(t)$ which is a straight line and we performed the calculations for ^{16}O both analytically and numerically and the calculations for ^{40}Ca only numerically.

The centre-of-mass correction to the $1\hbar\omega$ excitation is seen to be quite important.

After the subtraction of the spurious excitations we are left only with the octupole part of the $1\hbar\omega$ transitions, because in the scattering of two T = 0 nuclei we cannot excite the dipole mode.

The role of the octupole mode, together with other collective modes of excitation will be discussed in the next chapter.

VI-3 Corrections to the $2\hbar\omega$ Excitations

We now calculate the centre-of-mass correction to the $2\hbar\omega$ excitations. This means that first of all we have to calculate matrix elements like:

$$N_{xx} \langle 0 | R_x R_x | V 0 \rangle \qquad \text{(a)}$$

and (VI-13)

$$N_{xy} \langle 0 | R_x R_y | V 0 \rangle \qquad \text{(b)}$$

where

$$R_{xx} = \sum_{i=1}^{A} m_i \sum_{j=1}^{A} x_j$$
$$R_{xy} = \sum_{i=1}^{A} m_i \sum_{j=1}^{A} y_j \qquad \text{(VI-14)}$$

Introducing once again the operators Eq.(A-III-13) we can make the substitution:

$$R_x R_x \rightarrow \sum_{1}^{A}{}_{ij} \frac{a_{xi} a_{xj}}{2\beta^2} = A_x A_x \qquad \text{(a)}$$

$$R_x R_y \rightarrow \sum_{1}^{A}{}_{ij} \frac{a_{xi} a_{yj}}{2\beta^2} = A_x A_y \qquad \text{(b)} \qquad \text{(VI-14')}$$

Their normalization constants are

$$N_{xx} = \frac{\sqrt{2}\,\beta^2}{A} \quad ; \quad N_{xy} = \frac{2\beta^2}{A} \qquad \text{(VI-15)}$$

In order to calculate matrix elements like Eq.(VI-12), we notice first that the operators Eq.(VI-13) are tensor operators of second rank.

In Appendix III-2 we prove that if $T_{ij}(\underline{r})$ is a tensor operator of second rank, $V(\underline{r} - \underline{r}_o)$ is a spherical symmetric potential and $|0\rangle$ denotes a spherical symmetric Slater determinant, the following property holds

$$\langle 0 | T_{ij}(\underline{r}) V(\underline{r} - \underline{r}_o) | 0 \rangle = T_{ij}(\tilde{\underline{r}}_o) F(\tilde{\underline{r}}_o) + \delta_{ij} G(\tilde{\underline{r}}_o) \qquad \text{(VI-16)}$$

where $\tilde{\underline{r}}_o = \frac{\beta \underline{r}_o}{\sqrt{\alpha}}$, i = x,y,z; j = x,y,z, and $F(\tilde{\underline{r}}_o)$ and $G(\tilde{\underline{r}}_o)$ are two spherical symmetric functions.

For a fixed potential and a fixed nuclear ground state function, any matrix element of the type of Eq.(VI-16) is then determined once we know the functions $F(\tilde{\underline{r}}_o)$ and $G(\tilde{\underline{r}}_o)$. To obtain them let us introduce the operator Eq.(VI-14'-a) in Eq.(VI-13-a), then:

$$N_{xx} \langle 0 | R_x R_x V | 0 \rangle = N_{xx} \langle 0 | A_x A_x V | 0 \rangle$$

$$= N_{xx} \langle 0 | A_x [A_x, V] | 0 \rangle$$

$$= N_{xx} \langle 0 | [A_x, [A_x, V]] | 0 \rangle$$

$$= 4 N_{xx} \frac{1}{4\beta^4} \sum_i \langle i | \frac{\partial^2 V}{\partial x^2} | i \rangle \qquad \text{(VI-17)}$$

$$= \frac{\sqrt{2}}{A\beta^2} \int_{-\infty}^{\infty} V(\underline{r} - \underline{r}_0) \frac{\partial^2}{\partial x^2} \rho(\underline{r}) \, d^3 \underline{r}$$

In Appendix VI we show in detail how to get Eq.(VI-17).

The analytical forms of Eq.(VI-17) for ^{16}O and ^{40}Ca are:

^{16}O:

$$N_{xx} \langle 0 | R_x R_x V | 0 \rangle = \frac{4 V_0}{\sqrt{2} A} \frac{\alpha^3 \beta^3}{\alpha^{7/2}} e^{-\beta^2 r_0^2/\alpha} \left\{ \frac{2\beta^2 x_0^2}{\alpha} \cdot \left[\frac{2\beta^2 r_0^2}{\alpha} + (4\gamma - 3) \right] - \left[\frac{2\beta^2 \underline{r}_0^2}{\alpha} + (4\gamma - 1) \right] \right\} \qquad \text{(VI-18)}$$

and hence

$$F(\underline{\tilde{r}}_0) = \frac{V_0}{\beta^2} \frac{\alpha^3 \beta^3}{\alpha^{7/2}} e^{-\tilde{r}_0^2} \left\{ 4 \underline{\tilde{r}}_0^2 + 8\gamma - 6 \right\}$$

$$G(\underline{\tilde{r}}_0) = \frac{V_0}{\beta^2} \frac{\alpha^3 \beta^3}{\alpha^{7/2}} e^{-\underline{\tilde{r}}_0^2} \left\{ - \left(2 \underline{\tilde{r}}_0^2 + 4\gamma - 1 \right) \right\} \qquad \text{(VI-19)}$$

^{40}Ca

$$N_{xx} \langle 0 | R_x R_x V | 0 \rangle = \frac{4 V_0}{\sqrt{2} A} \frac{\alpha^3 \beta^3}{\alpha^{9/2}} e^{-\beta^2 \underline{r}_0^2/\alpha} \cdot$$

$$\cdot \left\{ \frac{2\beta^2 x_0^2}{\alpha} \left[\frac{2\beta^4 \underline{r}_0^4}{\alpha^2} + \frac{2\beta^2 \underline{r}_0^2}{\alpha} (5\gamma - 4) \right. \right. \qquad \text{(VI-20)}$$

$$\left. + \left(10\gamma^2 - 15\gamma + \frac{13}{2} \right) \right] - \left(\frac{2\beta^4 \underline{r}_0^4}{\alpha^2} + \frac{2\beta^2 \underline{r}_0^2}{\alpha} (5\gamma - 2) \right.$$

$$\left. \left. + \left(10\gamma^2 - 5\gamma + \frac{5}{2} \right) \right) \right\}$$

and

$$F(\tilde{r}_0) = \frac{V_0}{\beta^2}\,\frac{a^3\beta^3}{\alpha^{9/2}}\,e^{-\tilde{r}_0^2}\left\{4\tilde{r}_0^4 + 4(5\gamma-4)\tilde{r}_0^2 + (20\gamma^2-30\gamma+13)\right\}$$

$$G(\tilde{r}_0) = \frac{V_0}{\beta^2}\,\frac{a^3\beta^3}{\alpha^{9/2}}\,e^{-\tilde{r}_0^2}\left\{-\left[2\tilde{r}_0^4 + (10\gamma-4)\tilde{r}_0^2 + (10\gamma^2-5\gamma+\tfrac{5}{2})\right]\right\} \qquad \text{(VI-21)}$$

APPENDIX VI

Part 1
Proof of Eq.(VI-17).

Let us first calculate the double commutator $\left[A_x,\left[A_x,V\right]\right]$

$$\left[A_x,\left[A_x,V\right]\right]=\frac{1}{2\beta^2}\sum_{ij\kappa}\left[a_{xi},\left[a_{xj},V_\kappa\right]\right]=$$

$$=\frac{1}{2\beta^2}\sum_{ij}\left[a_{xi},\left[a_{xj},V_j\right]\right]=$$

$$=\frac{1}{2\beta^2}\sum_i\left[a_{xi},\left[a_{xi},V_i\right]\right] \qquad \text{(A-VI-1)}$$

$$=\frac{1}{2\beta^2}\frac{m\omega}{2\hbar}\left[\left(x_i+\frac{i}{m\omega}p_{xi}\right),\left[\left(x_i+\frac{i}{m\omega}p_{xi}\right),V_i\right]\right]$$

$$=\frac{1}{2\beta^2}\frac{\beta^2}{2}\left(-\frac{1}{m^2\omega^2}\right)\left[p_{xi},\left[p_{xi},V_i\right]\right]$$

$$=\frac{1}{2\beta^2}\frac{\beta^2}{2}\frac{1}{\beta^4}\frac{\partial^2}{\partial x_i^2}V_i$$

$$=\frac{1}{4\beta^4}\frac{\partial^2}{\partial x_i^2}V_i$$

Using this result in Eq.(VI-17) we obtain

$$N_{xx}\langle 0|R_xR_xV|0\rangle=N_{xx}\langle 0|\left[A_x,\left[A_x,V\right]\right]|0\rangle \qquad \text{(A-VI-2)}$$

$$=\frac{N_{xx}}{\beta^4}\sum_i\langle i|\frac{\partial^2}{\partial x^2}V|i\rangle$$

Here again <i| are the single particle orbital states. Introducing the density function, Eq.(A-IV-2) can be written as

$$N_{xx}\langle 0|R_xR_xV|0\rangle=\frac{N_{xx}}{\beta^4}\int_{-\infty}^{\infty}\rho(\underline{r})\frac{\partial^2V(\underline{r}-\underline{r}_0)}{\partial x^2}\,d^3\underline{r}$$

where we integrated by parts twice and used the fact that both $\rho(\underline{r})$ and $V(\underline{r} - \underline{r}_o)$ vanish at infinity.

Part 2
Proof of

$$\langle 0|T_{ij}(\underline{r})\, V(\underline{r}-\underline{r}_0)|0\rangle = T_{ij}(\underline{r}_0)\, F(\underline{r}_0) + \delta_{ij}\, G(\underline{r}_0) \qquad \text{(A-VI-3)}$$

where

$$T_{ij}(\underline{r}) = \sum_{1}^{A}{}_n\; T_{ij}^{n}(\underline{r}_n)$$

is a tensor operator of 2nd rank given by a sum of single particle operators, and

$$V(\underline{r}-\underline{r}_0) = \sum_n V(|\underline{r}_n - \underline{r}_0|)$$

is a spherical symmetric potential, and $|0\rangle$ is the ground state of a closed shell nucleus, given by a Slater determinant. Then we find

$$\tau_{ij}(\underline{r}_0) \equiv \langle 0|T_{ij}(\underline{r})\, V(|\underline{r}-\underline{r}_0|)|0\rangle \qquad \text{(A-VI-4)}$$

$$= \sum_n \int d^3\underline{r}\; \varphi_n^*(\underline{r})\, T_{ij}(\underline{r})\, V(|\underline{r}-\underline{r}_0|)\, \varphi_n(\underline{r})$$

Let us suppose now that

$$\underline{r}_0 = R\, \underline{r}_0' \quad , \quad \text{i.e.} \quad (\underline{r}_0)_i = R_{ij}\,(\underline{r}_0')_j$$

and

$$\underline{r} = R\, \underline{r}' \qquad \text{(A-VI-5)}$$

where Q is an operator which generates a rotation.

From Eq.(A-VI-4) we get

$$\tau_{ij}(R\,\underline{r}_0') = \sum_n \int \varphi_n^*(\underline{r})\,T_{ij}(\underline{r})\,V(|\underline{r}-R\,\underline{r}_0'|)\,\varphi(r)\,d^3\underline{r} \qquad \text{(A-VI-6)}$$

$$= \sum_n \int \varphi_n^*(R\,\underline{r}')\,T_{ij}(R\,\underline{r}')\,V(|R\,\underline{r}'-R\,\underline{r}_0'|)\,\varphi_n(R\,\underline{r}')\,d^3\underline{r}'$$

where we used

$$d^3\underline{r} = d^3\underline{r}'$$

But due to the rotational invariance of our functions and operators and to the fact that we are dealing with closed shell nuclei, it holds

$$\sum_n \varphi_n^*(\underline{r})\,\varphi_n(\underline{r}) = \sum_n \varphi_n^*(R\,\underline{r}')\,\varphi_n(R\,\underline{r}')$$

$$= \sum_n \varphi_n^*(\underline{r}')\,\varphi_n(\underline{r}') \qquad \text{(A-VI-7)}$$

$$V(|R\,\underline{r}'-R\,\underline{r}_0'|) = V(R\,|\underline{r}'-\underline{r}_0'|) = V(|\underline{r}'-\underline{r}_0'|)$$

$$T_{ij}(\underline{r}) = T_{ij}(R\,\underline{r}') = R_{ii'}\,R_{jj'}\,T_{i'j'}(\underline{r}')$$

Then Eq.(A-VI-6) becomes

$$\tau_{ij}(R\,\underline{r}_0') = R_{ii'}\,R_{jj'}\sum_n \int \varphi_n(\underline{r}')\,T_{i'j'}(\underline{r}')\,V(|\underline{r}'-\underline{r}_0'|)\,\varphi(\underline{r}')\,d^3\underline{r}' \qquad \text{(A-VI-8)}$$

$$= R_{ii'}\,R_{jj'}\,\tau_{i'j'}(\underline{r}_0')$$

Eq.(A-VI-8) shows that $\tau_{ij}(\underline{r}_o)$ transforms as a tensor of 2nd rank, further if $T_{ij}(r)$ is an irreducible tensor, i.e. if

$$\sum_i T_{ii}(r) = 0;$$

then also

$$\sum_i \tau_{ii}(r_o) = 0$$

and $\tau_{ij}(\underline{r}_o)$ transforms as an irreducible tensor of 2nd rank.

$\tau_{ij}(\underline{r}_o)$ must then be the most general second rank tensor, function of a vector $\underline{r}_o$; its form has to be

$$\tau_{ij}(r_o) = T_{ij}(r_o)\, F(r_o) + \delta_{ij}\, G(r_o) \qquad \text{(A-VI-9)}$$

since $T_{ij}(\underline{r}_o)$ $F(\underline{r}_o)$ and δ_{ij} $G(\underline{r}_o)$, with $F(\underline{r}_o)$ and $G(\underline{r}_o)$ rotational invariant functions, are the only two second rank tensors we can construct out of a vector $\underline{r}_o$.

TABLE (VI-1)

^{16}O

b = 0 fm

E_α (MeV)	$1\hbar\omega$ Numerical	C.M.1 Analytical	C.M.1 Numerical	$1\hbar\omega$-C.M.1 Numerical	$2\hbar\omega$	C.M.2	$2\hbar\omega$-C.M.2
10	24.12	16.20	16.10	8.02	0.02	0.0005	0.02
20	66.52	59.20	59.08	7.74	1.84	0.0003	1.84
30	67.60	60.64	60.60	7.00	7.60	0.05	7.55
40	57.44	51.40	51.38	6.06	13.80	0.20	13.60
50	47.04	42.00	41.97	5.07	17.68	0.32	17.36
60	38.48	34.27	34.27	4.20	19.32	0.40	18.92
70	31.80	29.04	28.25	3.55	19.68	0.44	19.24
80	26.56	23.56	23.57	2.99	19.28	0.45	18.83
90	22.48	19.92	19.92	2.56	18.56	0.44	18.12
100	19.20	17.00	17.02	2.18	17.72	0.43	17.29
110	16.60	14.68	14.69	1.91	16.84	0.42	16.42
120	14.48	12.80	12.80	1.68	16.04	0.40	15.64

Centre-of-mass corrections to the results of Table V-1

Units are (MeV·10^{-22} sec)

TABLE(VI-2)

^{40}Ca

b = 0 fm

E_α (MeV)	$1\hbar\omega$	C.M.1	$1\hbar\omega$-C.M.1	$2\hbar\omega$	C.M.2	$2\hbar\omega$-C.M.2
10	59.40	34.31	25.09	7.23	0.02	7.21
20	98.99	71.10	27.89	12.30	0.009	12.29
30	89.09	65.01	24.08	26.51	0.02	26.49
40	71.32	51.92	19.04	35.99	0.08	35.91
50	56.34	40.86	15.48	38.94	0.13	38.81
60	44.99	32.52	12.47	38.31	0.15	38.16
70	36.51	26.33	10.18	36.25	0.16	36.09
80	30.11	21.67	8.44	33.84	0.15	33.69
90	25.21	18.11	7.10	31.51	0.14	31.37
100	21.38	15.33	6.05	29.40	0.14	29.36
110	18.35	13.15	5.20	27.55	0.13	27.42
120	15.91	11.38	4.53	25.94	0.12	25.82

Centre-of-mass corrections to the results of Table V-2

Units are (MeV·10^{-22} sec)

Chapter VII

THE ROLE OF COLLECTIVE EXCITATIONS

The purpose of this chapter is to establish the connection between our description of the excitations which produce the imaginary part of the optical potential, and the collective description of them.

In section 1 we give a short review of the theoretical and experimental status of collective modes of nuclei. We present our calculations in section 2.

VII-1 Review of the Theoretical and Experimental Situation[28,29,30,31,32,33]

So far we have been discussing the target excitations in terms of one particle-one hole excitations in the framework of the H.O. S.M.

However, it is known that a coherent superposition of single particle excitations gives rise to collective vibrational modes which are shape oscillations of the nucleus. They are known as giant resonances and can be classified as isoscalar or isovector depending on whether the neutrons and protons move in phase or out of phase.

According to the H.O.S.M., vibrational states will group at excitations energies

$$E_x = N \hbar\omega \quad , \quad N = 0, 1, 2, 3, \ldots$$

In fig.(VIII-1) the schematic level sequence of the H.O.S.M. is presented again and some possible transitions are indicated.

From transitions with $\Delta N = 1$ the so-called giant dipole resonance (G.D.R.) is obtained. The G.D.R. has been interpreted as a vibration of the neutrons against the protons; therefore it is characterised by T = 1

and is an isovector collective state.

According to the H.O.S.M. it should be located at $E_x = 1\hbar\omega \sim 40\ A^{-1/3}$ MeV, but it has been found experimentally at $E_x \simeq 77\ A^{-1/3}$ MeV.

The apparent discrepancy is due to the fact that in an isovector mode the nuclear interaction is repulsive thus increasing the expected excitation energy.

The giant quadrupole resonance (G.Q.R.) comes from transitions with $\Delta N = 2$, ($E_x = 2\hbar\omega$), and it can exist both with $T = 0$ and $T = 1$. There is actually also another quadrupole resonance coming from the transitions with $\Delta N = 0$, ($E_x = 0\hbar\omega$), which correspond to transition of a nucleon between two subshells of the same major shell.

The H.O.S.M. estimate for the excitation energy would give $E_x \simeq 80\ A^{-1/3}$ MeV, while experimentally the isoscalar G.Q.R. has been observed at $E_x \simeq 63\ A^{-1/3}$ MeV. The difference in this case reflects the fact that in the isoscalar mode the nuclear interaction is attractive and hence the excitation energy is pushed down.

Two other collective modes, the monopole and octupole ones, are also possible, although they have not yet been well identified experimentally. The monopole resonance (E0) belongs to the $2\hbar\omega$ excitation; it is very interesting as it is a compressional mode: its properties could give a measure of the compressibility of the nuclear matter.

The octupole mode comes partially from the $1\hbar\omega$ excitations and partially from the $3\hbar\omega$ ones. It can exist both as isoscalar and isovector.

A better estimate of the excitation energy can be obtained using the Bohr and Mottelson[28] model of collective vibrational modes.

The model assumes that the oscillation in the nucleonic density, in a system of independent particles, produces a variation in the average

one-body potential. As a consequence, the change of the one-body potential induces excitations in the motion of nucleons. When the induced density variations are exactly those needed to generate the oscillator potential, a self-sustained collective motion is realised.

The situation is summarised in Tables (VII-1), (VII-2).

VII-2 Collective excitations and the imaginary part of the O.P.

In order to understand how the absorption of flux from the elastic channel is affected by the presence of collective excitations, we have calculated an expression such as Eq.(III-3), in which the only excited states included are those obtained by operating on the ground state $|0\rangle$ with a tensor operator $O_{ijk...}$ defined in Eq.(VII - 2).

The new formula is

$$\tilde{O}(r_0) = -\frac{1}{2\hbar}\int_{-\infty}^{\infty} dt \int_{-\infty}^{\infty} dt' \, N_0^2 \langle 0| V(\underline{r}-\underline{r}_0) O^{+}_{ijk...} |0\rangle\langle 0| O_{ijk...} V(\underline{r}'-\underline{r}'_0) |0\rangle \times e^{i\bar{\omega}(t-t')}, \qquad \text{(VII-1)}$$

where $O_{ijk...}$ is a tensor operator of rank m defined[34] as a set of 3^m operators which under rotation transform according to

$$O'_{ijk...} = \sum_{\ell mn...} a_{i\ell}\, a_{jm}\, a_{kn}\, O_{\ell mn} \qquad \text{(VII-2)}$$

and $\bar{\omega} = m\omega$.

For m = 1 Eq.(VII-2) gives the centre-of-mass operator $\underline{R}$, whose effect we already discussed. In the elastic scattering of T = 0 nuclei the G.D.R. cannot be excited, therefore after the centre-of-mass subtraction the strength of the $1\hbar\omega$ excitations in our calculations is to be attributed to the octupole mode.

For m = 2 the spurious centre-of-mass state is generated by the second rank centre-of-mass operator R^2 as discussed in Chapter VI. The giant quadrupole state is generated by the quadrupole operator

$$Q_{\alpha\beta} = \sum_{1}^{A} i \; 3 r_{i\alpha} r_{i\beta} - r_i^2 \delta_{\alpha\beta} \quad ; \; \alpha, \beta \equiv x, y, z, \qquad \text{(VII-3)}$$

and the giant monopole state by the scalar operator

$$M = \sum_{1}^{A} i \; r_i^2 \qquad \text{(VII-4)}$$

Only those parts of $Q_{\alpha\beta}$ and M which include the $2\hbar\omega$ excitations should be included. It is most convenient to use the representation of the giant quadrupole and monopole states by the creation and annihilation operators defined in Appendix III.

Hence the monopole state is

$$|M\rangle = N_M \left(\sum_i a_{ix}^{+2} + a_{iy}^{+2} + a_{iz}^{+2} \right) |0\rangle \qquad \text{(VII-5)}$$

and the five components of the quadrupole state can be taken as

$$|Q_1\rangle = N_{Q_1} \left(\sum_i 2 a_{ix}^{+2} - a_{iy}^{+2} - a_{iz}^{+2} \right) |0\rangle \qquad \text{(a)} \qquad \text{(VII-6)}$$

$$|Q_2\rangle = N_{Q_2} \left(\sum_i a_{iy}^{+2} - a_{iz}^{+2} \right) |0\rangle \qquad \text{(b)}$$

$$|Q_3\rangle = N_{Q_3} \left(\sum_i a_{ix}^{+} a_{iy}^{+} \right) |0\rangle \qquad \text{(c)}$$

$$|Q_4\rangle = N_{Q_4} \left(\sum_i a_{iy}^{+} a_{iz}^{+} \right) |0\rangle \qquad \text{(d)}$$

$$|Q_5\rangle = N_{Q_5} \left(\sum_i a_{ix}^{+} a_{iz}^{+} \right) |0\rangle \qquad \text{(e)}$$

The normalization constants of the above states are calculated in Appendix VII.

In order to calculate Eq.(VII-1) for the quadrupole and monopole giant resonances, we need the matrix element of the potential $V(|\underline{r} - \underline{r}_o|)$ between the ground state and the states of Eqs.(VII-5) and (VII-6).

The matrix elements can be calculed as follows

$$\begin{aligned}
\langle \alpha\beta | V(\underline{r}-\underline{r}_0) | 0 \rangle &= \langle 0 | \textstyle\sum_i a_{i\alpha} a_{i\beta} \sum_j V(\underline{r}_j - \underline{r}_0) | 0 \rangle \\
&= \langle 0 | \textstyle\sum_i [a_{i\alpha} a_{i\beta}, V(\underline{r}_j - \underline{r}_0)] | 0 \rangle \\
&= \langle 0 | \textstyle\sum_i \left(a_{i\alpha} [a_{i\beta}, V] + [a_{i\alpha}, V] a_{i\beta} \right) | 0 \rangle \\
&= \hbar \langle 0 | \textstyle\sum_i a_{i\alpha} \frac{\partial V}{\partial r_{i\beta}} + \frac{\partial V}{\partial r_{i\alpha}} a_{i\beta} | 0 \rangle \\
&= \hbar l \int \left(r_\alpha \frac{\partial V}{\partial r_\beta} + r_\beta \frac{\partial V}{\partial r_\alpha} \right) \rho(\underline{r}) d^3\underline{r} + \\
&\quad + \hbar^2 \left[\langle 0 | \frac{\partial}{\partial r_\alpha} \left(\frac{\partial V}{\partial r_\beta} | 0 \rangle \right) + \langle 0 | \frac{\partial V}{\partial r_\alpha} \left(\frac{\partial}{\partial r_\beta} | 0 \rangle \right) \right] \\
&= \frac{1}{2} \int \left(r_\alpha \frac{\partial V}{\partial r_\beta} + r_\beta \frac{\partial V}{\partial r_\alpha} \right) \rho(\underline{r}) d^3\underline{r} + \frac{\hbar^2}{2} \times \\
&\qquad \times \langle 0 | \frac{\partial^2 V}{\partial r_\alpha \partial r_\beta} - \frac{\partial^2 V}{\partial r_\beta \partial r_\alpha} | 0 \rangle \qquad \text{(VII-7)} \\
&= \frac{1}{2} \int \left(r_\alpha \frac{\partial V}{\partial r_\beta} + r_\beta \frac{\partial V}{\partial r_\alpha} \right) \rho(\underline{r}) d^3\underline{r} \\
&= r_{0\alpha} r_{0\beta} F(\underline{r}_0) + \delta_{\alpha\beta} G(r_0)
\end{aligned}$$

where we used

$$a_\alpha = l r_\alpha + \hbar \frac{\partial}{\partial r_\alpha} \quad \text{and} \quad [a_\alpha, a_\alpha^+] = 2\hbar l = 1 \quad \therefore \quad l = \frac{1}{2\hbar}$$

$\rho(\underline{r})$ is the nuclear density function defined as

$$\rho(\underline{r}) = \sum_1^A i \; |\varphi_i(\underline{r})|^2$$

Finally we get:

$$
\begin{aligned}
&\langle \Pi_1 | V(\underline{r}-\underline{r}_0)|0\rangle = N_\Pi \left[r_0^2 F(\underline{r}_0) + 3 G(\underline{r}_0)\right] \\
&\langle Q_1 | V(\underline{r}-\underline{r}_0)|0\rangle = N_{a_1} (2x_0^2 - y_0^2 - z_0^2) F(\underline{r}_0) \\
&\langle Q_2 | V(\underline{r}-\underline{r}_0)|0\rangle = N_{a_2} (y_0^2 - z_0^2) F(\underline{r}_0) \\
&\langle Q_3 | V(\underline{r}-\underline{r}_0)|0\rangle = N_{a_3} x_0 y_0 F(\underline{r}_0) \\
&\langle Q_4 | V(\underline{r}-\underline{r}_0)|0\rangle = N_{a_4} y_0 z_0 F(\underline{r}_0) \\
&\langle Q_5 | V(\underline{r}-\underline{r}_0)|0\rangle = N_{a_5} x_0 z_0 F(\underline{r}_0)
\end{aligned}
\qquad \text{(VII-8)}
$$

The analytical expressions of $F(\underline{r}_0)$ and $G(\underline{r}_0)$ are

^{16}O

$$F(\underline{r}_0) = 2V_0 \frac{a^3\beta^3}{\alpha^{7/2}} e^{-\beta^2 r_0^2/\alpha} \left\{ 4\frac{\beta^2 r_0^2}{\alpha} + (12\gamma - 2) \right\} \qquad \text{(VII-9)}$$

$$G(\underline{r}_0) = -2V_0 \frac{a^3\beta^3}{\alpha^{7/2}} e^{-\beta^2 r_0^2/\alpha} \left\{ 2\frac{\beta^2 r_0^2}{\alpha} + (6\gamma + 1) \right\} \qquad \text{(VII-10)}$$

^{40}Ca

$$F(\underline{r}_0) = 2V_0 \frac{a^3\beta^3}{\alpha^{9/2}} e^{-\beta^2 r_0^2/\alpha} \left\{ 4\frac{\beta^4 r_0^4}{\alpha^2} + (28\gamma - 8)\frac{\beta^2 r_0^2}{\alpha} + (40\gamma^2 - 18\gamma + 5) \right\} \qquad \text{(VII-9')}$$

$$G(\underline{r}_0) = -2V_0 \frac{a^3\beta^3}{\alpha^{9/2}} e^{-\beta^2 r_0^2/\alpha} \left\{ 2\frac{\beta^4 r_0^4}{\alpha^2} + 14\gamma\frac{\beta^2 r_0^2}{\alpha} + (16\gamma^2 + 5\gamma + \frac{1}{2}) \right\} \qquad \text{(VII-10')}$$

and the expressions for the density function have already been given in Eqs.(VI-11,11').

Using the above matrix elements in Eq.(VII-1) we have calculated the quadrupole and monopole contribution to the $2\hbar\omega$ excitations in ^{16}O and ^{40}Ca.

Table (VII-3-4) shows the results obtained using a straight line trajectory, while the results of Table (VII-5-6) were obtained using a classical trajectory in the folding potential. The way in which the classical trajectory has been calculated is described in the next chapter.

The quadrupole excitation which we have calculated belongs to the $2\hbar\omega$ transition and hence it represents the G.Q.R. In the H.O.S.M. the

G.Q.R. is obtained at an energy $E_x = 2\hbar\omega \simeq 80\ A^{-1/3}$ MeV. However, as we have already pointed out, the G.Q.R. has been experimentally located at an energy $E_x \sim 63\ A^{-1/3}$ MeV.

In order to see if this shift in energy affects the probability of excitation of the resonance, we repeated our calculation using an H.O. frequency ω' such that $2\hbar\omega' = 63\ A^{-1/3}$ MeV.

But it is known that the quadrupole operator satisfies the energy-weighted sum rule

$$S = \sum_n (E_n - E_0) |\langle n|Q|0\rangle|^2$$

$$= \langle 0|Q(H-E_0)|Q|0\rangle$$

$$= \frac{1}{2}\langle 0|[Q,[H,Q]]|0\rangle$$

$$= \frac{\hbar^2 A}{m}\langle 0|\sum_i r_i^2|0\rangle \qquad \text{(VII-11)}$$

$$= \frac{\hbar^2 A}{m}\ \frac{3}{5}\ R^2$$

where H is the many particle hamiltonian and $|n\rangle$ are exact eigenstates of H with eigenvalues E_n. Q is any of the components of the quadrupole operator, e.g.

$$Q = \sum_1^A{}_i\ (2x_i^2 - y_i^2 - z_i^2)$$

The oscillator strength associated with the quadrupole resonance is then

$$S_a = E_a |\langle q|Q|0\rangle|^2 \qquad \text{(VII-12)}$$

where $|q\rangle$ is the quadrupole resonance state. The energy of the resonance can be shifted from $E_a = 2\hbar\omega$ to $E_{Q'} = 2\hbar\omega'$ provided that the strength S_Q remains the same, i.e.

$$S_{a'} = E_{a'} |\langle q' | Q | 0 \rangle|^2 = S_a$$

from which one gets

$$|\langle q' | Q | 0 \rangle|^2 = \frac{E_a}{E_{a'}} |\langle q | Q | 0 \rangle|^2$$

In our calculation the above correction has been made simply renormalizing the state $N_{Q_{ij}} \langle 0|Q_{ij}$ by a factor $\sqrt{E_Q/E_{Q'}}$.

The results obtained in this way are shown in the third column of tables (VII-3,4).

The results of Tables (VII-3,4) were obtained using a straight line trajectory with constant velocity. In this case the giant quadrupole and monopole resonances represent a very big part of the $1\hbar\omega$ excitations. For many incident energies of the α-particle they are more than the 90% of the total $2\hbar\omega$ corresponding values.

On the other hand, in the case in which the path is the classical trajectory (Tables VII-5 - 6) the collective excitations are very small compared to the total $2\hbar\omega$ values. The reason for obtaining such a small collective motion can be explained comparing the crossing time of the α-particle inside the real potential of the target with the period of the shell model harmonic oscillator. For ^{40}Ca the period of the oscillator is $T_{H.O.} = \frac{2\pi}{\omega} = 3.54 \cdot 10^{-22}$ sec.* (at $E_\alpha = 100$ MeV, say). Hence the ratio between the two time is $T_{H.O.}/T$ crossing ~ 2.

*The crossing time of the α-particle does not depend very much on the incident energy, since it is accelerated by a potential of the order of -300 MeV. It is $T_{crossing} \sim 1.5 \cdot 10^{-22}$ sec.

In a simple intuitive picture we can imagine that the target receives a push when the α-particle comes in and it starts to deform along the α-incident direction, but before it can deform completely it receives another push in the opposite direction from the α-particle which is now going out.

There is therefore a kind of cancellation effect and no collective motion can be seen.

Brink and Mavrommatis have calculated the time integral of the imaginary potential using the collective model to describe the target. They also found[43] that when $T_{H.O.}/T$ crossing ~ 2 the collective excitations are strongly reduced.

In Tables (VII-3,4) the column marked $\tilde{Q}$ shows the results obtained for $-\int \mathrm{Im}\, V_{opt}$ when only the giant quadrupole state is included and its energy is taken from the experimental value $E_x = 2\hbar\omega' \sim 63\, A^{-\frac{1}{3}}$ MeV. From Eq.(V-8') we know that when the trajectory is a straight line, as in this case, the time integral of the imaginary potential is given by a function

$$F(d) \propto \frac{1}{\omega_{\kappa n}^2} \frac{\omega_{\kappa n}^2}{v^2} f\left(\frac{\omega_{\kappa n}}{v}\right)$$

where $d \propto \omega_{kn}/v$, $\omega_{kn} = N\omega$ with $N = 1,2,..$, and v is the velocity of the α-particle.

The shift in the energy of the G.Q.R. corresponds to a change in ω such that $\left(\frac{\omega}{\omega'}\right)^2 = \left(\frac{80}{63}\right)^2 \sim 1.6$. The maximum of the above function occurs to an energy $E_M = \frac{1}{2} m v_M^2$ and is

$$\pi_{ax} = \frac{1}{\omega_{\kappa n}^2} \frac{\omega_{\kappa n}^2}{v_M^2} f\left(\frac{\omega_{\kappa n}}{v_M}\right)$$

If we shift the energy and renormalize the quadrupole state by $\sqrt{E_Q/E_{Q'}} = \sqrt{1.27}$, we obtain a new maximum

$$M'_{a\lambda} = \frac{1}{\omega'^2_{\pi\nu}} \frac{\omega'^2_{\pi\nu}}{\nu^2_{n'}} f\left(\frac{\omega_{\pi'\nu}}{\nu_{n'}}\right) \frac{\bar{E}a}{\bar{E}a'}$$

with $E_{M'} = E_M/1.6$ and $M'_{a\lambda} = M_{a\lambda} \cdot 1.6 \cdot 1.27$ which agrees with the results $\tilde{Q}$ of Tables (VII-3,4) for the position and value of the new maximum.

APPENDIX VII

We wish to calculate the normalization constants of the giant monopole and quadrupole states given in Eqs.(VII-5,6).

Let us first consider a state

$$|\alpha\beta\rangle = \sum_{1}^{A} i\ a_{i\alpha}^{+}\, a_{i\beta}^{+}\, |0\rangle$$

then we have

$$\begin{aligned}
\mathcal{N}_{\alpha\beta} \equiv \langle\alpha\beta|\alpha\beta\rangle &= \langle 0|\bar{\Sigma}_i a_{i\alpha}\, a_{i\beta}\, \bar{\Sigma}_i a_{i\alpha}^{+}\, a_{i\beta}^{+}\, |0\rangle \\
&= \langle 0|\bar{\Sigma}_i \left[a_{i\alpha}\, a_{i\beta},\ a_{i\alpha}^{+}\, a_{i\beta}^{+}\right]|0\rangle \\
&= \langle 0|\bar{\Sigma}_i \left(a_{i\alpha}\left[a_{i\beta}, a_{i\alpha}^{+} a_{i\beta}^{+}\right] + \left[a_{i\alpha}, a_{i\alpha}^{+} a_{i\beta}^{+}\right] a_{i\beta}\right)|0\rangle \\
&= \langle 0|\bar{\Sigma}_i \left(a_{i\alpha} a_{i\alpha}^{+} + a_{i\beta}^{+}\, a_{i\beta}\right)|0\rangle \\
&= \langle 0|\bar{\Sigma}_i \left(a_{i\alpha}^{+} a_{i\alpha} + \left[a_{i\alpha}, a_{i\alpha}^{+}\right] + a_{i\beta}^{+}\, a_{i\beta}\right)|0\rangle \\
&= \langle 0|\bar{\Sigma}_i \left(n_{i\alpha} + n_{i\beta} + 1\right)|0\rangle \\
&= \langle 0|\bar{\Sigma}_i \left(2 n_{i\alpha} + 1\right)|0\rangle \\
&= \langle 0|\bar{\Sigma}_i \left(\tfrac{2}{3} n_i + 1\right)|0\rangle \\
&= \tfrac{2}{3} N + A
\end{aligned}$$

where $a_{i\alpha}^{\dagger}\, a_{i\alpha}$ is the number operator in state i and N

$$N = \Sigma_i n_i \quad \begin{cases} = 12 & {}^{16}O \\ = 60 & {}^{40}Ca \end{cases}$$

A is the mass number.

Similarly

$$\mathcal{N}^{\sigma}_{\alpha\alpha} = 2\left(\frac{2}{3}N + A\right) = 2\,\mathcal{N}^{\sigma}_{\alpha\beta}$$

For the monopole state $|M\rangle$ we obtain

$$N_\pi^{\,2} \langle \pi | \pi \rangle = 1$$

$$N_M^{\,2}\; 3\,\mathcal{N}^{\sigma}_{\alpha\alpha} = 1 \quad \longrightarrow \quad N_\pi = \frac{1}{\sqrt{6\,\mathcal{N}^{\sigma}_{\alpha\beta}}} = \frac{1}{\sqrt{6\left(\frac{2}{3}N+A\right)}} = \frac{1}{\sqrt{2(2N+3A)}}$$

And for the quadrupole components

$$N_{Q_1}^{2} \langle Q_1 | Q_1 \rangle = 1$$
$$N_{Q_1}^{2}\; 6\,\mathcal{N}^{\sigma}_{\alpha\alpha} = 1 \quad \longrightarrow \quad N_{Q_1} = \frac{1}{\sqrt{12\,\mathcal{N}^{\sigma}_{\alpha\beta}}} = \frac{1}{\sqrt{4(2N+3A)}}$$

$$N_{Q_2}^{2} \langle Q_2 | Q_2 \rangle = 1$$
$$N_{Q_2}^{2}\; 2\,\mathcal{N}^{\sigma}_{\alpha\alpha} = 1 \quad \longrightarrow \quad N_{Q_2} = \frac{1}{\sqrt{4\,\mathcal{N}^{\sigma}_{\alpha\beta}}} = \sqrt{\frac{3}{4(2N+3A)}}$$

$$N_{Q_3}^{2} \langle Q_3 | Q_3 \rangle = 1$$
$$N_{Q_3}^{2}\; \mathcal{N}^{\sigma}_{\alpha\beta} = 1 \quad \longrightarrow \quad N_{Q_3} = \frac{1}{\sqrt{\mathcal{N}^{\sigma}_{\alpha\beta}}} = \sqrt{\frac{3}{(2N+3A)}}$$

and

$$N_{Q_4} = N_{Q_5} = N_{Q_3} = \sqrt{\frac{3}{(2N+3A)}}$$

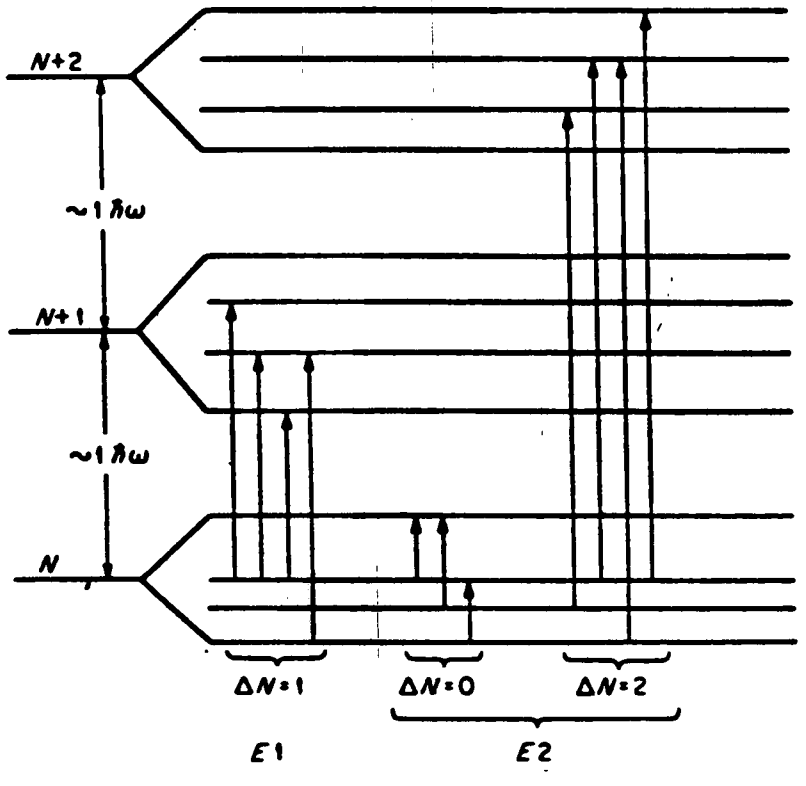


FIG.(VII-1)

Schematic level sequence of the H,O.S.M., some possible transitions are indicated

TABLE VII-1

H.O.S.M. Transition	Name of Resonance	E.W.S.R.	Excited State	Excitation		Energy(MeV) Experimental
				H.O.S.M.	Bohr and Mottelson	
$\Delta N = 0$	Quadrupole (E2) low-frequency $T=0$	20 ÷ 30%	2^+ (low lying)	$0\hbar\omega$	$25A^{-\frac{1}{2}}$	
$\Delta N = 1$	G.D.R.(E1) $T=1$	$\sim$ 100%	1^-	$1\hbar\omega \simeq 40A^{-1/3}$	$78A^{-1/3}$	$77A^{-1/3}$
	Octupole(E3) low-frequency $T=0$	20 ÷ 30%	3^-			$30A^{-1/3}$
	Octupole(E3) low-frequency $T=1$					$64.7A^{-1/3}$
$\Delta N = 2$	Quadrupole (E2) (high-frequency) IS G.Q.R. $T=0$ IV G.Q.R. $T=1$	A < 40 < 30% 40 < A < 100 60% A > 100 90% 60%	2^+	$2\hbar\omega \simeq 80A^{-1/3}$	$58A^{-1/3}$ $135A^{-1/3}$	$63A^{-1/3}$ $120A^{-1/3}$
	Monopole (E0) $T=0$	$\sim$ 10%(?)	0^+			$77A^{-1/3}$
$\Delta N = 3$	Octupole(E3) (high-frequency) $T=0$	75%	3^-	$3\hbar\omega \simeq 120A^{-1/3}$		$110A^{-1/3}$

TABLE VII-2

GIANT QUADRUPOLE RESONANCE

Nucleus	Excitation Energy (MeV)	Γ (MeV)	Experiment	Reference
^{16}O	21	7	(α,α'), E_α = 147 MeV	(31)
^{40}Ca	18	3.5	(α,α'), E_α = 96.9 MeV	(33)

CAPTIONS FOR TABLES (VII-3,4)

1st column — α-particle incident energy in MeV

2nd column — $-\int \mathrm{Im}\, V_{opt}\, dt$ in $\left[\mathrm{MeV}\ 10^{-22}\ \mathrm{sec}\right]$ from Eq.(III-19) including only $2\hbar\omega$ excitations

3rd column — $-\tilde{O}(\underline{r}_o)$ from Eq.(VII-1) in $\left[\mathrm{MeV}.10^{-22}\ \mathrm{sec}\right]$ for the giant quadrupole resonance with the energy shift described at page 82, Chapter VII.

4th column — $-\tilde{O}(r_o)$ from Eq. (VII-1) in $\mathrm{MeV}.10^{-22}$ sec for the giant quadrupole resonance.

5th column — The same as column 4th but for the giant monopole resonance

6th column — Sum of the results of column 4th and 5th

7th column — Percent of the collective states contained in the total $2\hbar\omega$ excitations

TABLE VII-3

^{16}O

b = 0 fm

E_α (MeV)	$2\hbar\omega$	$\tilde{Q}$	Quadrupole	Monopole	Q + M	$\frac{Q + M}{2\hbar\omega}$ 100
10	0.02	0.09	0.00047	0.00046	0.00093	4.7
20	1.84	6.46	0.36	0.29	0.65	35.3
30	7.60	10.38	2.62	2.98	5.60	73.7
40	13.80	8.64	4.59	7.19	11.78	85.4
50	17.68	5.74	5.07	10.79	15.86	89.7
60	19.32	3.40	4.58	13.20	17.78	92.0
70	19.68	1.83	3.73	14.58	18.31	93.0
80	19.28	0.87	2.85	15.24	18.09	93.8
90	18.56	0.34	2.08	15.42	17.50	94.3
100	17.72	0.09	1.47	15.30	16.77	94.6
110	16.84	0.004	1.00	15.00	16.00	95.0
120	16.04	0.01	0.65	14.59	15.24	95.0

Straight line trajectories

TABLE VII-4

^{40}Ca

b = 0 fm

E_α (MeV)	$2\hbar\omega$	$\tilde{Q}$	Quadrupole	Monopole	Q + M	$\frac{Q + M}{2\hbar\omega}$ 100
10	7.23	0.32	0.12	0.15	0.27	3.7
20	12.30	18.64	1.66	0.38	2.04	16.6
30	26.51	19.62	8.15	5.72	13.87	52.3
40	35.99	12.37	10.47	11.91	22.38	62.2
50	38.94	6.50	9.27	15.77	25.04	64.4
60	38.31	2.99	7.03	17.57	24.60	64.2
70	36.25	1.15	4.92	18.08	23.00	63.4
80	33.84	0.3	3.25	17.89	21.14	62.5
90	31.51	0.02	2.05	17.33	19.38	61.5
100	29.40	0.03	1.22	16.60	17.82	60.6
110	27.55	0.02	0.68	15.81	16.49	59.9
120	25.94	0.44	0.33	15.01	15.34	59.1

Straight line trajectories

TABLE VII-3

^{40}Ca

b(fm)	Q	M	Q + M	2ħω	Q	M	Q + M	2ħω	Q	M	Q + M	2ħω
0	0.47	0.71	1.18	12.7	0.64	0.46	1.10	11.77	0.46	0.52	0.98	10.65
1	0.26	0.91	1.17	12.6	0.41	0.45	0.86	11.56	0.34	0.33	0.67	10.29
2	0.48	0.27	0.75	12.5	0.24	0.22	0.46	10.96	0.21	0.05	0.26	9.27
3	0.15	0.37	0.52	12.1	0.22	0.03	0.25	10.23	0.25	0.01	0.26	7.99
4	0.27	0.06	0.33	11.6	0.29	0.01	0.30	9.41	0.14	0.03	0.17	6.83
5	0.35	0.002	0.35	11.2	0.20	0.04	0.24	8.92	0.009	0.003	0.01	6.86
5.2	0.29	0.002	0.31	11.2	0.16	0.04	0.20	8.95	0.003	0.0001	0.004	7.28
5.4	0.37	0.002	0.37	11.1	0.13	0.03	0.16	9.03	0.0009	0.0004	0.001	8.03
5.6	0.27	0.04	0.31	11.0	0.10	0.03	0.13	9.22	0.0011	0.00008	0.0002	9.39
5.8	0.32	0.03	0.35	11.0	0.07	0.02	0.09	9.51	$1.5\ 10^{-4}$	$0.7\ 10^{-4}$	$2.2\ 10^{-4}$	12.10
6	0.36	0.02	0.38	11.0	0.05	0.01	0.06	9.98	$0.25\ 10^{-6}$	$0.13\ 10^{-6}$	$0.38\ 10^{-6}$	19.32
6.2	0.34	0.03	0.37	11.0	0.03	0.01	0.04	10.71	$0.0\ 10^{-8}$	0.0	0.0	8.22
6.4	0.23	0.05	0.28	11.1	0.01	0.01	0.02	11.98	0.0	0.0	0.0	1.15
7	0.0	0.0	0.0	0.01	0.00	0.00	0.00	0.09	0.0	0.0	0.0	0.10
8	0.0	0.0	0.0	0.0003	0.00	0.00	0.00	0.002	0.0	0.0	0.0	0.0039
	E_α = 30 MeV				E_α = 56 MeV				E_α = 104 MeV			

Classical trajectories

TABLE VII-6

^{16}O E_α = 104 MeV

b (fm)	$2\hbar\omega$	Q	M	Q + M
0	7.62	0.46	0.87	1.33
1	7.18	0.28	0.42	0.7
2	5.98	0.24	0.008	0.25
3	5.11	0.15	0.02	0.17
4	6.76	0.003	0.001	0.004
5	1.09	0.0	0.0	0.0
6	0.029	0.0	0.0	0.0
7	0.0009	0.0	0.0	0.0
8	0.00002	0.0	0.0	0.0

Classical trajectories

Chapter VIII

SEMICLASSICAL TREATMENT OF RELATIVE MOTION

In this chapter we drop the simple approximation of a straight line trajectory introduced in chapter V, section 2, and proceed to the solution of the classical equation of motion (V-14).

We already know from classical mechanics that central force motion is always motion in a plane; the classical trajectory of the α-particle is then given by the solution of the equation of motion:

$$\mu \ddot{x} = -\frac{\partial V(r)}{\partial x}$$
$$\mu \ddot{y} = -\frac{\partial V(r)}{\partial y} \qquad \text{(VIII-1)}$$

where we used cartesian coordinates for semplicity and uniformity with our previous calculations.

The potential that generates the motion is:

$$V(\underline{r}) = V_R(\underline{r}) + V_C(\underline{r}) \qquad \text{(VIII-2)}$$

$V_R(\underline{r})$ is the real part of our optical potential in 1st order perturbation theory and is given by the folding procedure;

$$V_R(\underline{r}_0) = \langle 0 | V(\underline{r} - \underline{r}_0) | 0 \rangle$$
$$= \sum_i \int \varphi_i(\underline{r}) V(\underline{r} - \underline{r}_0) \varphi_i(\underline{r}) \, d^3\underline{r} \qquad \text{(VIII-3)}$$
$$= \int \rho(\underline{r}) V(\underline{r} - \underline{r}_0) \, d^3\underline{r}$$

$V_c(r)$ is the Coulomb potential: if we use the uniformly charged sphere approximation for the target nucleus, its form is:

$$V_c(r) = \begin{cases} \frac{z_1 z_2 e^2}{2 R_c}\left(3 - \frac{r^2}{R_c^2}\right) & r \le R_c \\ \frac{z_1 z_2 e^2}{r} & r > R_c \end{cases} \qquad \text{(VIII-3)}$$

$R_c \equiv$ charge radius = mass radius.

If we want to take into account the actual charge distribution in the target, we can calculate directly the force due to the Coulomb potential in the following way:

$$F_c(r) = e^2 z_1 \frac{Q(r)}{r^2} \; ; \qquad \begin{aligned} F_c(x) &= F_c(r)\frac{x}{r} \\ F_c(y) &= F_c(r)\frac{y}{r} \end{aligned} \qquad \text{(VIII-4)}$$

where $Q(r) = \int_0^r \rho(\underline{r}')\, d^3\underline{r}'$ (VIII-5)

is the charge distribution function and $\rho(\underline{r}')$ is the density function defined as

$$\rho(\underline{r}) = \sum_1^A{}_i \; |\varphi_i(\underline{r})|^2 \qquad \text{or}$$

$$= \langle 0 | \delta^3(\underline{r} - \underline{r}') | 0 \rangle \qquad \text{(VIII-6)}$$

where $\phi_i(\underline{r})$ are the shell-model single particle wave functions and $|0\rangle$ is the many-body ground state. We calculated the trajectory using the Coulomb force of Eq.(VIII-4), which however, neglects the projectile charge distribution. Then we repeated the calculation using the

Coulomb force corresponding to the potential Eq.(VIII-3').

We found that the results are the same within a factor 10^{-3}, and therefore in our successive calculations we used the uniformly charged sphere approximation.

The analytical expressions of $\rho(\underline{r})$ and of the folding potential are

^{16}O $$\rho(\underline{r}) = 4 \frac{\beta^3}{\pi^{3/2}} e^{-\beta^2 \underline{r}^2} (1 + 2\beta^2 \underline{r}^2)$$

^{40}Ca $$= 4 \frac{\beta^3}{\pi^{3/2}} e^{-\beta^2 r^2} \left(\frac{5}{2} + 2\beta^4 \underline{r}^4 \right) \qquad \text{(VIII-7)}$$

Folding potential

^{16}O $$V(\underline{r}) = 4 V_0 \sqrt{\frac{\gamma^3}{\alpha^5}} e^{-\beta^2 \underline{r}^2/\alpha} \left\{ \frac{2\beta^2 \underline{r}^2}{\alpha} + (4\gamma + 1) \right\} \qquad \text{(VIII-8)}$$

^{40}Ca $$V(r) = 4 V_0 \sqrt{\frac{\gamma^3}{\alpha^7}} e^{-\beta^2 \underline{r}^2/\alpha} \left\{ \frac{2\beta^4 \underline{r}^4}{\alpha^2} + 10\gamma \frac{\beta^2 \underline{r}^2}{\alpha} + (10\gamma^2 + 5\gamma + \frac{5}{2}) \right\}$$

In order to solve the set of equations of motion Eq.(VIII-1) we first transformed it in a set of simultaneous linear differential equations of the first order like:

$$v_x = \frac{dx}{dt}$$
$$\mu \dot{v}_x = - \frac{\partial V(\underline{r})}{\partial x} \qquad \text{(VIII-9)}$$

$$v_y = \frac{dy}{dt}$$
$$\mu \dot{v}_y = - \frac{\partial V(\underline{r})}{\partial y}$$

The set of equations Eq.(VIII-9) was solved by the Runge-Kutta[35] method of the fourth order, using the initial conditions:

$$x_0 \equiv x(-T) = -12 \text{ fm}$$

$$y_0 \equiv y(-T) = b$$

$$v_x(-T) = \sqrt{\frac{2(E_\alpha - V(r))}{m}}$$

$$v_y(-T) = 0$$

where

$$r_0 = \sqrt{x_0^2 + y_0^2}$$

and

$$T = \frac{x_0}{v_x}$$

We used a number of points N = 65 and a step length h = 2T/N .

The reason for the above choice of x_o, T, N , h, was that we had to get uniformity with the general structure of our computing programme, which is described in the next chapter.

In order to check the stability of the Runge-Kutta method we tried also several calculations increasing the number of points by a factor 2 and then decreasing the step length, but we found our results rather insensitive to the change (i.e. within a factor 10^{-4}).

Figs. (VIII-2,3,4,5,6) show the trajectories of the α-particle in the potential of ^{40}Ca (Fig.VIII-1) for E_α = 29,31,56, 104, 166 MeV. They correspond to initial impact parameter b = 0 ÷ 7 fm.

APPENDIX VIII

δ-function:

$$\int d^3\underline{r}\ \delta^3(\underline{r}-\underline{r}') = 1 \qquad \text{(A-VIII-1)}$$

Gaussian:

$$N\int d^3\underline{r}\ e^{-(\underline{r}-\underline{r}')^2/a^2} = 1 \qquad \text{(A-VIII-2)}$$

$$N = (a^2\pi)^{-3/2}$$

δ-function $\longleftrightarrow$ Gaussian relationship:

$$\delta^3(\underline{r}-\underline{r}') = \lim_{a\to 0} \frac{1}{a^3\pi^{3/2}}\ e^{-(\underline{r}-\underline{r}')^2/a^2} \qquad \text{(A-VIII-3)}$$

Nuclear density function:

$$\rho(\underline{r}) = \langle 0|\delta^3(\underline{r}-\underline{r}')|0\rangle = \lim_{a\to 0}\left\{N\langle 0|\ e^{-(\underline{r}-\underline{r}')^2/a^2}|c\rangle\right\} \qquad \text{(A-VIII-4)}$$

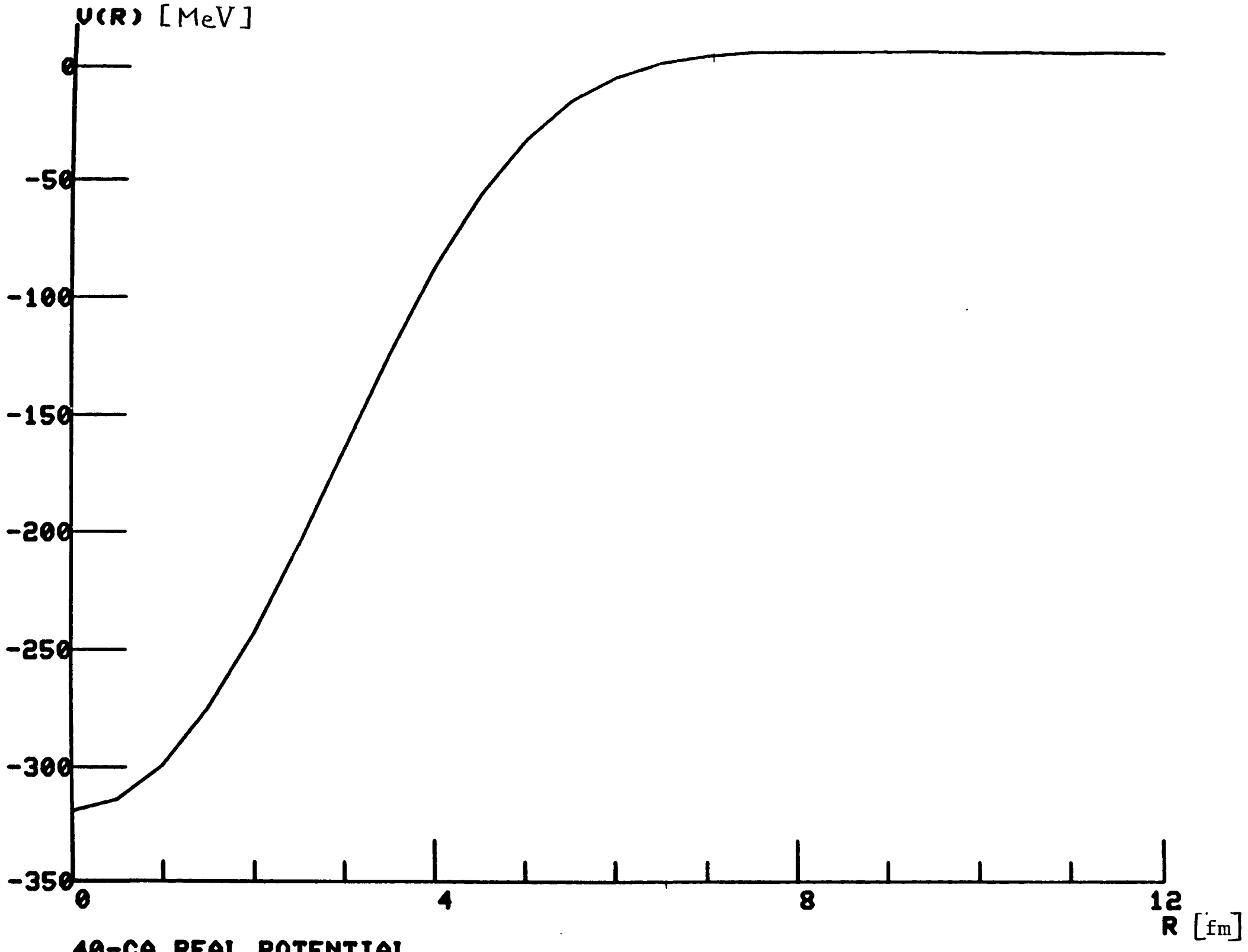
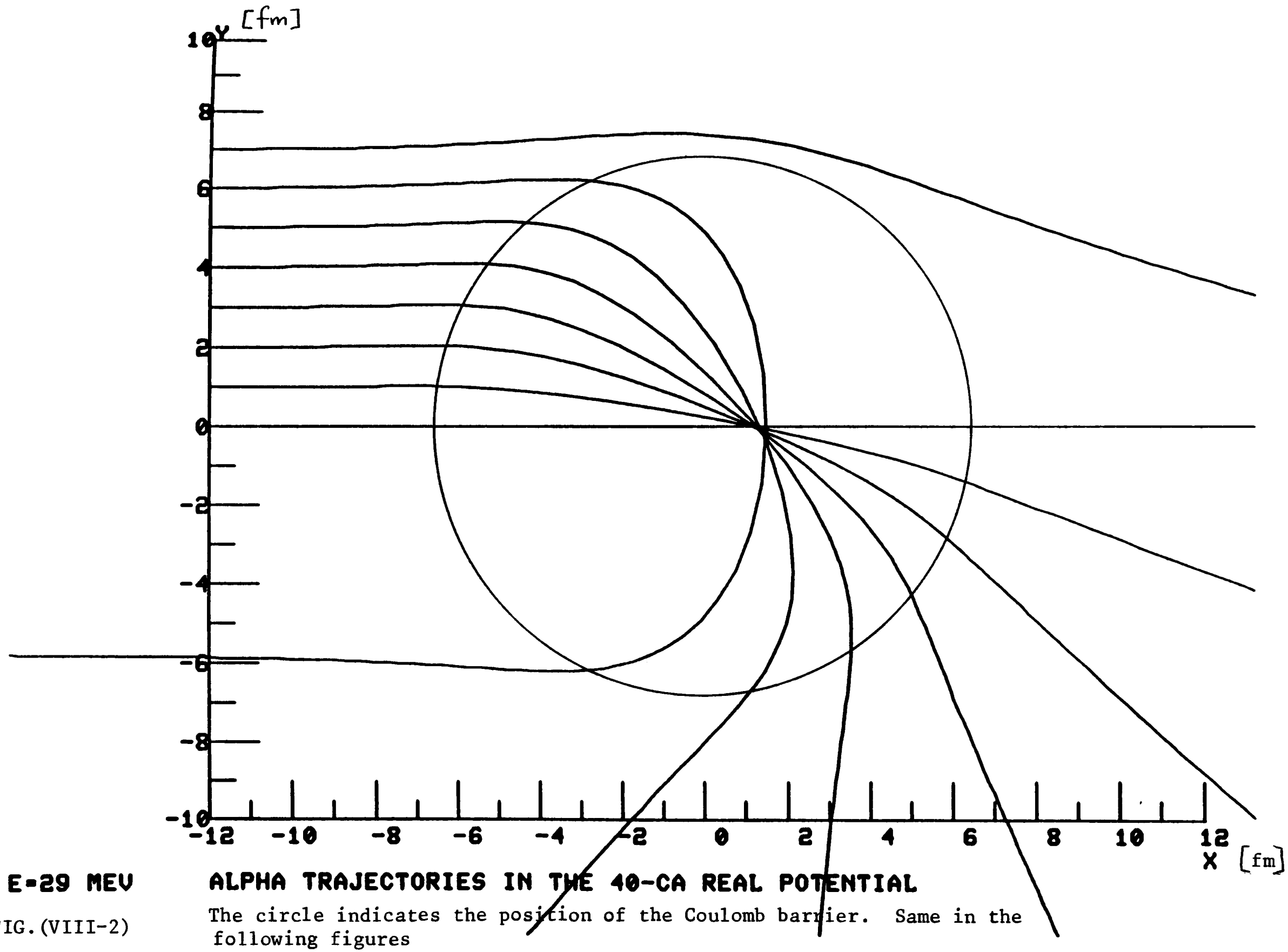
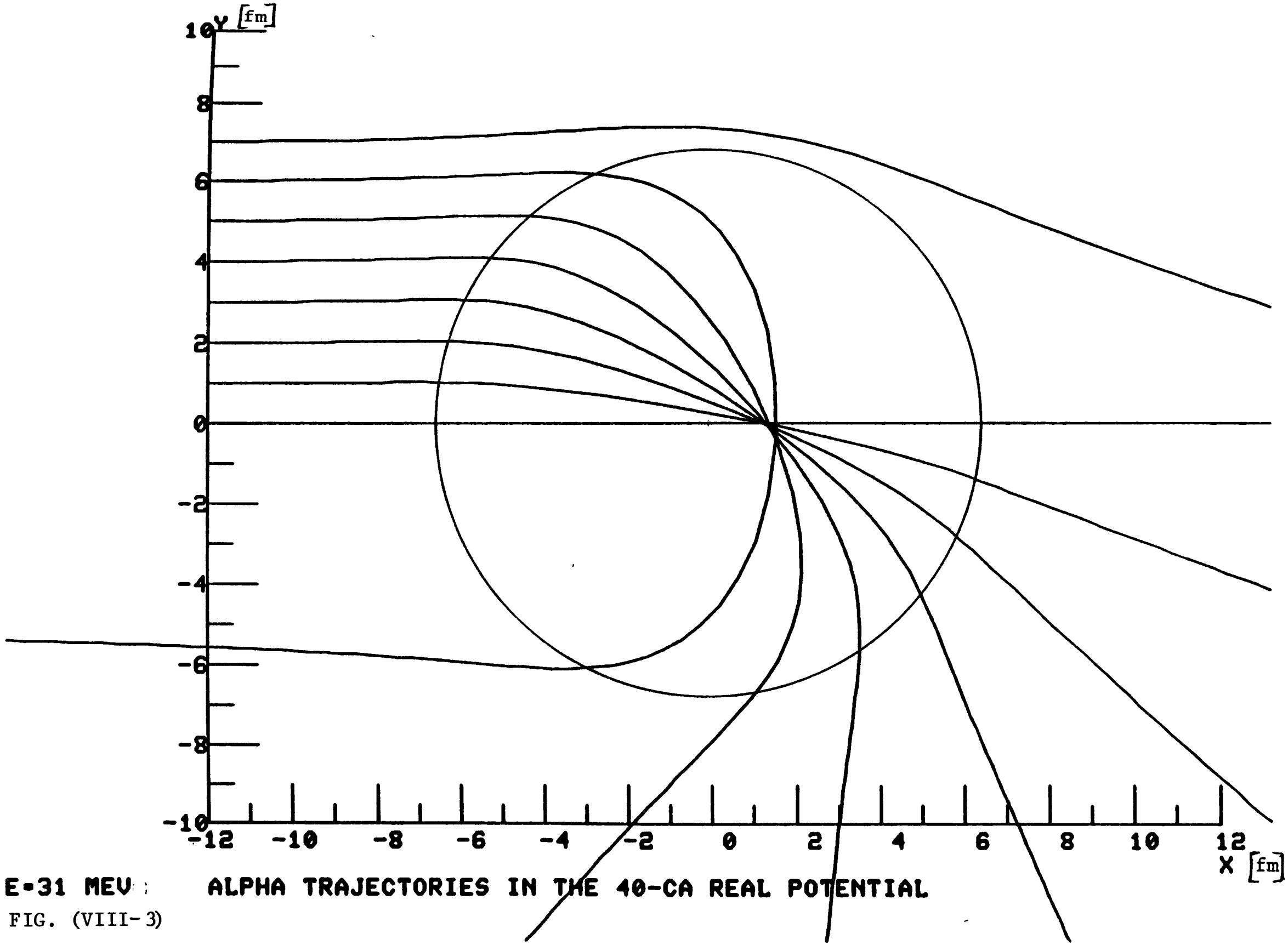


FIG.(VIII-1) **40-CA REAL POTENTIAL**



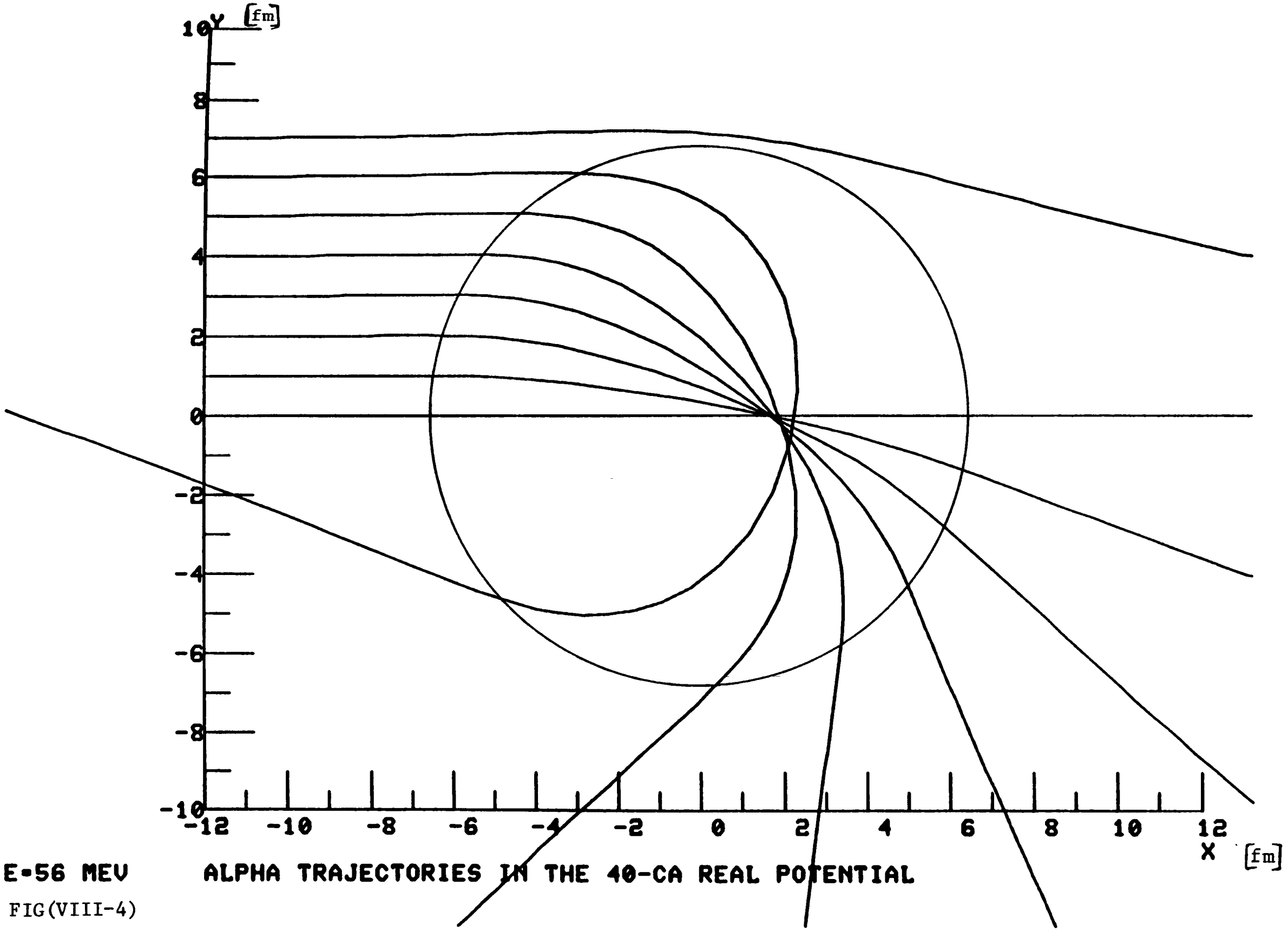
E=29 MEV **ALPHA TRAJECTORIES IN THE 40-CA REAL POTENTIAL**

FIG.(VIII-2) The circle indicates the position of the Coulomb barrier. Same in the following figures



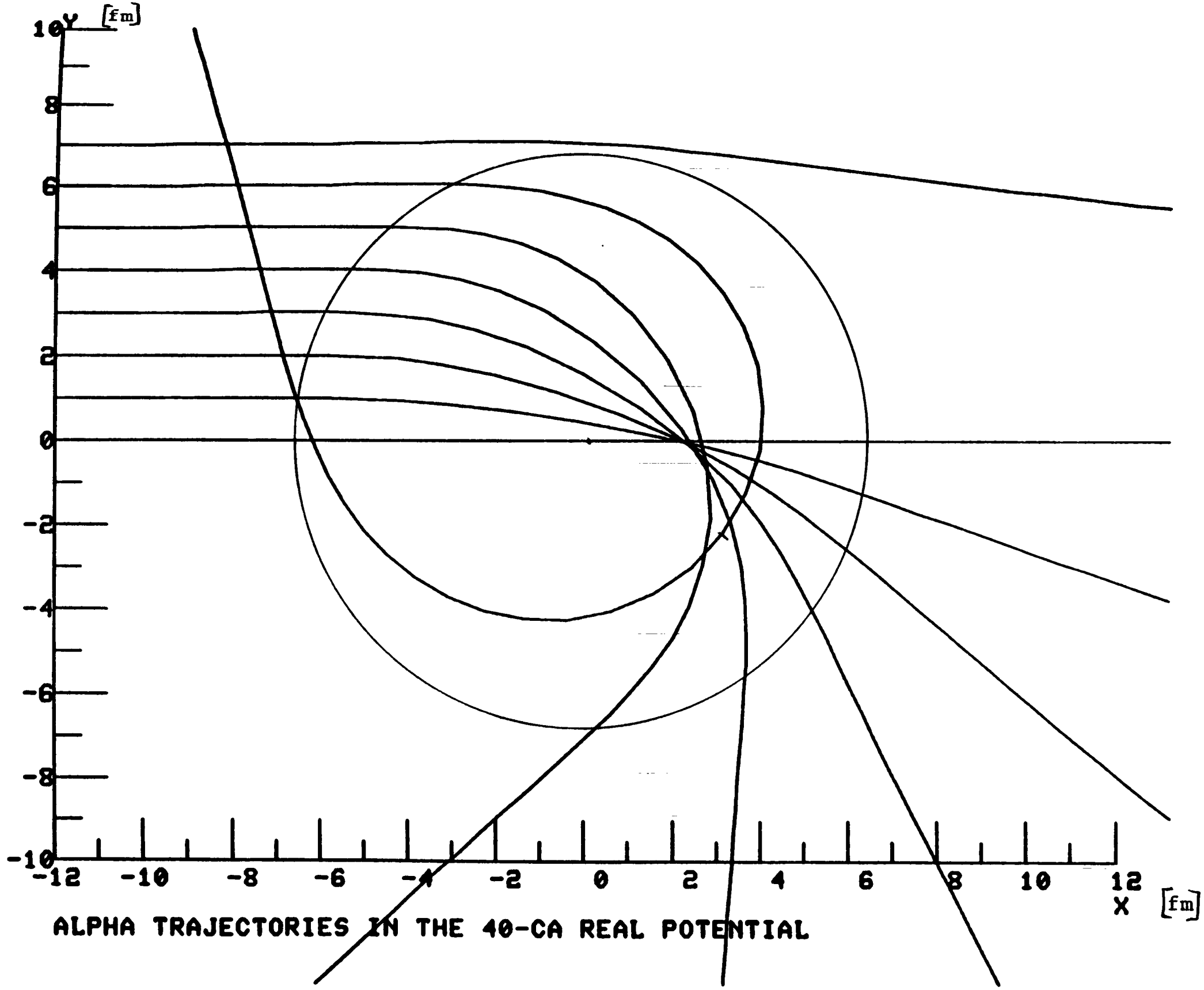
E=31 MEV : ALPHA TRAJECTORIES IN THE 40-CA REAL POTENTIAL

FIG. (VIII-3)



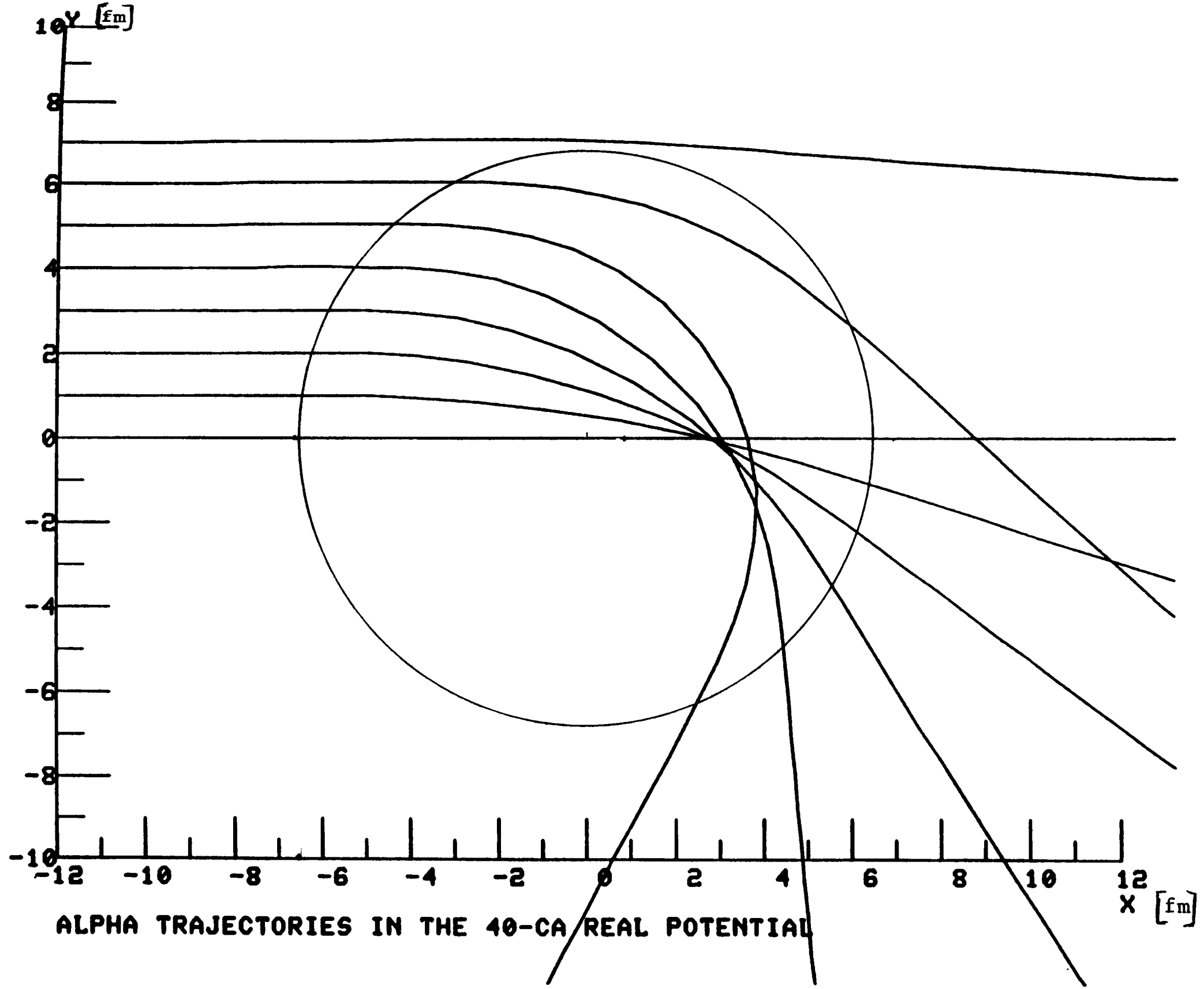
E=56 MEV ALPHA TRAJECTORIES IN THE 40-CA REAL POTENTIAL

FIG(VIII-4)



E=104 MEV ALPHA TRAJECTORIES IN THE 40-CA REAL POTENTIAL

FIG.(VIII-5)



E=166 MEV ALPHA TRAJECTORIES IN THE 40-CA REAL POTENTIAL

FIG.(VIII-6)

Chapter IX

NUMERICAL RESULTS

IX-1 Calculations with the Straight Line Trajectories

We begin this chapter by describing calculations of the time integral of the imaginary part of the optical potential using the perturbative formula Eq.(III-19). The first calculations were made for ^{16}O as a target using the straight line trajectories and including the contributions from $1\hbar\omega$ and $2\hbar\omega$ excitations. They were made both analytically with the correlation function method described in Chapter V and numerically using a computer code OPTPOT which calculates Eq.(III-19) by numerical integration.

Eq.(III-19) can be transformed as follows

$$\int_{-\infty}^{\infty} Im\, V_{opt}(r(t))\,dt = -\frac{1}{2\hbar}\sum_{\substack{n\langle\\ k\rangle}} \left| \int_{-\infty}^{\infty} \langle n|V|k\rangle\, e^{i\omega_{kn}t}\, dt \right|^2$$

$$= -\frac{1}{2\hbar}\sum_{\substack{n\langle\\ k\rangle}} \left\{ \left| \int_{-\infty}^{\infty} \langle n|V|k\rangle \cos(\omega_{kn}t)\,dt \right|^2 + \left| \int_{-\infty}^{\infty} \langle n|V|k\rangle \sin(\omega_{kn}t)\,dt \right|^2 \right\}.$$

The matrix elements in this equation were obtained from the recurrence formula described in Appendix IV and the time integrals were calculated using Simpson's rule.

We found that the integrands $\langle n|V|k\rangle \cos(\omega_{kn}t)$ and $\langle n|V|k\rangle \sin(\omega_{kn}t)$ tend to zero rapidly outside an interval $(-r, r)$ with $r = 12$ fm. Therefore we integrated over a total time $2T = \frac{2r}{v}$ (sec), where v is the velocity of the α-particle, and we used a total number of points $N = 65$;

the step length was chosen to be $h = 2T/N$. The reason for choosing $N = 65$ was that we found a very good agreement with the previous analytical results, for this value of N, while no significant improvement was obtained by increasing N further.

The results of the numerical and analytical calculations are shown in Table V-1 for ^{16}O. In most cases they agree and they are accurate within 2%. The two calculations use completely different formulae, so that the agreement between the results provides a check for both calculations. (Table (VI-1,2) follow page 60).

The sum in Eq.(III-19) over the occupied and unoccupied states can be regarded as a series in terms of different orders of excitation $N\hbar\omega$ with $N = 1,2,\ldots$. In order to check the convergence of this series we calculated numerically, several orders of excitation both for ^{16}O and ^{40}Ca. Table (V-2) shows the contributions coming from different orders of excitation in ^{40}Ca. The largest excitation is the $2\hbar\omega$ one and its contribution to the time integral of the optical potential is of the order of $-40\left[\text{MeV}.\ 10^{-22}\ \text{sec}\right]$ in ^{40}Ca. The contribution of higher excitations diminishes at all incident energies but less rapidly at high incident energies than at low energies. This indicates that with the increase in the incident energy more inelastic channels start to open. However, very high excitations do not contribute (cf. Tables V), since the $8\hbar\omega$ excitation in ^{40}Ca is already 10^{-2} times smaller than the $2\hbar\omega$ excitation and therefore it can be neglected.

The same trend was found in ^{16}O for which the $5\hbar\omega$ excitations are 10^{-2} times smaller than the $2\hbar\omega$ excitation.

As discussed in Chapter VI the formula (III-19) contains contributions from spurious centre-of-mass excitations. These contributions have been calculated and the results are shown in Tables (VI-1,2)

for ^{16}O and ^{40}Ca respectively. In both cases the spurious centre-of-mass term is a very large part of the $1\hbar\omega$ contribution.* The $2\hbar\omega$ states occur at E_α = 20 MeV, where E_α is the incident energy of the α-particle, while the $2\hbar\omega$ states are most strongly excited at E_α = 50 MeV. Similarly the largest excitation of higher states occurs at higher incident energies.

IX-2 Comparison with Phenomenological Potentials

Now we wish to extract some information about the optical potential itself, using the results of the time integral $\int$ Im $V(\underline{r}(t))$ dt.

First we try to understand the relation between our theory of the optical potential and some phenomenological optical potentials. For this purpose we selected from the literature several imaginary potentials with a form factor of the Woods-Saxon type

$$W(r) = -\frac{W_0}{1+e^{(r-R)/a}} \qquad \text{(IX-1)}$$

and performed the time integral with the same trajectories used in our perturbation calculations. The time integral was made with the same time interval and with the same step length as in the perturbation calculations.

Fig. (IX-1) shows the results for a target of ^{16}O and E_α = 104 MeV. The phenomenological potential was taken from ref.(36), its form factor is given in Eq.(IX-1) and the parameters are

$$W_0 = 29.7 \text{ MeV} \; ; \; R = 3.53 \text{ fm} \; , \; a = 0.72 \text{ fm} \qquad \text{(IX-2)}$$

* The $2\hbar\omega$ excitations are only slightly affected by the spurious center of mass part. It is interesting to note in tables (V-2) and (V1-2) that the maximum excitation of the $1\hbar\omega$ states occurs at E_α = 20 MeV, ...

The full curve shows $\int$ Im $V(\underline{r}(t))$ dt from our calculation of Eq.(III-19), while the dashed curve is $\int W(\underline{r}(t))$ dt with $W(r)$ given by Eqs. (IX-1,2)

The abscisa indicates the value of the impact parameters corresponding to the different trajectories used. In this case the trajectories are straight lines. Therefore in Fig.(IX-1) each point has coordinate

$$\left(b, \int \mathrm{Im}\, V(\underline{r}(t))\, dt \right)$$

where $\underline{r}(t) = \underline{v}t + \underline{b}$ and $v = \sqrt{\frac{2E_\alpha}{m}}$.

Figs.(IX-2,3,4,5,6) represent the same kind of calculation but for α-scattering on ^{40}Ca at E_α = 29, 31, 56, 104, 166 MeV, respectively. The parameters of the phenomenological potentials are as follows (36,37,38,39,40,41).

Ref.	E_α(Mev)	W_o(MeV)	R(fm)	a(fm)	ν
(36)	29	16.6	4.925	0.564	
(37)	31	19.8	5.20	0.522	
(38)	56	21.05	5.13	0.54	
(39)	104	19.8	5.53	0.559	
(40)	166	20.7	5.54	0.55	
(41)		29.91	(3.853+0.035Eα)	0.558	2.653

The potential of F. Michel[41] has an energy dependent radius and its form factor is

$$W(r) = -\frac{W_o}{\left[1 + e^{(r-R)/va}\right]^\nu} \qquad \text{(IX-3)}$$

The parameter υ in the denominator was chosen in order to give a potential which goes to zero on the surface more slowly than the usual Woods-Saxon.

As can be seen from Figs.(IX-1-6) our calculations do not reproduce the time integral of any of the phenomenological potentials used exactly, although the order of magnitude and the general trends are the same.

Michel potential Eq.(IX-3) differs from the others since it can be used over a range of energies, while each of the other potentials is determined for a specific energy. In the potential (IX-3) the radius R changes with the incident energy of the α-particle E_α according to

$$R \simeq 3.853 + 0.035\, E_\alpha \quad [fm] \qquad \text{(IX-4)}$$

This fact leads to systematic differences between the results with this potential and the results with other phenomenological potentials or our calculations.

The first difference is that Michel's potential gives a time integral which is always bigger than ours at large impact parameters. This is not unexpected since this potential has a larger effective diffuseness than a Woods-Saxon. Our results instead show a rather good agreement with phenomenological potentials with a Woods-Saxon form factor.

Michel's potential also has the property that the time integral of Im $V(\underline{r})$ decreases with the incident energy E_α. This is related to the trajectories we have used in this set of calculations. The trajectories are in fact straight lines and the α-particle has a

velocity which is constant also in the region of the target nucleus. Therefore at high energies this region is crossed in a time interval smaller than at low energies and thus the time integral decreases with the energy.

The trend discussed above seems to be reproduced also by our calculations and the Woods-Saxon phenomenological potential.

However, we would expect that the total absorption of flux from the elastic channel, which we are calculating by means of the time integral of the Im $V(\underline{r}(t))$, should increase with the incident energies. The approximation of a straight line trajectory does not appear to be satisfactory in this respect, and therefore calculations with more realistic trajectories seem to be called for.

IX-3 Calculations with Classical Trajectories

A second series of calculations was made using the classical trajectories in the folding potential calculated by Eqs.(VIII-3,3') from the α-nucleon potential.

In Figs.(IX-7,8,9,10,12) we show the results obtained at the same incident energies discussed in the previous section, but using the classical trajectories instead of the simple straight lines.

In this case, in the region of the target, the α-particle is accelerated by a potential which has a strength of order of -300 MeV in ^{40}Ca (cf. Fig.VIII-1), hence its velocity inside does not depend very much on the initial velocity (i.e. on the energy). As a consequence, the results of the time integral of Michel's potential and of the Woods-Saxon potentials, have now the expected energy dependence: the overall strength of the time integral increases with the energy for the phenomenological potentials. The path integral calculations

give an absorption stronger than the phenomenological potentials at low energies, but the difference between them diminishes when the incident energy increases.

This behaviour indicates, in our opinion, that the semiclassical approach we are using becomes more reliable at high energies. We did not try any calculation at incident energies higher than E_α = 166 MeV because the phenomenological α-nucleon interaction[23-b] we are using fits data only at low to medium energies.

The dependence of the results at large impact parameters is the same as discussed in section 2. Our calculations agree with the results obtained with Woods-Saxon potentials, while Michel's potential gives rise to quite a strong absorption even for impact parameters larger than 7 fm. (Remember that with our model of the real potential, the Coulomb barrier is located at ∿ 7 fm. in ^{40}Ca).

At low impact parameters our results show the same behaviour of the phenomenological potentials in the case of E_α = 29, 31 and 56 MeV, while at higher energies, i.e. E_α = 104 and 166 MeV, our time integral tends in general to increase with the impact parameter while the phenomenological results tend to decrease. This discrepancy is probably due to the strength of the effective α-nucleon interaction which is not big enough to give the correct excitation at high incident energy.

The most interesting region of impact parameters is the one between 5 and 6 fm. There the time integral of the optical potential starts to increase slightly in absolute value, while for smaller impact parameters it was almost constant. From the figures of Chapter VIII representing the classical trajectories of the α-particle in the ^{40}Ca real potential, one can see that the values of impact parameters between 5 and 6 fm. correspond to the trajectories scattered at backward

angles. The well defined peak shown by $\int \mathrm{Im}\, V_{opt}(\underline{r}(t))\, dt$ at all energies, but in particular at $E_\alpha = 104$ MeV corresponds to an orbiting trajectory (cf. Fig.VIII-5). In this case the absorption is very strong and the approximation of a real trajectory is no longer justified.

At this stage we would like to recall that when we introduced the path integral approach, in Chapter II, we said that Eq.(II-25)

$$\int_{t'}^{t''} V_{opt}(\underline{r}(t))\, dt = i\hbar \ln \langle 0 | U(\underline{r}(t), t'', t') | 0 \rangle$$

is difficult to satisfy for all possible paths and we promised to identify the paths which give the main contribution to the path integral.

From the results discussed in this chapter one can identify the important paths with the classical trajectories corresponding to scattering at backward angles at low to medium energies and with the trajectories close to the one that shows an orbiting at high energies. If we think in terms of the real potential of the target which appears in the radial Schrödinger equation

$$V(r) = V_N(r) + V_C(r) + \frac{\ell(\ell+1)}{2\mu r^2}\hbar^2 \qquad \text{(IX-5)}$$

we can give a prescription for the identification of the important paths to be used in Eq.(II-25): they are the classical trajectories corresponding to scattering near the top of the barrier of potential (IX-5).

Next we explain why the trajectories corresponding to scattering at backward angles are more important than the others.

It is already well known[36,41,42] that α-elastic scattering on ^{40}Ca shows the so-called ALAS phenomenon for $E_\alpha < 40$ MeV, namely a strong enhancement of the differential cross section at backward angles.

Brink and Takigawa[36] have proposed an explanation of this phenomenon within a semiclassical theory. If the imaginary part of the optical potential is weak enough the partial wave scattered near the top of the barrier of potential (IX-9) can penetrate inside the real potential. It will re-emerge after being reflected at the most internal turning point of the potential. When such a situation occurs one can therefore have information on the real potential at very close distances.

Before concluding this chapter we show how our results for $\int \mathrm{Im}\, V_{opt}(\underline{r}(t))\, dt$ can be related to more interesting physical quantities.

In a semiclassical description of the projectile motion the angular momentum ℓ is related to the impact parameter b by

$$m v b = \hbar \left[\ell(\ell+1)\right]^{1/2} \simeq \hbar\, \ell \qquad \text{for large } \ell. \tag{IX-6}$$

The time integral of the optical potential for a trajectory with impact parameter b can therefore be related to the imaginary part of the phase shift of the partial wave with angular momentum ℓ in the following way.

In Chapter II it was shown that

$$|S_\ell|^2 = \exp\left\{\frac{2}{\hbar}\int \mathrm{Im}\, V_{opt}(r(t))\, dt\right\} \tag{IX-7}$$

where $\mathrm{Im}\, V_{opt} < 0$.

For scattering of spin zero particles the S-matrix is given in terms of the phase shift by

$$S_\ell = e^{2i\delta_\ell} \tag{IX-8}$$

From Eqs.(XI-7,8) we find

$$-4\,\mathrm{Im}\,\delta_\ell = \frac{2}{\hbar}\int \mathrm{Im}\, V_{opt}(r(t))\,dt$$

and the probability that the system is left in its ground state after the scattering is

$$P_{0\to 0} = e^{-4\,\mathrm{Im}\,\delta_\ell} \tag{IX-9}$$

The above probability $P_{0 \to 0}$ is the most significant physical quantity and we give in Table (IX-1) some values of it in correspondence to typical values of the time integral.

TABLE IX-1

$-\int \mathrm{Im}\, V_{opt}(r(t))\, dt$ ($\mathrm{MeV}\cdot 10^{-22}$ sec)	Im δ_e	e^{-4} Im δ_e
5	0.38	0.2
10	0.76	$0.5\cdot 10^{-1}$
15	1.14	$0.1\cdot 10^{-1}$
20	1.52	$0.2\cdot 10^{-2}$
25	1.89	$0.5\cdot 10^{-3}$
30	2.28	$0.1\cdot 10^{-3}$
35	2.66	$0.2\cdot 10^{-4}$
40	3.04	$0.5\cdot 10^{-5}$
45	3.42	$0.1\cdot 10^{-5}$
50	3.79	$0.2\cdot 10^{-6}$
55	4.18	$0.5\cdot 10^{-7}$
60	4.56	$0.1\ 10^{-7}$

Caption for figures in Chapter IX

$\int \mathrm{Im}\, V(\underline{r}(t))\, dt$ vs. impact parameter

Full curve is our calculation.

Dashed curves are time integrals of the phenomenological potentials given at page 93 and 94.

Double dashed curves are time integrals of Michel's potential.

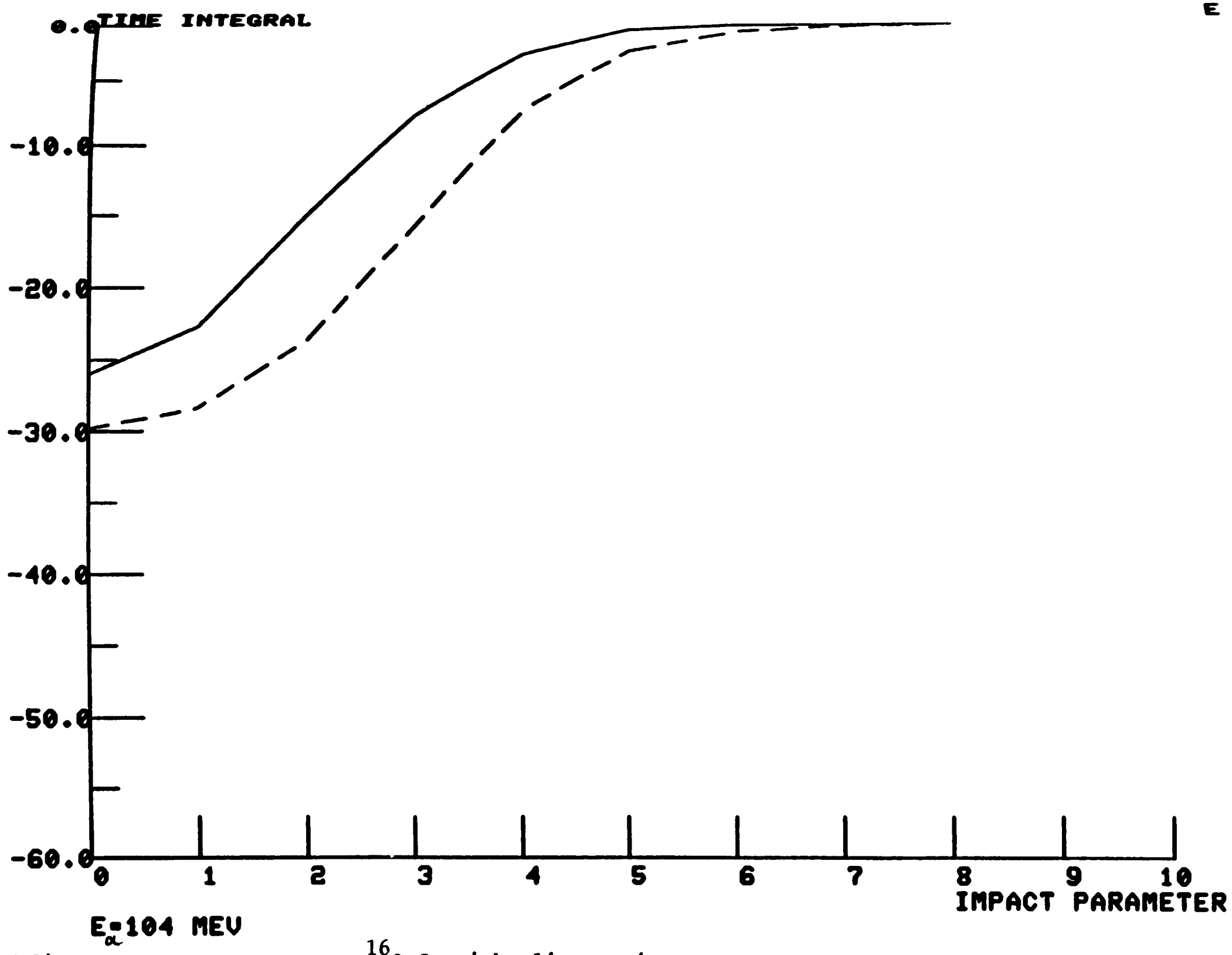


FIG.(IX-1) ^{16}O Straight line trajectory

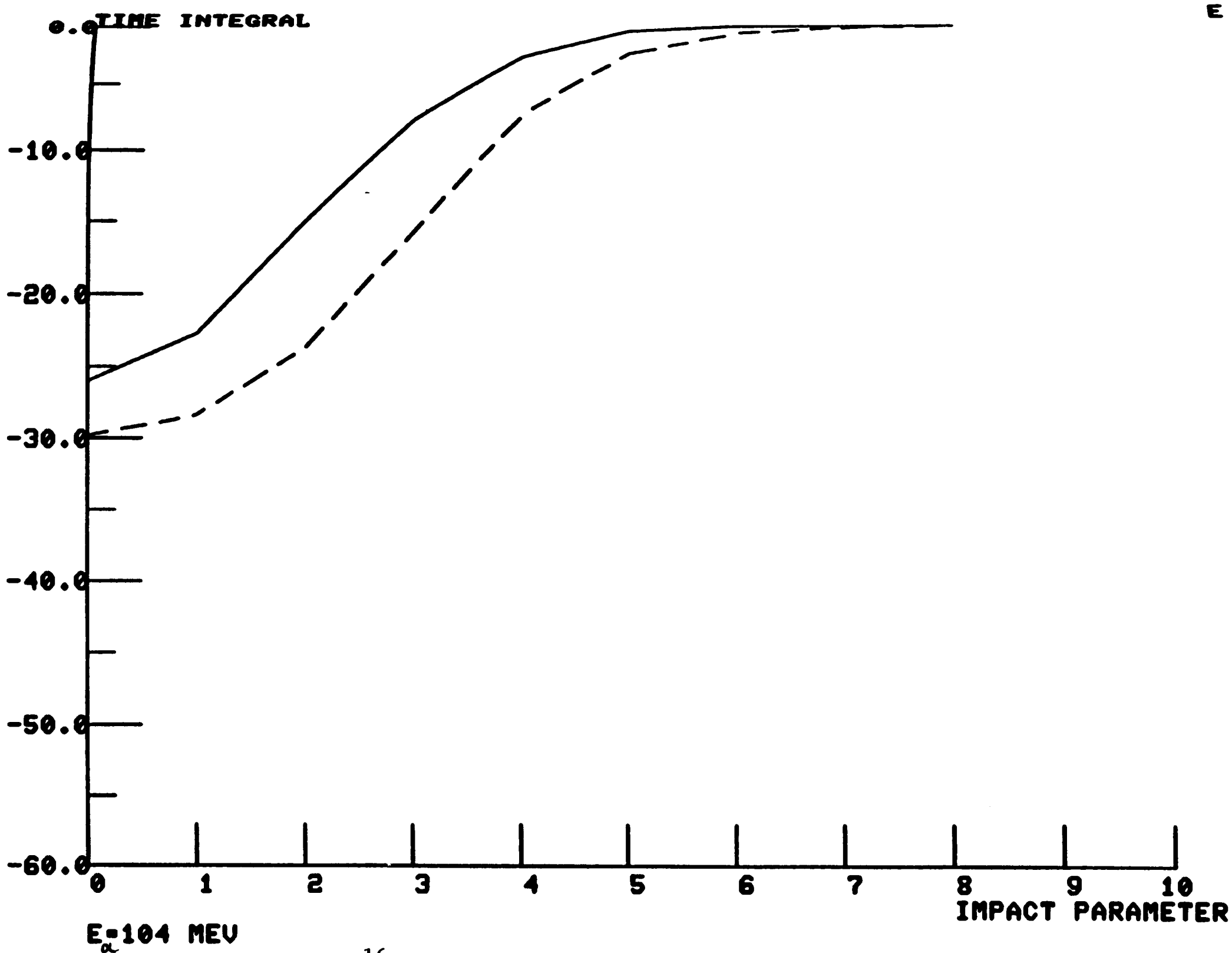


FIG.(IX-1) ^{16}O Straight line trajectory

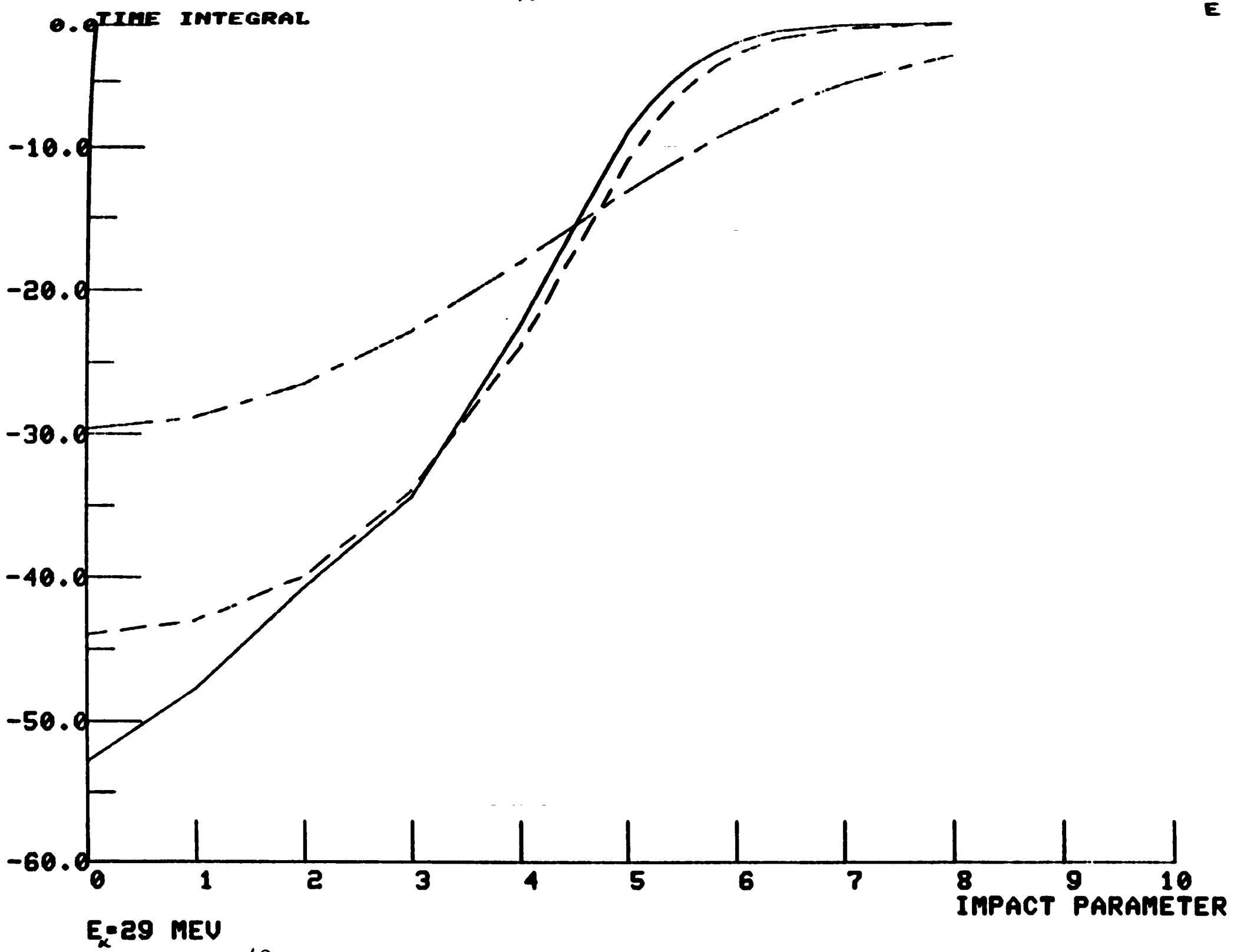


FIG.(IX-2) ^{40}Ca, straight line trajectory. The same in the following figures, with various values of E_α

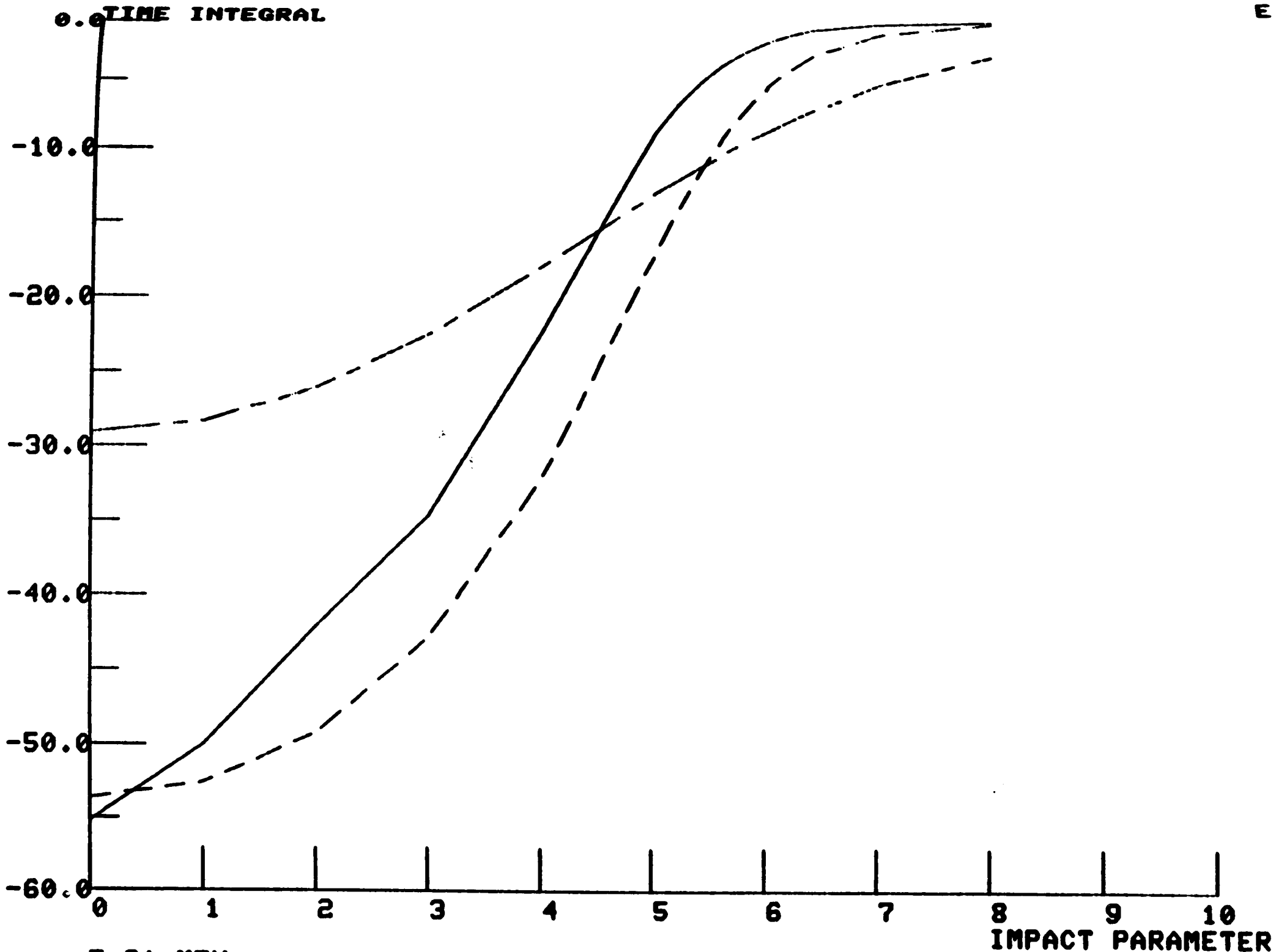

TIME INTEGRAL
E
0.0
-10.0
-20.0
-30.0
-40.0
-50.0
-60.0
0
1
2
3
4
5
6
7
8
9
10
IMPACT PARAMETER
E=31 MEV

FIG.(IX-3)

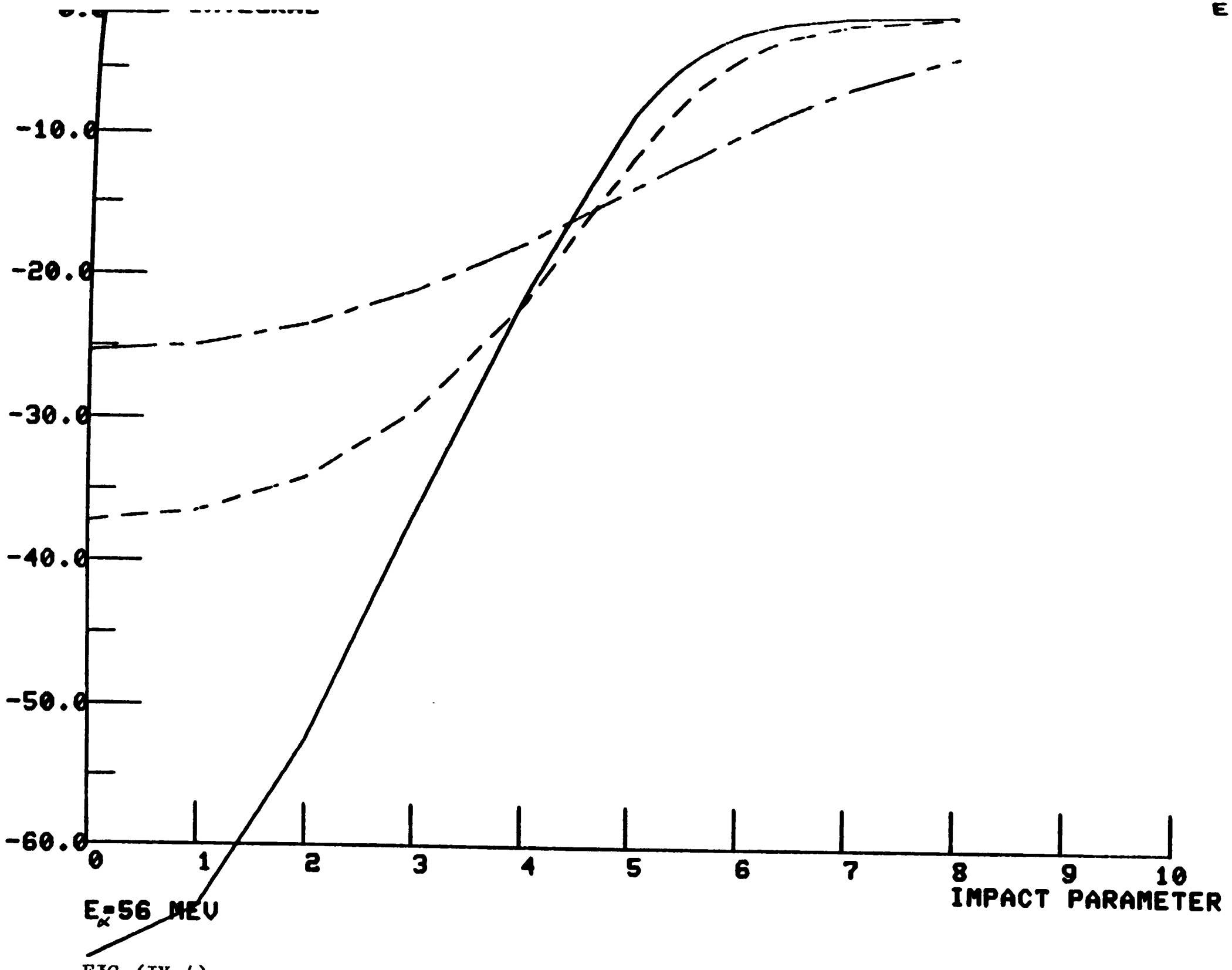

-10.0
-20.0
-30.0
-40.0
-50.0
-60.0
0
1
2
3
4
5
6
7
8
9
10
IMPACT PARAMETER
E∝=56 MEV

FIG.(IX-4)

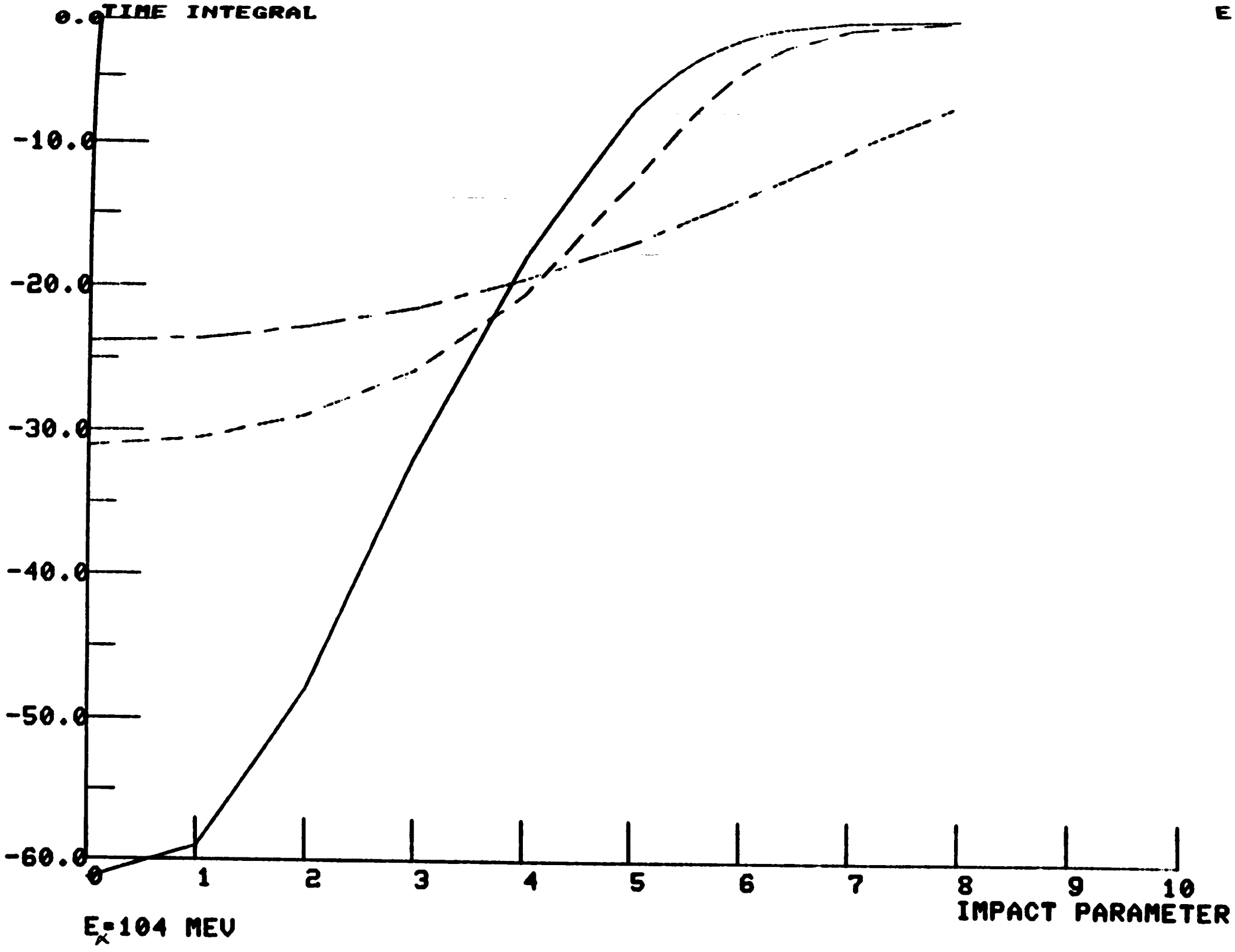

TIME INTEGRAL
E
0.0
-10.0
-20.0
-30.0
-40.0
-50.0
-60.0
0
1
2
3
4
5
6
7
8
9
10
IMPACT PARAMETER
E$_x$=104 MEV

FIG.(IX-5)

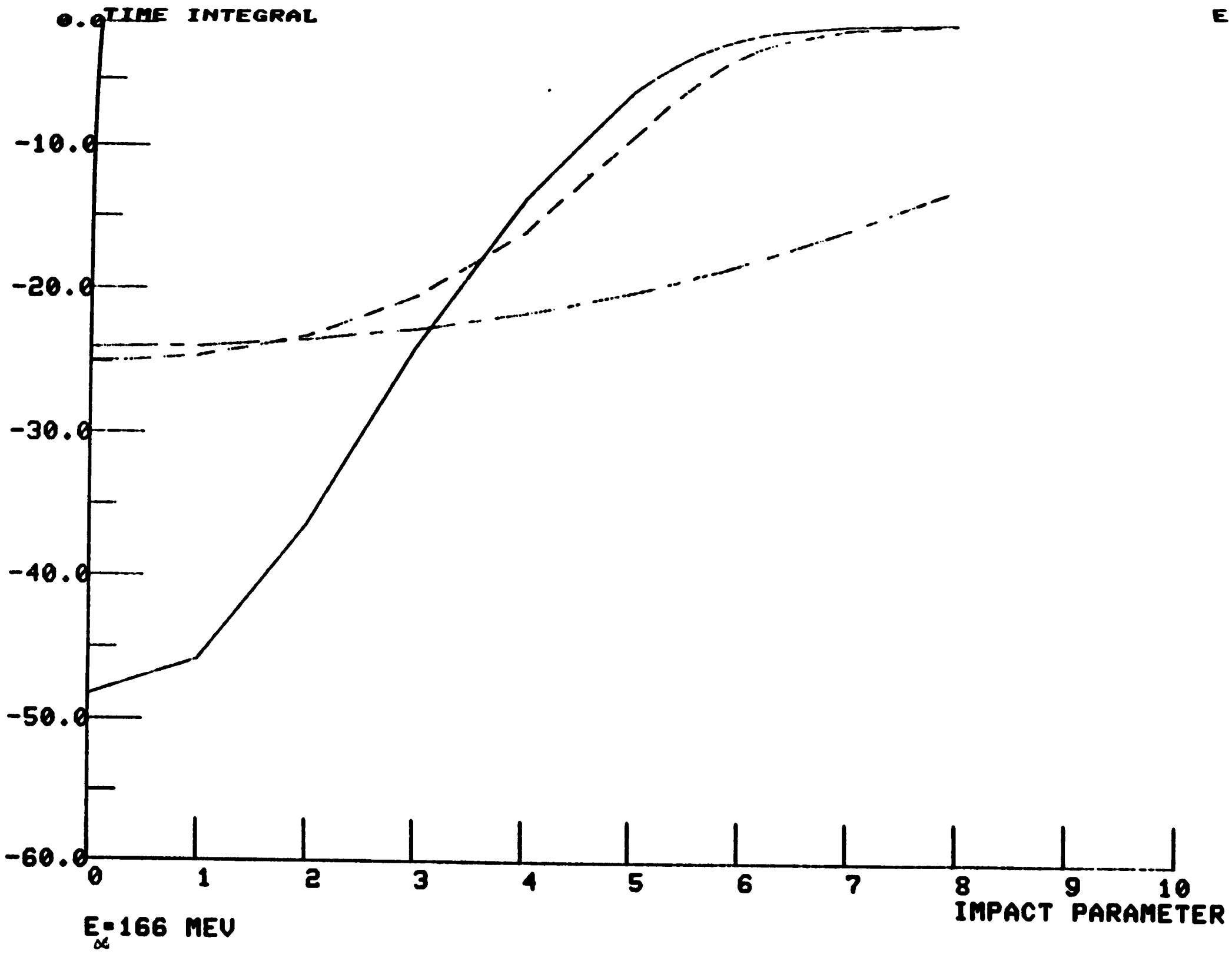

TIME INTEGRAL
E
0.0
-10.0
-20.0
-30.0
-40.0
-50.0
-60.0
0
1
2
3
4
5
6
7
8
9
10
IMPACT PARAMETER
E=166 MEV
∝

FIG.(IX-6)

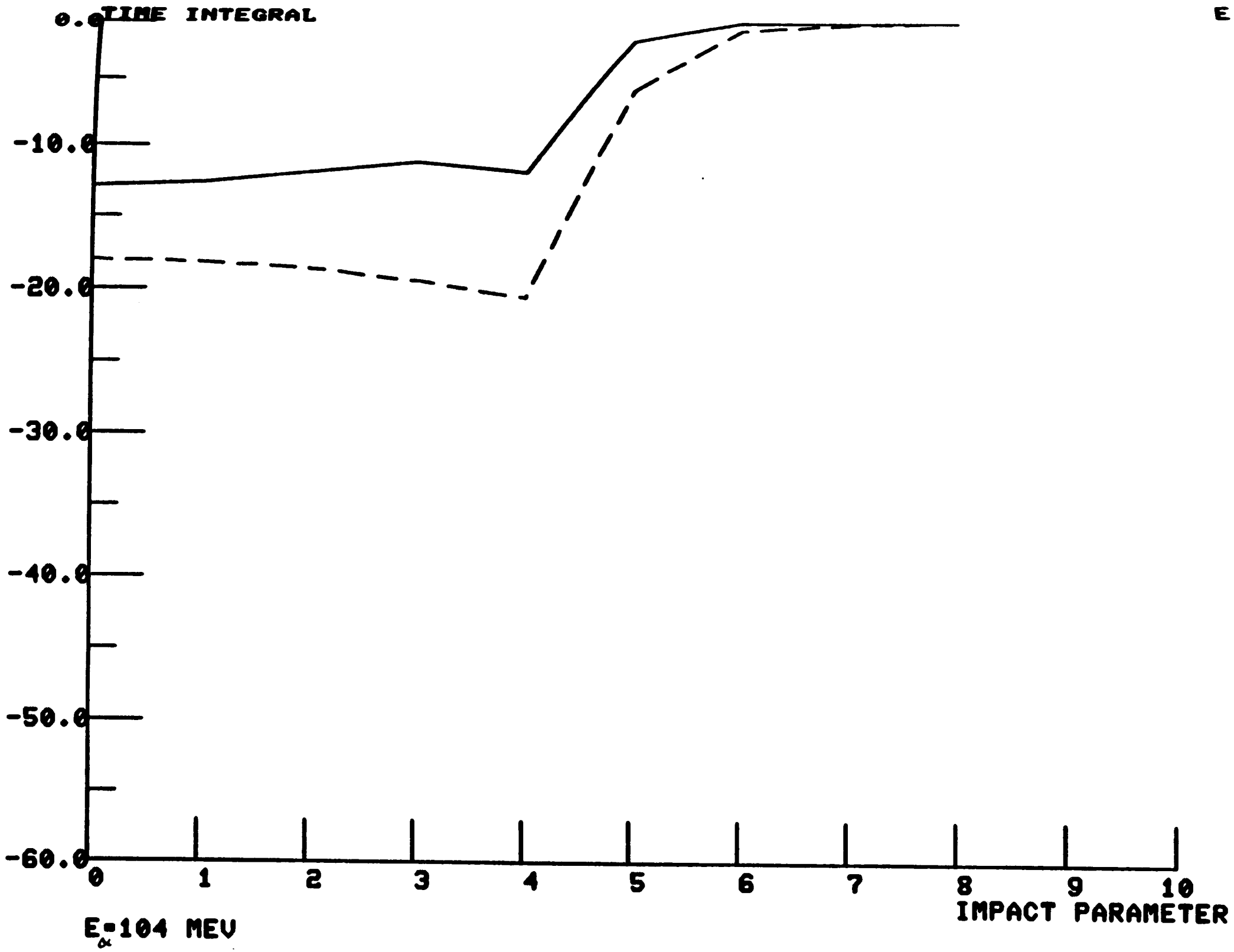


FIG.(IX-7) ^{16}O, Classical trajectory

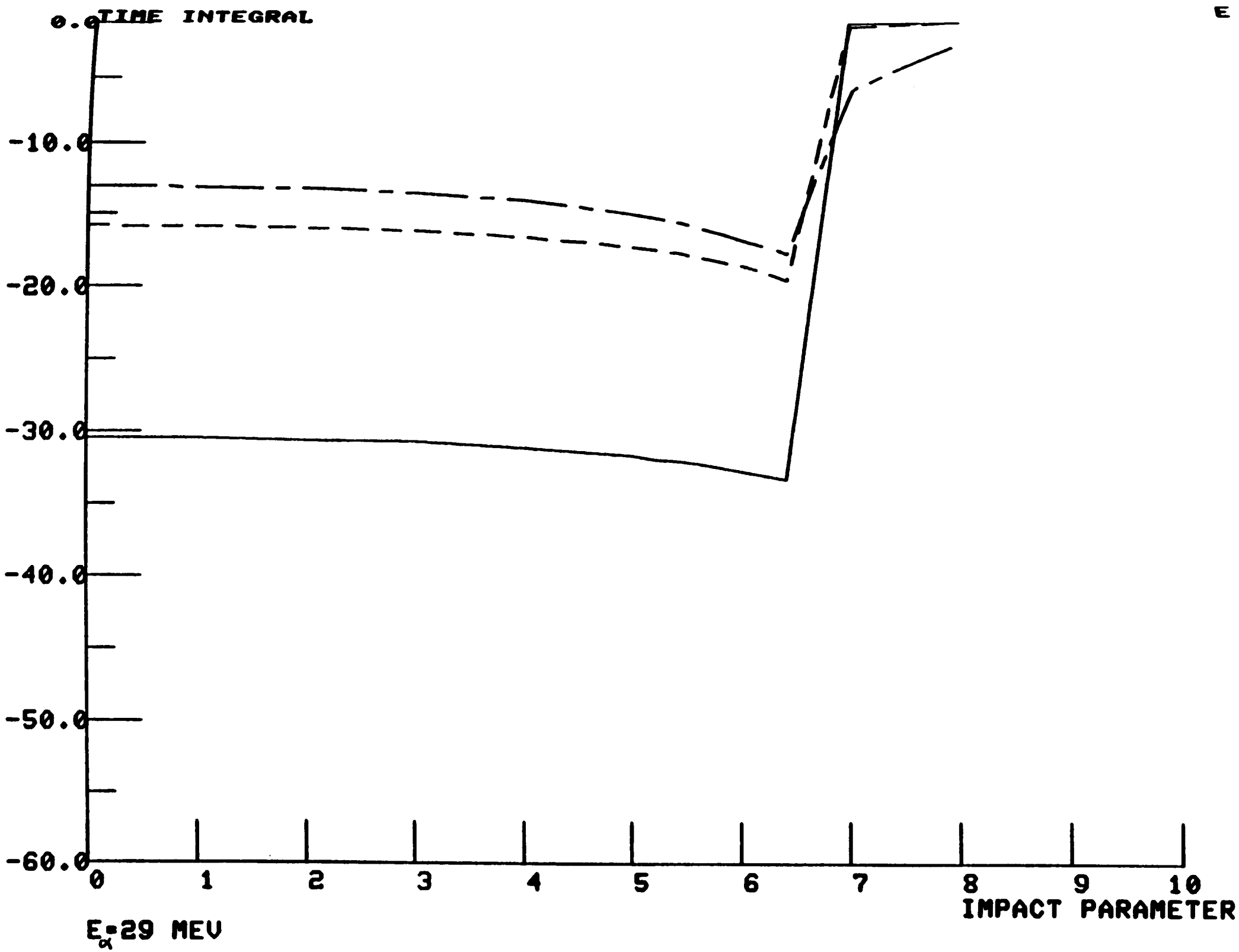


FIG. (IX-8) ^{40}Ca, classical trajectory. The same in the following figures with various values of E_α

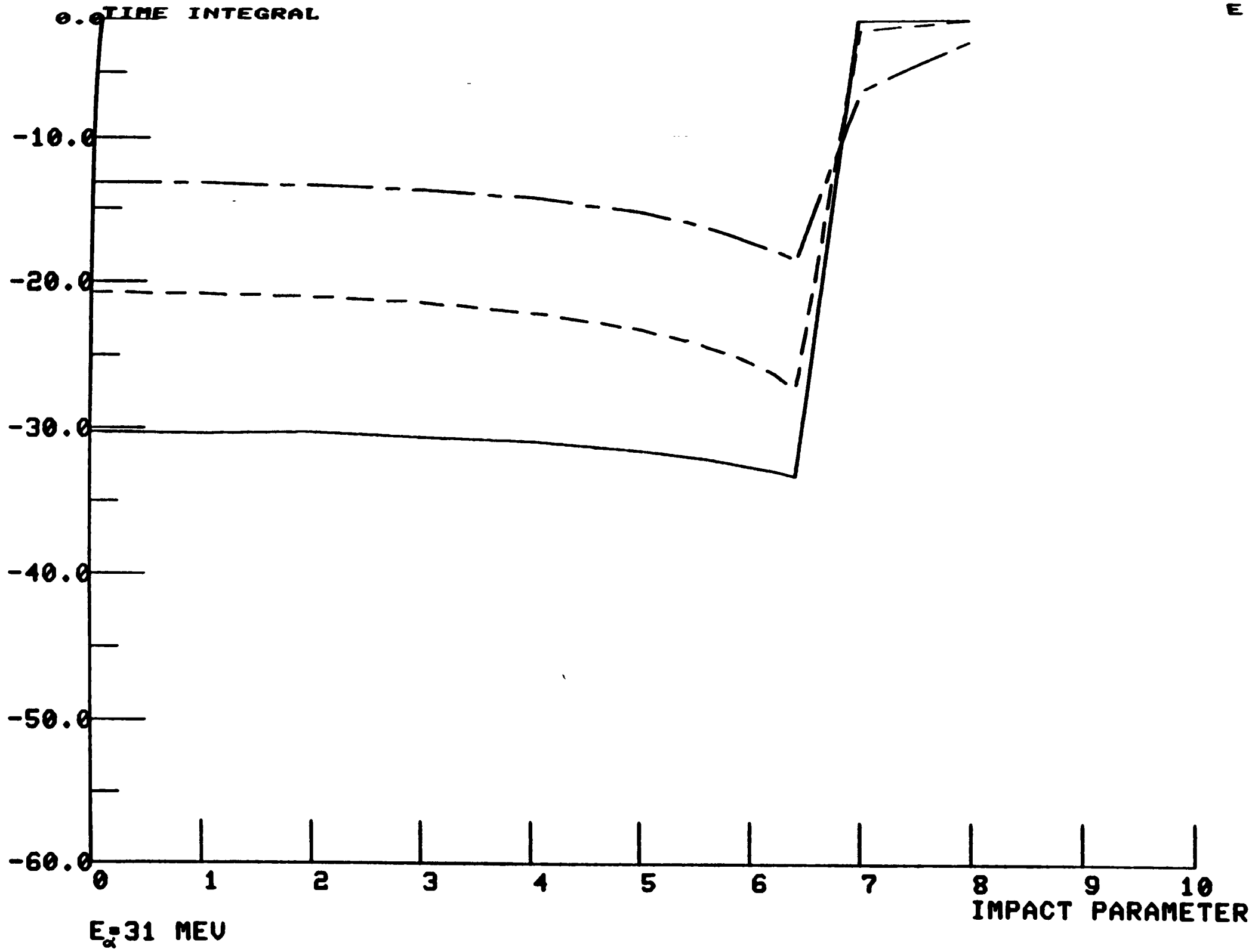

TIME INTEGRAL
0.0
-10.0
-20.0
-30.0
-40.0
-50.0
-60.0
0
1
2
3
4
5
6
7
8
9
10
IMPACT PARAMETER
E_α=31 MEV

FIG. (IX-9)

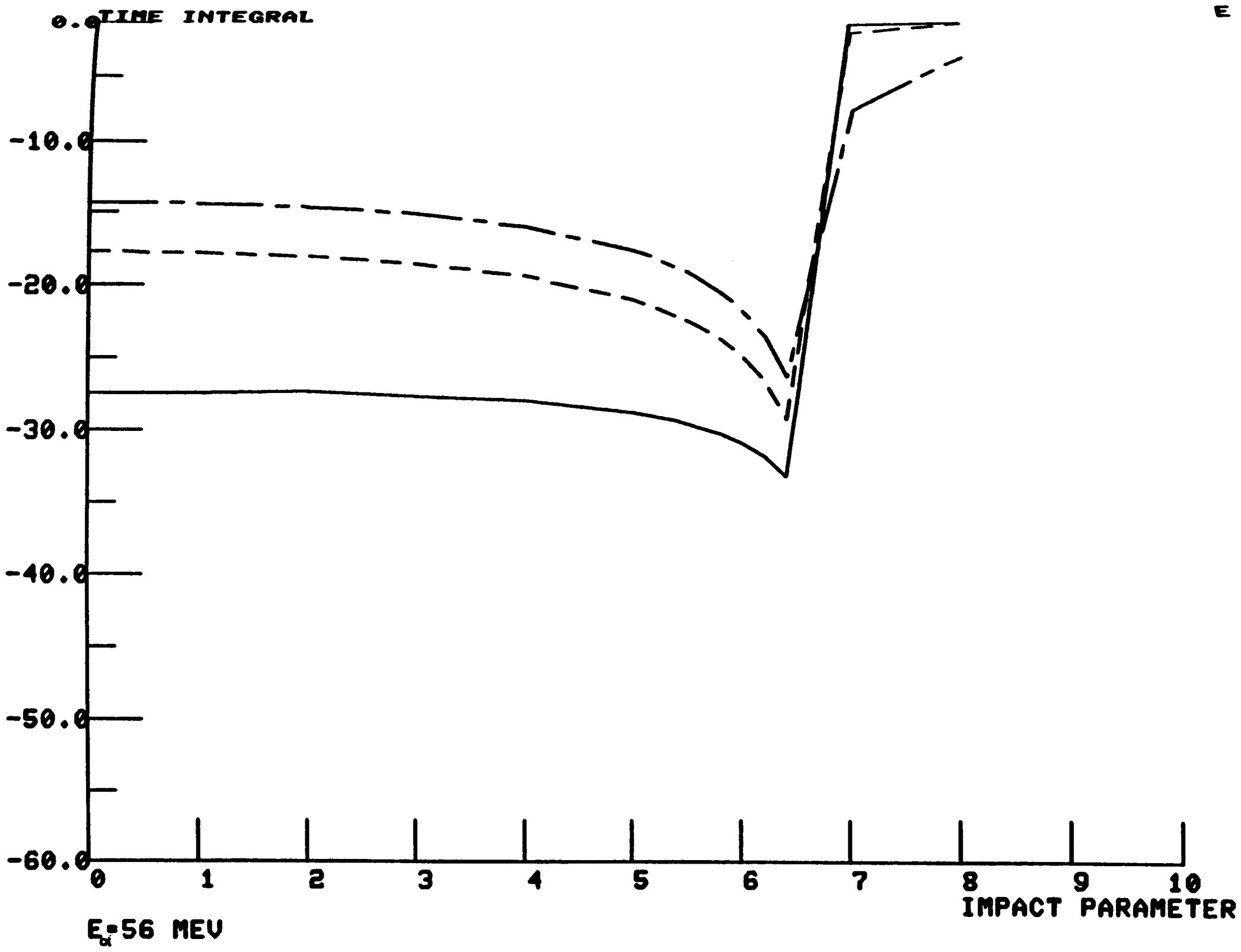

TIME INTEGRAL
0.0
-10.0
-20.0
-30.0
-40.0
-50.0
-60.0
0
1
2
3
4
5
6
7
8
9
10
IMPACT PARAMETER
E_α=56 MEV

FIG. (IX-10)

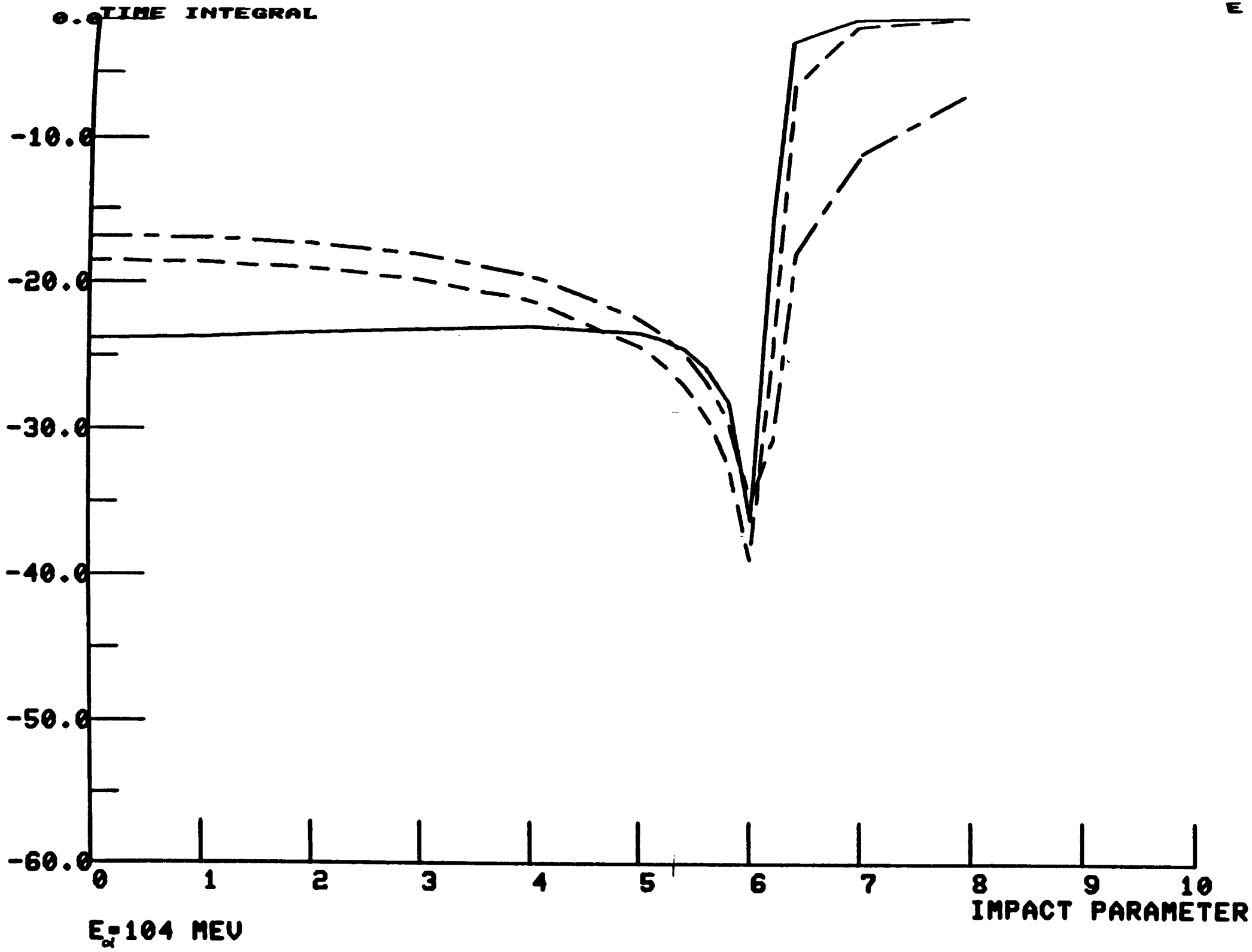

TIME INTEGRAL
0.0
-10.0
-20.0
-30.0
-40.0
-50.0
-60.0
0
1
2
3
4
5
6
7
8
9
10
IMPACT PARAMETER
E_α=104 MEV

FIG. (IX-11)

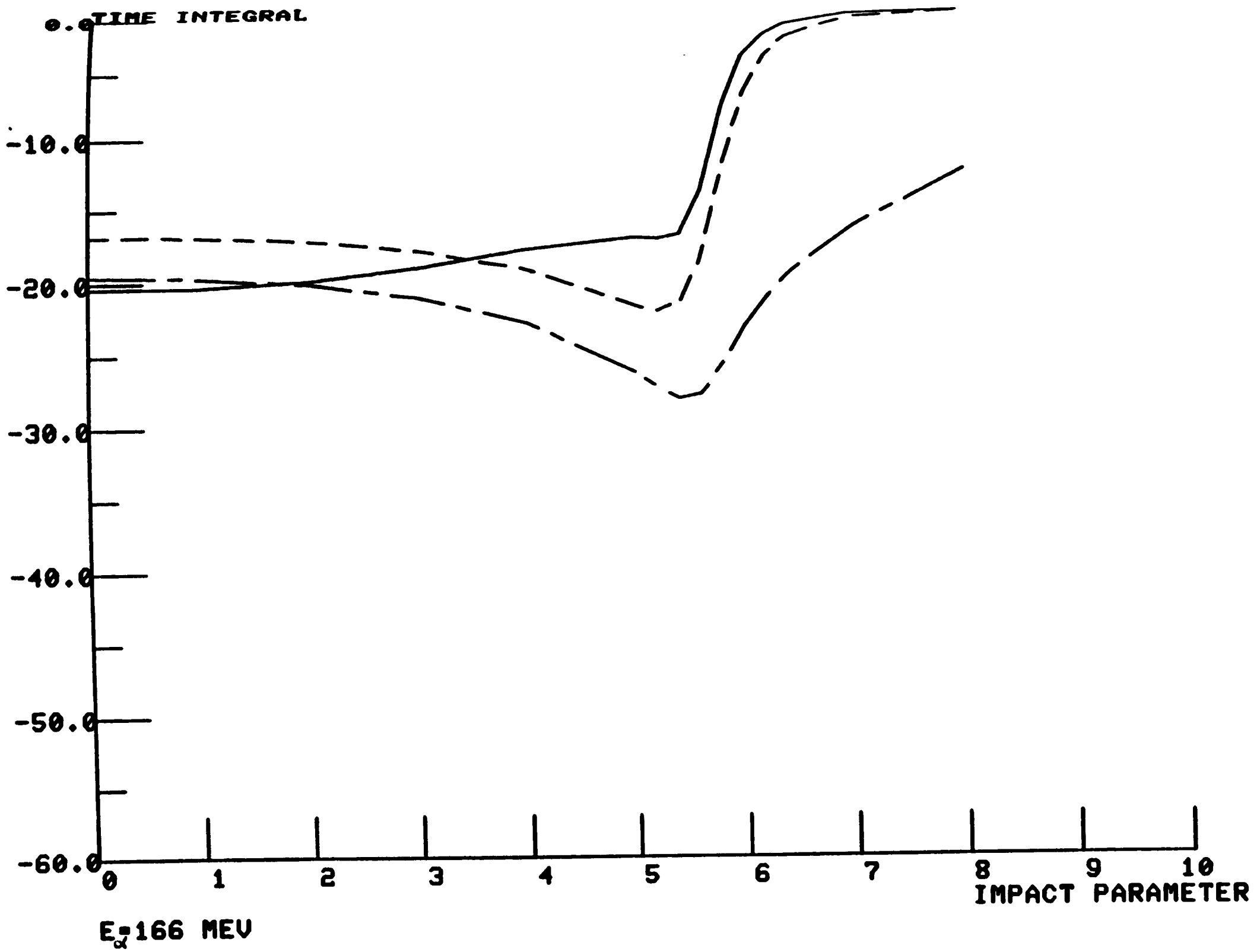

TIME INTEGRAL
0.0
-10.0
-20.0
-30.0
-40.0
-50.0
-60.0
0
1
2
3
4
5
6
7
8
9
10
IMPACT PARAMETER
E_α=166 MEV

FIG. (IX-12)

CHAPTER X

NON PERTURBATIVE CALCULATION OF THE OPTICAL POTENTIAL

As discussed in the next chapter, all calculations of the optical potential made so far use perturbation theory. It is interesting to have some indication of the validity of this approximation. In particular it is important to know how weak the α-nucleon effective interaction has to be in order for the perturbation expansion to be valid.

Another problem connected with the optical potential is the approximation made in the real part. All the approaches already existing calculate only the first order term (folding potential), and assume that the second order contribution is negligible.

In this chapter we show how the time integral of the optical potential Eq.(II-25), coming from the path integral approach can be obtained in an approximation better than perturbation theory, by using a coupled channels calculation of the amplitude $\langle 0|U|0\rangle$.

X-1 Coupled Equations

In Chapter III it was shown that in an independent particle description of the target nucleus, the time integral of the optical potential, Eq.(II-25), becomes

$$\int_{-\infty}^{\infty} V_{opt}(\underline{r}(t))\,dt = i\hbar \ln\{\det\langle \chi_i | \varphi_j\rangle\} = i\hbar \ln \det(a_{ij}) \qquad \text{(X-1)}$$

where the single particle wave functions χ_i and ϕ_j were obtained in Eqs.(III-6,6') and a_{ij} are the coefficients of the expansion

$$\varphi_i = \sum_j^N a_{ij}(t)\,\chi_j\, e^{-\frac{i}{\hbar}\varepsilon_j t} \qquad \text{(cf. Eq.(III-7))} \quad \text{(X-2)}$$

$i = 1, 2, \ldots A.$

In this framework the time evolution of the system is governed by the Schrödinger equations for the coefficients $a_{ij}(t)$

$$\dot{a}_{ik}(\underline{r}(t)) = -\frac{i}{\hbar}\sum_{j=1}^{N} a_{ij}(\underline{r}(t))\, V_{kj}(\underline{r}(t))\, e^{i\omega_{kj}t} \qquad (X\text{-}3)$$

$i = 1, 2, \ldots A.$

where $a_{ik}(r(t)) = \delta_{ik}$ when $t = -\infty$ and the potential matrix elements V_{kj} are

$$V_{kj} = \langle \chi_k | V(\underline{r} - \underline{r}(t) | \chi_j \rangle$$

The set of coupled equations represented by Eq.(X -3) was solved previously by applying second order perturbation theory. However it would be interesting to investigate whether the previous assumption is correct and if not what are its limits of applicability.

In order to do this the set of coupled Equations (X -3) has been solved by numerical integration using the Runge-Kutta method.

The matrix of the coefficients $\{a_{ij}\}$ is complex, hence separating the real and imaginary part of Eq.(X -1) we get

$$\int_{-\infty}^{\infty} \mathrm{Re}\, V_{opt}(\underline{r}(t))\, dt = -\hbar\left\{\arg(\det a_{ij}) + n\pi\right\} \qquad (X\text{-}4)$$

$n = 0, 1, 2, \ldots$

The term $n\pi$ is included in Eq.(X-4) because a calculation of $\arg(\det a_{ij})$ gives a result in the range $[0, \pi]$

$$\int_{-\infty}^{\infty} \mathrm{Im}\, V_{opt}(\underline{r}(t))\, dt = \hbar \ln |\det a_{ij}| \qquad (X\text{-}5)$$

Eq.(XII-4) for the real part of the optical potential contains both

the first order term (folding potential) and the correction from the second order term of the perturbation theory expansion.

Therefore if we subtract the time integral of the folding potential from the result of Eq.(XII-4) we are left with the correction coming from the excitations of the target, which so far we have not calculated.

Eq.(X-3) represents a set of 2N coupled equations since every coefficient is given by two equations for its real and imaginary parts.

We have then to solve the set of equations

$$\hbar \frac{\partial}{\partial t} \mathrm{Re}\, a_{ik} = \sum_j (\mathrm{Im}\, a_{ik} \cos(\omega_{jk} t) - \mathrm{Re}\, a_{ik} \sin(\omega_{jk} t)) V_{kj} \qquad \text{(X-6)}$$

$$-\hbar \frac{\partial}{\partial t} \mathrm{Im}\, a_{ik} = \sum_j (\mathrm{Re}\, a_{ik} \cos(\omega_{jk} t) + \mathrm{Im}\, a_{ik} \sin(\omega_{jk} t)) V_{kj}$$

with i = 1,2,...,A; j,k = 1,2,...,N, and the initial conditions are

$$a_{ij}(0) = \delta_{ij} \qquad \text{(X-7)}$$

The results for the time integral of Im V_{opt} are easily obtained from our computing code POTOPT according to Eq.(X-5). The way of studying the integral of the real part of the optical potential is slightly more complicated and it is described in the following section.

X-2 Real Part of the Optical Potential

In this section we present the numerical method used to extract information about the real part of the optical potential.

Solving the set of coupled equations (X-6) one can obtain Eq. (X-4), i.e.

$$\int_{-\infty}^{\infty} \mathrm{Re}\, V_{opt}(r(t))\, dt = -\hbar \left[\arg(\det a_{ij}) + n\pi\right]$$

$$n = 0, 1, 2, \ldots$$

Let us put

$$\vartheta \equiv \arg(\det a_{ij})$$

with

$$0 < \vartheta < \pi$$

in our convention.

In order to subtract the real potential coming from the folding term (1st order) from the correction given by the second order term, we need to know the phase $n\pi$. We proceed in the following way:

a) Fix the incident energy and the impact parameter. In this way the trajectory is determined and the steps described below have to be repeated for each new trajectory.

b) Make a set of calculations changing the strength of the effective potential V_o by a factor $\eta = \frac{1}{4}, \frac{1}{8}, \ldots$ etc.

c) There will be a regular change in θ proprotional to the change in V_o. By increasing the strength one can see when the value of θ has changed by π or 2π and so n can be found. Finally one gets

$$\int (V_f + \Delta V)\, dt = \Delta t\, (\vartheta + n\pi) \qquad \text{(X-8)}$$

where

$$V_f = \int V(\underline{r} - \underline{r}_o)\, \rho(\underline{r})\, d^3\underline{r} \qquad \text{(X-9)}$$

is the folding potential, ΔV is the second order correction coming from intermediate excitations. The factor 4 comes from the spin and isospin degeneracy of the single particle wave functions.

The next problem is to separate $\int V_f \, dt$ and $\int \Delta V \, dt$. This can be done again by looking at the results obtained with different strengths of the effective potential. For each value of η the time integral of the total real potential can be written

$$\bar{I}(\eta) = \eta \bar{I}_0 + \eta^2 \bar{I}_1 + \eta^3 \bar{I}_2 + \ldots \qquad \text{(X-10)}$$

where $I(\eta)$ is the quantity given by Eq.(X-8) and I_o is the time integral of the folding potential Eq.(X-9). Now we rewrite Eq.(X-10) by dividing both sides by η, we get:

$$\frac{\bar{I}(\eta)}{\eta} = \bar{I}_0 + \eta \bar{I}_1 + \eta^2 \bar{I}_2 + \ldots \qquad \text{(X-10')}$$

and for η very small $I(\eta)/\eta \simeq I_o$. Hence the time integral of the folding potential is obtained by dividing the total time integral calculated by the strength η, when η is very small. Finally $\int \Delta V \, dt$ is given by

$$\int \Delta V \, dt = 4\hbar(\vartheta + n\pi) - \int V_f \, dt \qquad \text{(X-11)}$$

The time integral of the folding potential can also be calculated by integrating the analytical expression of V_f given in Chapter VIII. We have done this in a few cases for ^{16}O with a straight line trajectory and b = 0 for several energies. The results obtained were in agreement with the ones obtained with the above procedure when $\eta = 1/8$.

X-3 Results

In the beginning we restricted ourselves to the simplest case and solved Eq.(X-6) for ^{16}O including only $1\hbar\omega$ excitations and using a straight line trajectory. We give here as an example the results obtained at E_α = 100 MeV for the trajectory with impact parameter b = 0 fm. The values are for $\int \mathrm{Im}\, V_{opt}(\underline{r}(t))\, dt$ in units of $\left[\mathrm{MeV}\ 10^{-22}\ \mathrm{sec}\right]$.

Table X-1

	V_o	$V_o/4$	$V_o/8$	$V_o/16$	$V_o/32$
Perturbation Theory	-19.20				
Coupled Channels	-29.45	-20.85	-20.01	-19.67	-19.69

where the coupled channel results have been multiplied by the appropriate factor η^{-2} in order to compare with the perturbation theory value.

This simple example shows that perturbation theory is rather accurate when the strength of the effective α-nucleon potential is 1/8 of V_o.

From the results of perturbation theory we already know that the most important excitations are the $2\hbar\omega$ ones. Therefore including both the $1\hbar\omega$ and $2\hbar\omega$ excitations one should be able to have a rather good description of the important inelastic channels involved in the collision. In the calculations discussed in this chapter the centre-of-mass corrections are not included. Then the comparison has to be made with the perturbation theory results for $\int \mathrm{Im}\, V_{opt}\, dt$ obtained before subtracting the spurious excitations. We made several sets of calculations both for ^{16}O and ^{40}Ca using the straight line trajectory first and the classical trajectory later on, at different impact parameters.

From all the results there is a clear indication that perturbation theory is accurate for a strength of about 1/8 of the value we have used (V_o = -53.8 MeV). When V_o is too small computational errors start to appear and the values obtained are not reliable any more.

We present here results obtained for ^{16}O using the straight line trajectory and for ^{40}Ca using the classical trajectory. From the following tables it can be seen that for oxygen the coupled channels calculations give a stronger absorption than perturbation theory, while for calcium they give a weaker absorption. If one compares with the figures of Chapter IX, it appears that for oxygen, with perturbation theory, we get a weaker absorption than the one obtained with a phenomenological potential, while for calcium our results gave a stronger absorption. Therefore it seems clear that by using a coupled channel calculation of $\langle 0|U|0\rangle$ we should reduce the discrepancy between the time integral of phenomenological potentials and our own, which was found before.

Next we discuss the values obtained for the time integral of the real part of the optical potential.

The first order term of the real potential does not depend on the intermediate excitations. Its value calculated from the results obtained including only $1\hbar\omega$ excitations should therefore be the same as the value calculated including both $1\hbar\omega$ and $2\hbar\omega$ excitations. The values shown in Tables (X-6,7) confirm this hypothesis and also the fact that the folding potential receives only a correction of a few percent from the second order term. This correction seems actually to change sign with the impact parameter and it is positive for scattering at the nuclear surface. This is perhaps an indication that the folding potential should be slightly corrected so as to be stronger at small distances and weaker at large distances.

TABLE X-2

^{16}O, WITH STRAIGHT LINE TRAJECTORIES, INCLUDING $1\hbar\omega + 2\hbar\omega$ EXCITATIONS

$\int \mathrm{Im}\, V_{opt}(\underline{r}(t))\, dt$ (MeV·10^{-22} sec)		E_α = 30 MeV	E_α = 50 MeV	E_α = 100 MeV	E_α = 50 MeV	E_α = 104 MeV
Perturbation Theory		- 75.20	- 64.72	- 36.52	- 22.82	- 0.8517
Coupled Channels	V_o	- 67.96	- 46.53	- 38.46	- 33.14	- 1.085
	$V_o/8$	- 75.70	- 66.85	- 37.52	- 24.32	- 0.8768
		b = 0 fm.			b = 3.024 fm.	b = 5 fm.

TABLE (X-3)

^{40}Ca, with classical trajectories, including $1\hbar\omega$ excitations only

$\int$Im $V_{opt}(\underline{r}(t))$ dt $\left[\text{MeV}.10^{-22}\ \text{sec}\right]$		Perturbation Theory	Coupled Channels		
			V_o	$V_o/4$	$V_o/32$
E_α=54 MeV	b = 5.4 fm	-16.25	-21.18	-17.24	-16.76
	b = 6 fm	-21.75	-28.84	-22.82	-22.04
E_α=104 MeV	b = 4 fm	- 9.58	-11.49	- 9.92	- 9.88
	b = 5.2 fm	-15.69	-19.52	-16.44	-16.16

TABLE (X-4)

^{40}Ca, with classical trajectories, including $1\hbar\omega$ + $2\hbar\omega$ excitations

$\int$Im $V_{opt}(\underline{r}(t))$ dt $\left[\text{MeV}.10^{-22}\ \text{sec}\right]$		Perturbation Theory	Coupled Channels	
			V_o	$V_o/8$
E_α=56 MeV	b = 1 fm	-17.57	-16.99	-17.27
	b = 5.4 fm	-25.29	-23.54	-25.44
	b = 6 fm	-31.73	-28.44	-32.01
E_α=104 MeV	b = 4 fm	-16.42	-15.27	-16.29
	b = 5.2 fm	-22.98	-19.95	-22.95

Values of $\int \mathrm{Re}\, V_{opt}\,(\underline{r}(t))\, dt = \int V_f\, dt + \int \Delta V\, dt = 4\hbar\,(\theta + n\pi)$

Time integral values are in $[\mathrm{MeV}\cdot 10^{-22}\ \mathrm{sec}]$. Values of θ are in radiants

TABLE (X-5)

^{16}O, with straight line trajectories, including $1\hbar\omega + 2\hbar\omega$ excitations

ηV_o	b = 0. fm		
	E_α = 30 MeV	E_α = 50 MeV	E_α = 100 MeV
	θ	θ	θ
V_o	0.05	2.30	1.25
$V_o/4$	0.33	2.64	1.82
$V_o/8$	1.7	1.29	0.9
$V_o/32$	0.41	0.32	0.22
n	4	3	2
$\int V_f\, dt$	-341.97	-264.85	-187.27
$\int \Delta V\, dt$	- 16.09	- 13.17	-10.98
$\frac{\int \Delta V\, dt}{\int V_f\, dt}\, 100$	4.7 %	4.9 %	5.8 %

TABLE (X-6)

^{40}Ca, with classical trajectories including only $1\hbar\omega$ excitations

ηV_o	E_α = 56 MeV		E_α = 104 MeV	
	b = 5.4 fm	b = 6 fm	b = 4 fm	b = 5.2 fm
	θ			
V_o	0.242	0.433	2.580	2.443
$V_o/4$	1.700	1.779	1.466	1.443
$V_o/32$	0.214	0.222	0.1841	0.181
$\int V_f\, dt$	-180.297	-187.037	-155.143	-152.494

TABLE (X-7)

As above, including $1\hbar\omega + 2\hbar\omega$ excitations

ηV_o	E_α = 56 MeV		E_α = 104 MeV	
	b = 5.4 fm	b = 6 fm	b = 4 fm	b = 5.2 fm
	θ			
V_o	0.214	0.174	2.611	2.299
$V_o/2$	0.232	0.3293	2.927	2.838
$V_o/8$	0.855	0.887	0.7363	0.723
n	2	2	1	1
$\int V_f\, dt$	-180.042	-186.90	-155.09	-152.283
$\int \Delta V\, dt$	8.982	16.893	3.633	9.040
$\frac{\int \Delta V\, dt}{\int V_f\, dt} \cdot 100$	4.98 %	9.03 %	2.34 %	5.93 %

Chapter XI

COMPARISON TO OTHER APPROACHES

XI-1 Introduction

In Chapter I we discussed Feshbach's theory and the folding theory of the optical potential and their applications made by N. Vinh Mau[6] and De Vries and Peng[9] respectively.

We chose to discuss the content of ref.(6) because it represents the only attempt made up to date to calculate the imaginary part of the α-nucleus optical potential by including intermediate excited states of the target explicitly. It is a second order perturbation theory calculation and hence it should be equivalent, in some approximation, to our perturbation formula of Chapter III.

De Vries and Peng have proposed very recently a microscopic model which calculates the nucleus-nucleus reaction cross section starting from the hypothesis that it is the nucleon-nucleon scattering which is mainly responsible for the target excitations. By using the Glauber approximation to describe the relative motion they make the assumption that the projectile trajectory is not modified in the field of the excited target. At the beginning of this work we made the same approximation; later on we introduced the classical trajectories of the α-particle in the static field of the target, but we kept the hypothesis that the target internal excitations do not influence the relative motion.

Section 2 below is devoted to the detailed comparison of N. Vinh Mau's work with our own. Section 3 compares the model of De Vries and Peng with the path integral approach in the framework of the shell model (cf. Chapter III).

XI-2 N. Vinh Mau's[6] calculations and the Path Integral Approach

Using the path integral formalism and calculating the transition amplitude $\langle 0|U|0\rangle$ by perturbation theory, we found in Chapter III that the time integral of the second order term of the optical potential is given by (cf. Eq.(III-3)):

$$\int_{-\infty}^{\infty} V_{opt}^{(2)}(\underline{r}(t))dt = -\frac{1}{\hbar}\sum_{n\neq 0}\int_{-\infty}^{\infty}dt\int_{-\infty}^{t}dt'\,\langle 0|V(\underline{r}(t))|n\rangle \langle n|V(\underline{r}(t'))|0\rangle\, e^{\frac{i}{\hbar}(\varepsilon_0-\varepsilon_n)(t-t')} \tag{XI-1}$$

We wish to show that the above equation is equivalent to Eq.(I-14). Changing the variables of integration as follows

$$T = \frac{1}{2}(t+t') \quad ; \quad \tau = t-t' \tag{XI-2}$$

we get

$$\int_{-\infty}^{\infty} V_{opt}^{(2)}(\underline{r}(t))\,dt = -\frac{i}{\hbar}\sum_{n\neq 0}\int_{-\infty}^{\infty}dT\int_{0}^{\infty}d\tau\; e^{\frac{i}{\hbar}(\varepsilon_0-\varepsilon_n)\tau}\cdot \tag{XI-3}$$

$$\times \langle 0|V\left(\underline{r}\left(T+\tfrac{\tau}{2}\right)\right)|n\rangle\langle n|V\left(\underline{r}\left(T-\tfrac{\tau}{2}\right)\right)|0\rangle .$$

Expanding the trajectory about T and setting

$$\underline{S} = \dot{\underline{r}}(T)\,\tau \tag{XI-4}$$

we can write

$$\begin{aligned}\underline{r}\left(T+\tfrac{\tau}{2}\right) &= \underline{r}(T)+\frac{\tau}{2}\,\dot{\underline{r}}(T)\\ &= \underline{r}(T)+\frac{1}{2}\underline{S}(\tau,T)\end{aligned} \tag{XI-4'}$$

$$\underline{r}\left(T-\tfrac{\tau}{2}\right) = \underline{r}(T)-\frac{1}{2}\underline{S}(\tau,T)$$

By analogy with Eq.(I-10,b) we define a local wave-number of the α-particle at position $\underline{r}$ inside the potential of the target $V^{(o)}_{\alpha N}(r)$ as

$$K^2_{n\alpha}(\underline{r}) = \frac{2m_\alpha}{\hbar^2}\left(E_\alpha - \varepsilon_n - V^{(o)}_{\alpha N}(\underline{r})\right) \qquad \text{(XI-5)}$$

and then

$$\varepsilon_n - \varepsilon_o = \frac{\hbar^2}{2m_\alpha}\left\{K^2_{n\alpha}(r) - K^2_{o\alpha}(r)\right\} \qquad \text{(XI-6)}$$

Using Eq.(XI-4) we write

$$(\varepsilon_o - \varepsilon_n)\tau = S\left(\frac{\hbar^2}{2m_\alpha}\right)\left\{K_{n\alpha}(\underline{r}(T)) - K_{o\alpha}(\underline{r}(T))\right\} \times \frac{K_{n\alpha}(\underline{r}(T)) + K_{o\alpha}(\underline{r}(T))}{|\dot{\underline{r}}(T)|} \qquad \text{(XI-7)}$$

Let us suppose now that $\dot{\underline{r}}(T)$ represents an average velocity of the α-particle inside the target. Then

$$m_\alpha |\dot{\underline{r}}(T)| \simeq \frac{1}{2}\hbar\left\{K_{n\alpha}(\underline{r}(T)) + K_{o\alpha}(\underline{r}(T))\right\} \qquad \text{(XI-8)}$$

With this assumption Eq.(XI-7) reduces to

$$\frac{(\varepsilon_o - \varepsilon_n)\tau}{\hbar} \simeq S\left[K_{n\alpha}(\underline{r}(T)) - K_{o\alpha}(\underline{r}(T))\right]$$

and Eq.(XI-3) becomes

$$\int_{-\infty}^{\infty} V^{(2)}_{opt}(\underline{r}(t))dt = \int_{-\infty}^{\infty} d\tau \left(-\frac{i}{\hbar}\right) \sum_{n\neq 0} \frac{1}{|\dot{\underline{r}}(\tau)|} \int_0^{\infty} ds \; e^{is\left[\kappa_{n\alpha}(\underline{r}(\tau)) - \kappa_{0\alpha}(\underline{r}(\tau))\right]} \times$$

$$\times \langle 0|V(\underline{r}(\tau) + \frac{1}{2}\underline{s}(\tau))|n\rangle \cdot \times \langle n|V(\underline{r}(\tau) - \frac{1}{2}\underline{s}(\tau))|0\rangle \; . \qquad \text{(XI-9)}$$

Let us recall the formula which ref.(6) gives for the second order term of the O.P. (cf. Eq.(I-13)):

$$V^{(2)}_{opt}(\underline{r}) = -\frac{i}{\hbar} \sum_{n\neq 0} \left(\frac{K_n}{K_{n\alpha}(r)K_{0\alpha}(r)} \frac{m_\alpha}{\hbar}\right) \int_0^{\infty} ds \; e^{is(K_{n\alpha}(r) - K_{0\alpha}(r))} \times$$

$$\times \langle \varphi_0|V(r + \frac{1}{2}s)|\varphi_n\rangle\langle\varphi_n|V(r - \frac{1}{2}s)|\varphi_0\rangle \qquad \text{(XI-10)}$$

Comparing Eqs.(XI-9) and (XI-10) we see that the $V^{(2)}_{opt}(r)$ we can extract from Eq.(XI-9) is the same as the one given in Eq.(XI-10) except that the factor $\frac{\hbar}{m_\alpha|\dot{\underline{r}}(T)|}$ is replaced by $\frac{K_M}{K_{M\alpha}(r)K_{0\alpha}(r)}$. The two expressions seem to be consistent with each other except for the factor $\frac{K_M}{K_{M\alpha}(r)}$ which in ref.(6) appears inside the Green function Eq.(I-9). In order to understand the origin of the above factor we calculate the α-particle Green's function as follows:

$$G_{\varepsilon_\alpha}(\underline{r},\underline{r}') = \sum_\beta \frac{\varphi_\beta(r)\varphi_\beta^*(r')}{\varepsilon_\alpha - \varepsilon_\beta - E_M + i\eta} \qquad \text{(XI-11)}$$

where $\phi_\beta(r)$ are eigenstates of the α particle in the potential V(r) with energy ε_β. Next we change variables as follows

$$\bar{r} = \frac{1}{2}(\underline{r} + \underline{r}') \quad ; \quad s = \underline{r} - \underline{r}' \qquad \text{(XI-12)}$$

and approximate the wave functions ϕ_β by plane waves near the point $\bar{r}$.

$$\varphi_\beta(r) = N_\beta \, e^{i \underline{k}_\beta(\bar{r}) \cdot \underline{r}}$$

where

$$k_\beta(r) = \sqrt{\frac{2m_\alpha}{\hbar^2}\left(\varepsilon_\beta - V^{(0)}_{\alpha N}(r)\right)} \qquad \text{(XI-13)}$$

and N_β is a normalization factor. Then Green's function becomes

$$\int |N_\beta|^2 \frac{d\varepsilon_\beta \, d\Omega \, \rho(\varepsilon_\beta) \, e^{i k_\beta(\bar{r}) \cdot (\underline{r} - \underline{r}')}}{\left(E_\alpha - \varepsilon_\beta - \bar{\varepsilon}_n + i\eta\right)} \qquad \text{(XI-14)}$$

The normalization and density of states are related by the requirement that the wave functions $\phi_\beta(r)$ form a complete set

$$\sum_\beta \varphi_\beta(r) \varphi^*_\beta(r') = \delta^3(r - r') \qquad \text{(XI-15)}$$

or

$$\int |N_\beta|^2 \rho(\varepsilon_\beta) \, d\varepsilon_\beta \, d\Omega \; e^{i k_\beta(\bar{r}) \cdot (r - r')} = \delta^3(r - r') \qquad \text{(XI-16)}$$

This should be compared with the integral representation of the δ-function

$$\frac{1}{(2\pi)^3} \int d^3 \underline{k}_\beta \; e^{i k_\beta (r - r')} = \delta^3 (r - r') \qquad \text{(XI-17)}$$

giving

$$|N_\beta|^2 \rho(\varepsilon_\beta)\, d\varepsilon_\beta\, d\Omega = \frac{1}{(2\pi)^3}\, d^3K_\beta \qquad \text{(XI-18)}$$

Using the definition of the momenta $K_\beta(\bar{r})$ and $K_{M\alpha}(\bar{r})$ Green's function reads

$$G_{E\alpha}(\underline{r},\underline{r}') = \frac{2m_\alpha}{\hbar^2}\int \frac{e^{i\underline{K}_\beta(\bar{r})\cdot(\underline{r}-\underline{r}')}}{K^2_{M\alpha} - K^2_\beta + i\eta}\, \frac{d^3K_\beta}{(2\pi)^3}$$

$$= -\frac{m_\alpha}{2\pi\hbar^2}\,\frac{\exp(iK_{M\alpha}|\underline{r}-\underline{r}'|)}{|\underline{r}-\underline{r}'|} \qquad \text{(XI-19)}$$

where

$$K_{M\alpha}(\bar{r}) = \sqrt{\frac{2m_\alpha}{\hbar^2}\left(E_\alpha - E_M - V^{(0)}_{\alpha N}(\bar{r})\right)} \qquad \text{(XI-20)}$$

If the above Eq.(XI-19) is used for the Green function in N. Vinh Mau's formula then the factor

$$\frac{K_M}{K_{M\alpha}\,K_{0\alpha}} \longrightarrow \frac{1}{K_{0\alpha}}$$

and Eqs.(XI-9) and (XI-10) become consistent. The extra factor $K_M/K_{M\alpha}$ in ref.(6) comes from a plane wave approximation of the Green function which is different from (XI-19) which uses a normalization which is different from the δ-function normalization (XI-15). She

argues that the δ-function normalization should not be used because only states in a narrow energy range contribute to the integral in Eq.(XI-14).

As we have seen in Chapter I and in the first part of this section, the imaginary part of the optical potential coming from Feshbach's theory can be calculated only by making several approximations. From the work of N. Vinh Mau it appears that the first difficulty is encountered in the approximate calculation of Green's function for the α-particle inside the target. The approximation of plane waves if feasible only inside a large enough potential and in the internal region of the potential itself. The next approximation consists in supposing that all important excited states have the same average energy. In our formalism this restriction does not appear. We found instead that by using Eq.(III-19) it is possible to calculate any order of excitation and we were able to understand which are actually the most populated intermediate states. Besides, an explicit calculation of the collective excitations and of the centre-of-mass corrections is possible.

On the other hand, the approach of ref.(6) is more consistent than ours from a purely theoretical point of view. It starts by calculating the α-nucleon effective interaction, while we used a phenomenological effective potential which can be used only over a limited range of energies.

XI-3 The Path Integral approach and the Microscopic Model of De Vries and Peng

In this section we compare the microscopic model which De Vries and Peng use to calculate the nucleus-nucleus reaction cross section, with the path integral approach to the optical potential. In particular we will consider the formulation of the path integral approach in terms

of the shell model description of the target which was introduced in Chapter III.

De Vries and Peng calculate the reaction cross-section by the formula

$$\sigma_R = 2\pi \int b\,db \left[1 - exp\left(-\int \sigma_T^{\alpha n} \rho\, dz\right)_b\right] \qquad \text{(XI-21)}$$

where we are using the α-nucleon cross-section instead of the nucleon-nucleon cross-section in order to make a comparison with our work.

Eq.(XI-21) was discussed in Chapter I, where it was also shown that using the optical potential obtained by the folding model, one can write

$$\sigma_R = 2\pi \int b\,db \left[1 - exp\left(\frac{2}{\hbar} \int Im\, V_{opt}(\underline{r}(t))\, dt\right)\right] \qquad \text{(XI-22)}$$

Now let us consider our formula for $\int \mathrm{Im}\, V_{opt}(\underline{r}(t))\, dt$ as given in Eq.(III;19). It can be written as

$$\int_{-\infty}^{\infty} Im\, V_{opt}(\underline{r}(t))\, dt = -\frac{1}{2\hbar} \sum_{\substack{n< \\ \kappa>}} \int_{-\infty}^{\infty} dt \int_{-\infty}^{\infty} dt'\, \varphi_n(\underline{r})\varphi_\kappa(\underline{r})\, V(\underline{r}-\underline{r}(t)) \times$$
$$\times \varphi_n(\underline{r}')\varphi_\kappa(\underline{r}')\, V(\underline{r}'-\underline{r}(t'))\, e^{\frac{i}{\hbar}(\varepsilon_\kappa-\varepsilon_n)(t-t')} \times \qquad \text{(XI-23)}$$
$$\times\, d^3\underline{r}\, d^3\underline{r}'$$

where $\phi_n(\underline{r})$ are the single particle wave functions and they are real in our calculation.

To show the relation of the above formula with Eq.(XI-21) we

first note that in ref.(9) the effects of the Pauli principle have been neglected. If the same assumption is made in Eq.(XI-23), the sum over the unoccupied states can be substituted by a sum over all possible states $\sum_0^\infty{}_k$. We have then

$$\sum_0^\infty{}_\kappa \varphi_\kappa(\underline{r})\varphi_\kappa(\underline{r}') = \delta^3(\underline{r}-\underline{r}')$$

The next assumption is that the time interval (t - t') over which the interaction between the projectile and the target is effective is very small compared to a characteristic response time of the system, i.e.

$$t - t' \ll \frac{1}{\omega_{\kappa n}}$$

where

$$\omega_{\kappa n} = \frac{\varepsilon_\kappa - \varepsilon_n}{\hbar}$$

Then the exponential in Eq.(XI-23) can be approximated to

$$e^{\frac{i}{\hbar}(\varepsilon_\kappa - \varepsilon_n)(t-t')} \simeq 1.$$

Eq.(XI-23) reduces thus to

$$\int I_{nn} V_{\alpha\bar{\alpha}}(\underline{r}(t))dt \simeq -\frac{1}{2\hbar}\int_{-\infty}^{\infty}dt\int_{-\infty}^{\infty}dt'\,\rho(\underline{r})\,V(\underline{r}-\underline{r}(t))V(\underline{r}'-\underline{r}'(t'))d^3\underline{r} \quad \text{(XI-24)}$$

where

$$\rho(\underline{r}) = \bar{\sum}_n |\varphi_n(\underline{r})|^2$$

is the nuclear density function.

Introducing now Glauber's approximation for the projectile trajectory we have

$$\underline{r}(t) = \underline{v}t + \underline{b} \qquad \text{with} \qquad \underline{b} \equiv (b_x, b_y, 0)$$
$$\underline{v} \equiv (0, 0, v)$$

and Eq.(XI-24) becomes

$$\text{R.H.S. (of Eq.(XI-24))} = -\frac{1}{\hbar}\int dt \int dt' \rho(x,y,z) \cdot \qquad \text{(XI-24')}$$
$$\times V(x-b_x, y-b_y, z-vt) V(x-b_x, y-b_y, z-vt') dx\,dy\,dz$$

Assuming that the density $\rho(x,y,z)$ is a slowly varying function in the x and y directions compared to the range of the potential V, we can write:

$$\rho(x,y,z) \simeq \rho(b_x, b_y, z)$$

Now we change the variables of integrations in Eq.(XI-24') as follows

$$z_1 = z - vt \longrightarrow dt = \frac{dz_1}{v}$$
$$z_2 = z - vt' \longrightarrow dt' = \frac{dz_2}{v}$$

obtaining

$$\text{R.H.S (of Eq.(XI-24'))} = -\frac{1}{\hbar}\frac{1}{v^2}\iiint \Big[\rho(b_x, b_y, z) V(x-b_x, y-b_y, z_1) \cdot \qquad \text{(XI-24")}$$
$$\times V(x-b_x, y-b_y, z_2) dx\,dy\,dz_1\,dz_2\Big] dz$$
$$= -\frac{1}{\hbar v^2}\int dz\, \rho(b_x, b_y, z) \iint dx'dy'\,dz_1\,dz_2 \cdot$$
$$\times V(x', y', z_1) V(x', y', z_2)$$

The last integral in the above equation is the α-nucleon total cross section. In order to show that explicitly let us remember the definition of the total corss section:

$$\sigma_T^{\alpha n} = \int |f(\vartheta,\varphi)|^2 \sin\vartheta \, d\vartheta \, d\varphi$$

To compare with our work the transition amplitude should be calculated by the Born approximation

$$f(\vartheta,\varphi) = -\frac{m}{2\pi\hbar^2} \int d^3\underline{r} \; V(\underline{r}) \; e^{i\underline{q}\cdot\underline{r}}$$

where $\underline{q} = \underline{K} - \underline{K}'$ is the momentum transfer between the initial (K) and final (K') momentum. If the angle θ between $\underline{K}'$ and $\underline{K}$ is small we can approximately write:

$$\begin{aligned} |\underline{k} - \underline{k}'|^2 &= k^2 + k'^2 - 2kk'\cos\vartheta \\ &= 2k^2(1-\cos\vartheta) \\ &= 4k^2 \sin^2\frac{\vartheta}{2} \\ &\simeq (k\vartheta)^2 \end{aligned}$$

Therefore is now

$$q = k\vartheta \qquad \text{with} \quad q \equiv (q_x, q_y, 0)$$

and

$$\sin\vartheta \simeq \vartheta$$

The cross section becomes

$$\sigma_T^{an} = \left(\frac{m}{2\pi\hbar^2}\right)^2 \frac{1}{\kappa^2} \int d^2\underline{q} \iint d^3\underline{r}\, d^3\underline{r}'\, e^{i\underline{q}\cdot(\underline{r}-\underline{r}')}\, V(\underline{r})\, V(\underline{r}')$$

$$= (2\pi)^2 \left(\frac{m}{2\pi\hbar^2}\right)^2 \frac{1}{\kappa^2} \int d^3\underline{r}\, d^3\underline{r}'\, \delta(x-x')\,\delta(y-y')\, V(\underline{r})\, V(\underline{r}') \qquad \text{(XI-25)}$$

$$= \frac{1}{\hbar^2 v^2} \int dx\, dy\, dz\, dz'\, V(x,y,z)\, V(x,y,z')$$

Substituting this result in Eq.(XI-24") we finally get:

$$\int \mathrm{Im}\, V_{opt}(\underline{r}(t))\, dt = -\frac{\hbar}{2} \int dz\, \sigma_T^{an}\, \rho(b_x, b_y, z) \qquad \text{(XI-26)}$$

Eq.(XI-26) represents the same result obtained in Chapter I, Eq.(I-22) where the optical potential was calculated by the folding model. Substituting Eq.(XI-26) into Eq.(XI-22) we would get again Eq.(XI-23).

We have therefore shown that the imaginary part of the optical potential calculated by the path integral formalism is equivalent to the same optical potential calculated within the folding theory (in the high energy limit).

The advantage of the path integral approach is that it includes the effects of the Pauli principle for the internal wave functions of the target. Furthermore, it takes into account explicitly the location in energy of the intermediate excited state, by means of the factor $e^{\frac{i}{\hbar}(\varepsilon_\kappa - \varepsilon_n)(t-t')}$. This factor is neglected both in the folding approach and in Feshbach's approach, as calculated by N. Vinh Mau.

CONCLUSIONS

In this work we have proposed a new approach to the optical potential based on Feynman's path integral formalism. It is a semiclassical theory in which the relative motion of the projectile with respect to the target can be separated from the internal excitations of the nuclei. Such a theory is particularly suitable for the study of heavy-ion scattering. However it has never been applied before. Therefore, in order to have some feeling for its ability to describe scattering phenomena, we have applied it to α-elastic scattering. Targets studied were ^{16}O and ^{40}Ca and they were described by the shell model. In this case both projectile and target have spin zero and this simplifies the problem.

Our formula for the optical potential is

$$\int_{-\infty}^{\infty} V_{opt}(\underline{r}(t))dt = i\hbar \ln \langle 0|U|0\rangle$$

where $V_{opt}(\underline{r}(t)) = Re\, V_{opt}(\underline{r}(t)) + i\, Im\, V_{opt}(\underline{r}(t))$

The above expression can be calculated provided one has some prescription for the choice of the path $\underline{r}(t)$ and for the evaluation of the transition amplitude $\langle 0|U|0\rangle$. We have argued that $\underline{r}(t)$ can be taken as the classical trajectory of the projectile in the real part of V_{opt}. The transition amplitude $\langle 0|U|0\rangle$ has been calculated both by perturbation theory and by solving a set of coupled channel equations. The solution by perturbation theory gave us some expressions consistent with existing theories of the optical potential.

We have shown that the path integral approach can be applied without making some approximations which other theories require. Furthermore

it gives more information about the importance of the different intermediate excitations. One can calculate separately contributions from different shells, centre-of-mass corrections and collective modes. Comparison with phenomenological potentials has given rather good qualitative agreement when we were using perturbation theory to calculate $\int \mathrm{Im}\, V_{opt}(\underline{r}(t))\, dt$. The discrepancy in the absorption given by our formalism and by the phenomenological potentials seems to be reduced when the coupled channel calculation of $\langle 0|U|0\rangle$ is used.

Here we would like to make some remark about the strength of the effective interaction we have been using. There are indications that it is perhaps too strong. It gives us a folding potential with a depth of $\sim$ -320 MeV for ^{40}Ca (cf. Fig. VIII-1), while in ref.(6) by using a different effective α-nucleon interaction, N. Vinh Mau obtained a potential with a depth of $\sim$ - 250 MeV. Furthermore from the figures of Chapter IX it can be noticed that in the case of ^{40}Ca we obtain an absorption stronger than that given by phenomenological potentials. The fact that one has to use a phenomenological α-nucleon effective interaction seems therefore to constitute a drawback for the approach we are proposing.

Most of this thesis has been devoted to the study of the imaginary part of the optical potential. It seems to us that the following conclusions can be drawn from our results:

a) The absorption of flux from the elastic channel is mainly due to single nucleon excitations. This holds at low to medium energies of the incident α-particle. Calculations at very high energy require an effective interaction different than the one we have used because it fits only data at low to medium energies.

b) Phenomenological potentials have now some theoretical justification. In particular Woods-Saxon potentials rather than Woods-Saxon to some power seem to be reproduced by our calculations (cf. figures in Chapter IX).

c) The absorption occurs along a classical orbit of the projectile in the target folding potential. The orbits that give the main contribution to the path integral correspond to particles scattered near the top of the Coulomb plus centrifugal barrier. Orbiting trajectories correspond to a strong absorption and in this case the approximation of a weak imaginary potential breaks down. One should therefore calculate an imaginary trajectory in the full V_{opt} of the target.

d) Perturbation theory is not the only way of calculating the optical potential. We have discussed in Chapter X an alternative, more accurate, procedure. According to our comparisons with phenomenological potential it seems to us that it is important to take into account the correction to the perturbation results, as indicated by the coupled channel calculations.

Finally we have confirmed that the real part of the optical potential is given to a very good approximation by the folding procedure plus or minus a correction of a few percent coming from the second order term.

Our calculations do not include explicitly the effect of direct reactions like pick up and knock out. However the H.O.S.M. intermediate states which we have used form a complete set and therefore they should implicitly include the possibility of having the above mentioned reactions.

We have the feeling that the path integral approach gives a good theory for a microscopic calculation of the optical potential. In particular the meaning of the imaginary part has been clarified. The important excitations are known and also the best way of calculating their effect on

the absorption from the elastic channel. Very few approximations are involved compared to other theories and the numerical calculations are not particularly difficult. Therefore one feels encouraged to proceed further with this approach, trying to describe more complicated scattering reactions.

A quite interesting case to study is α-scattering on non-closed shell targets. In this case the mechanism of excitation is rather complicated since there are many $0\hbar\omega$ transitions which correspond to motion of a nucleon within the same major shell. For example the $0\hbar\omega$ transitions are responsible for the low lying quadrupole resonance.. Furthermore the ALAS effect discussed in Chapter IX in correlation with the ^{40}Ca target disappears in other isotopes like ^{44}Ca and this case could also be studied with our model.

There are also several applications that can be made in the case of heavy-ion collisions and a discussion of them can be found in the original ref.(7) by D.M. Brink, where the path integral approach to the optical potential was first proposed. There is finally a question on whether or not one can extract the optical potential from the path integral.

The real part of the potential is well described by the folding potential and our approach does not give a big correction to this procedure. As far as the imaginary part is concerned, semiclassical theories of heavy-ion scattering indicate that the time integral of $\mathrm{Im}\, V_{opt}$ is the important quantity. One can in fact directly obtain from it the probability that the system is left in its ground state.

However, fits to experimental data require the knowledge of V_{opt} as a function of the distance $\underline{r}$. The optical potential appearing in our formalism is local, although energy dependent and it should be therefore appropriate to describe experimental data. Then one is tempted

to find a method to extract the potential from the path integral. This is at present beyond the scope of our thesis but we hope to study this problem in the near future.

REFERENCES

1. H. Feshbach, Ann. Rev. Nucl. Sci., 8 (1958) 49
2. H. Feshbach, Ann. Phys., 5 (1958) 357.
3. G.W. Greenlees, G.J. Pyle and Y.C. Tang, Phys. Rev. 171 (1968) 1115.
4. J.P. Vary and C.B. Dover, Proceedings of the Second High Energy Heavy-Ion Summer Study, Lawrence Berkeley Lab. (July, 1974).
5. G.R. Satchler and W.G. Love, Phys. Rep. 55 (1979) 183.
6. N. Vinh Mau, Phys. Lett., 71B (1977) 5.
7. D.M. Brink in "Microscopic Optical Potentials", Proceedings, Hamburg 1978, Ed. by H. V. v. Geramb.Springer-Verlag.
8. G.F. Perey and D.S. Saxon, Phys. Lett., 10 (1964) 107.
9. R.M. De Vries and J.C. Peng, Phys. Rev., C22 (1980) 1055.
10. W. Noremberg and H.A. Weidenmüller, Introduction to the theory of Heavy-Ion Collisions,Springer-Verlag, 1976.
11. J. Broki, J. Randrup, W.J. Swiatecki, and C.F. Tsang, Ann. Phys., 105 (1977) 427.
12. F. Stancu and D.M. Brink, Nucl. Phys., A270 (1976) 236, and references therein.
13. R.P. Feynman and A.R. Hibbs, Quantum Mechanics and Path Integrals, McGraw-Hill Book Company, Inc. 1965.
14. E.S. Abers and B.W. Lee, Gauge Theories, Phys. Rep., 9C (1973) 1.
15. This Thesis, Appendix IV, page 50.
16. P. Pechukas, Phys. Rev. 181 (1969) 174.
17. T. Koeling and R.A. Malfliet, Phys. Rep., 22C (1975) 181.

18. A. Messiah, Mécanique Quantique, Dunod 1972, Vol.II.

19. A. Bohr and B.R. Mottelson, Nuclear Structure, Vol.I, W.A. Benjamin, Inc., 1969.

20. D.J. Thouless, Nucl. Phys., 21 (1960) 225; 22 (1961) 78.

21. a_1 - S. Sinha, Phys. Rep., 20C (1975) 1

a_2 - G.R. Satchler and W.G. Love, ref. (5) above.

a_3 - M. Lassaut and N. Vinh Mau, Phys. Lett., 70B (1977) 14.

a_4 - F. Duggan, M. Lassaut, F. Michel and N. Vinh Mau, Orsay Preprint IPNO/TH 80-10, 1980.

b - A. Budzanowski et al., Phys. Lett., 32B (1970) 431.

22. G.R. Satchler and W.G. Love, Phys. Lett., 65B (1976) 415.

23. a) C.G. Morgan and D.F. Jackson, Phys. Rev., 175 (1968) 1402.

b) J. Batty, E. Friedman and D.F. Jackson, Nucl. Phys., A175 (1971) 1.

c) D.F. Jackson and R.C. Johnson, Phys. Lett., 49B (1974) 249.

24. A.M. Bernstein, Adv. in Nucl. Phys., 3 (1970) 325.

25. A.A. Zaidi and S. Darmodjo, Phys. Rev. Lett., 19 (1969) 1446.

26. R.J. Glauber, Lectures in Theor. Phys., Vol.1, (1959) 315.

27. J.P. Elliott and T.H.R. Skyrme, Proc. Roy. Soc., A232 (1955) 561.

28. A. Bohr and B.R. Mottelson, Nuclear Structure, Vol.II, W.A. Benjamin Inc., 1975.

29. F.E. Bertrand, Ann. Rev. Nucl. Sci., 26 (1976) 457.

30. E.F. Garman, D. Phil. Thesis, Oxford 1980, unpublished.

31. K.T. Knöpfle, G.J. Wagner, H. Breuer, M. Rogge and C. Mayer-Börike, Phys. Rev. Lett., 35 (1975) 779.

32. M.N. Harakeh, A.R. Arends, M.J.A. de Voigt, A.G. Drentje, S.Y. van der Werf and A. van der Wonde, Nucl. Phys. A265 (1976) 189.

33. D.H. Youngblood, A.D. Bacher, D.R. Brown, J.D. Bronson, J.M. Moss and C.M. Rozsa, Phys. Rev., C15 (1977) 246.

34. A. de-Shalit and I. Talmi, Nuclear Shell Theory, Academic Press, 1963.

35. L. Fox and D.F. Mayers, Computing Methods for Scientists and Engineers, Clarendon Press, Oxford (1968).

36. D.M. Brink and N. Takigawa, Nucl. Phys., A279 (1977) 159 and references therein.

37. E.P. Lippincott and A.M. Berstein, Phys. Rev. 163 (1967) 1170.

38. P. Gaillard, R. Bouché, L. Feuvrais, M. Gaillard, A. Guichard, M. Gusakow, J.L. Leonhardt and J.R. Pizzi, Nucl. Phys., A131 (1969) 353.

39. G. Hauser, R. Löhken, G. Nowicki, H. Rebel, G. Schatz, G. Schweimer, J. Specht, Nucl. Phys., A182 (1972) 1.

40. L. Bimbot, B. Tatischeff, I. Brissaud, Y. Le Bornec, N. Frascaria and A. Willis, Nucl. Phys. A210 (1973) 397.

41. F. Michel, Ph.D. Thesis, University of Mons, 1976, unpublished.

42. F. Michel and R. Vanderpoorten, Phys. Rev., C16 (1977) 142.

43. D.M. Brink and E. Mavrommatis, private communication.